W-Pos462

THE ROLE OF A Na/Mg EXCHANGE MECHANISM IN THE REGULATION OF INTRACELLULAR FREE MAGNESIUM IN FROG SKELETAL MUSCLE

L. A. Blatter, Dept. of Physiology, University of Maryland School of Medicine, Baltimore, MD 21201

A new type of intracellular magnesium-selective microelectrode based on the neutral carrier ETH 5214 was used to measure the intracellular free magnesium concentration ($[Mg]_i$) in frog skeletal muscle fibers. At room temperature (18-20 °C) the average value for $[Mg]_i$ was 0.93 mmol/l (pMg_i = 3.03 ± S.D. 0.42; n = 38 experiments). The regulation of $[Mg]_i$ was studied by measuring $[Mg]_i$ and $[Na]_i$ with ion-selective microelectrodes during alterations of the membrane potential and the transmembrane sodium and magnesium gradients. Depolarization of the fiber by increasing external [K] from 2.5 to 12.5 mmol/l did not significantly influence $[Mg]_i$. Increasing extracellular [Mg] from 1 to 10 and 20 mmol/l caused a concentration-dependent and reversible rise in $[Mg]_i$ and a decrease in $[Na]_i$, whereas removal of external magnesium did not affect $[Mg]_i$. Removal of external sodium caused an increase in $[Mg]_i$ and a decrease of $[Na]_i$. The results show that $[Mg]_i$ in frog skeletal muscle is not in a thermodynamic equilibrium and suggest that a Na/Mg exchange mechanism may be involved in maintaining low levels of $[Mg]_i$.

W-Pos463

ION CHANNELS AND RECEPTORS IN HUMAN MUSCLE CELL LINES FROM NORMAL AND DUCHENNE MUSCULAR DYSTROPHY BIOPSIES.

E. Jaimovich, J Hidalgo, J.L. Liberona, S. Tascón, F. Cifuentes and R. Caviedes. Depto. Fisiología y Biofísica Universidad de Chile, Casilla 70005, Santiago 7, Chile.

Human skeletal muscle cell lines were established by transforming myocytes from surgical biopsies. Among several skeletal muscle markers, these cell lines have significant levels of dihydropyridine and alpha-Bungarotoxin receptors. Maximal binding for the latter is 3-5 pmoles/mg prot. (Kd=1.9 nM) in normal and dystrophic cells and increases 80% upon cell fusion. PN 200-110 binding in normal and dystrophic cells was 1.1-1.8 pmoles/mg prot. Higher affinity binding was apparent in dystrophic (Kd 0.3 nM) than in normal (Kd 1.6 nM) cells.

In normal cells, using Carbachol as an agonist (100-500 nM), single channel recordings in cell attached mode showed low duty cycle events of a conductance close to 20 pS. When the same patch was excised, several levels (up to 6) of events with a single channel conductance of 25 pS were observed as well as another channel of 49 pS. For the latter, Po in cell attached recordings, decreased with hyperpolarization (Vp +100 mV Po=0.26, Vp +140 mV Po=8 x 10-4).

Supported by: NIH GM 35981, FONDECYT 896 and DTI2123.

W-Pos464

AN ESTIMATE OF NEGATIVE FIXED CHARGE DENSITY IN SKELETAL MUSCLE OF THE FROG FROM POTENTIAL MEASUREMENTS IN SKINNED FIBERS.

D. Maughan, G. Hochheizer, and R. Godt*. Dept. Physiology & Biophysics, Univ. Vermont, Burlington VT 05405, and *Dept. Physiology & Endocrinology, Med. College of Georgia, Augusta, GA 30912.

Skinned muscle fibers contain charged myofibrillar proteins which should produce a Donnan equilibrium potential (V_d) across the myofibrillar boundary. From electroneutrality and estimates of ionic composition, one can compute a fixed charge density Z^- and corresponding V_d (Maughan & Godt, Biophys. J. *56*:717, 1989). Here we report a measurement of V_d in detergent-treated skinned fibers (sarcomere spacing 2.00 um) bathed in a solution which closely mimics *in vivo* conditions (ionic strength 0.20 M; 4% Dextran T500): V_d averaged -3.5±1.6 mV (n=410). Vanadate (1 mM), which inhibits myofibrillar ATPase, had no effect on V_d. From Donnan theory, computed Z^- = -55 meq/l, i.e., near the likely physiological value. When ionic strength was decreased to 0.13 M, V_d rose to -6.0 mV; computed Z^- remained unchanged, in accord with Donnan theory. Inexplicably, replacement of ATP (6.8 mM) with the poorly hydrolizable analogue ATPγS irreversibly abolished V_d in skinned fibers.

Support: NIH AR 31636 and DK 33833.

W-Pos465

MEASUREMENTS AND MODELLING OF MAGNETIC FIELDS FROM A SINGLE MUSCLE FIBER AND A SINGLE MOTOR UNIT. R.S. Wijesinghe, R.N. Friedman, J.M. van Egeraat, and J.P. Wikswo, Jr., Department of Physics and Astronomy, Vanderbilt University, Nashville, TN 37235.

We measured single motor unit action currents of human and frog muscles using a high-resolution SQUID magnetometer. Action currents in a single muscle fiber from a frog were measured using a room-temperature toroidal pickup coil and a current-to-voltage converter. Data analysis employed a mathematical model developed for an active muscle fiber in an anisotropic bundle. Based upon our model, a single human skeletal muscle fiber 1 mm below the surface of a 10 mm diameter bundle produces, at a point 1 mm above the bundle, a maximum magnetic field of 0.26 pT for the x-component, and at the same point, 0.8 and 0.012 pT for the y- and z-components, respectively. Therefore, the measured signal of 160 pT for a single motor unit in the human abductor pollicis brevis of thumb indicates that there are 615 fibers in one motor unit of this muscle. These techniques thus offer the possibility of non-invasive localization of motor units in humans and accurate characterization of action currents in isolated single fibers and fiber bundles.

W-Pos466

INWARD RECTIFIER K CHANNELS IN RAT FIBERS.
O.Delbono, B.A.Kotsias. I.I.Med."A.Lanari",
Univ. of Buenos Aires, Argentina.

The resting PK of frog skeletal fibers shows inward rectification: PK is high when Vm-EK is negative and low when Vm-EK is positive. Voltage clamp studies (2 electrodes) were made on short toe muscle fibers of the rat (1.2 mm) equilibrated in 65 mM K_2SO_4 to further examis this issue.

The V-I relationship of these fibers was more linear (S-shapped) than in frog fibers under similar conditions. A mean chord conductance of 3.8 mS/sq.cm was found with -35 mV hyperpolarization and 2.7 mS/sq.cm with 35 mV, which gives a conductance ratio of 1.4 (n=22). The currents showed very little time dependence and were reduced by TMA, TEA or Cs. The current is not altered when [K]i was raised from 150 to 190 mM without change in [K]o. This is what would be expected from constant field theory and different from frog fibers.

Our results show that in rat fibers there is a lower rectification in the presence of an outward driving force in comparison with frog fibers. This could result from the combined effect of an increased leakage through the linear pathway of the channel and a different gating mechanism of the inward rectifier.

W-Pos467

QUANTITATION OF SHAPE PARAMETERS DURING CHEMOTAXIS. S.H. Gilbert, K.E. Fogarty & F.S. Fay. Dept. of Physiology, UMMC, Worcester, MA.

Chemotaxis involves a complex sequence of reorganization of structures within the cell and changes in the shape and position of the cell on the substratum. Some components of subcellular reorganization are closely associated with processes responsible for locomotion, while others are simply effects of it. An important step in understanding molecular mechanisms is therefore to distinguish quantitatively between cause and effect. We are developing methods for tracking structures in digitized phase-contrast video images of newt eosinophils induced to make turns by changing the direction of a gradient of chemoattractant. Trajectories of centroids of the cell and its components are compared to determine how they move with respect to the substratum and each other. Structures whose patterns of motion within the frame of reference of the cell change in response to the stimulus are likely to be effectors of the response, while any whose motion on the substrate is like that of the cell are likely to be carried passively. As expected, the motion of lamellipodial centroids analyzed by our techniques indicates that they play an effector role in chemotaxis.

W-Pos468

PRELIMINARY CHARACTERIZATION OF AN ACTIN BASED ORGANELLE TRANSLOCATOR FROM NITELLA. M.N. Rivolta, R. Urrutia, J. Sellers*, B. Kachar. Lab. of Molecular Otology, NIDCD and * Lab. of Molecular Cardiology, NHLBI, NIH, Bethesda, Md (Intro. by J. Hammer III).

Cytoplasmic streaming at rates of 60 μm/s in the algae Nitella is generated by the gliding of endoplasmic reticulum cisternae along stationary actin filament cables (Kachar and Reese, J. Cell Biol. 106:1545, 1988). High speed supernatants (150,000g for 90 min) of low ionic strength extracts, prepared in the presence of 25mM NaF, translocate fluorescently labeled actin filaments at 60 μm/s in the in vitro sliding actin filament assay (Kron and Spudich, PNAS, 83:6272, 1986). The extract has K^+-EDTA, Ca^{++} and Mg^{++}-ATPase activities of 7.9, 3.5 and 3.7 nmol/min/mg respectively. Actin (47μM) stimulates the Mg^{++} ATPase activity 3.5 fold. Western blots of proteins coprecipitated from the high speed extract with actin in the absence of ATP revealed a band of 105kDa when probed with anti-Acanthamoeba myosin I polyclonal antibodies and faint bands of 240kDa, 180kDa and 105kDa when probed with anti-Acanthamoeba myosin II antibodies. Antibodies against myosin I, but not against myosin II, partially inhibited movement of actin filaments in the in vitro assay.

W-Pos469

STOCHASTIC SIMULATIONS OF ROTATION AND PROTON FLOW IN THE BACTERIAL FLAGELLAR MOTOR. B. Kleutsch and P. Läuger, Dept. of Biology, University of Konstanz, D-7750 Konstanz, F.R.G.

The rotatory motor of bacterial flagella is driven by a transmembrane electrochemical gradient of protons. A microscopic model is analysed based on the assumption that protons passing through the motor use a channel-like pathway formed by ligand groups located partly on the rotor, partly on the stator. Proton translocation is linked to the displacement of stator elements which are elastically bound to the cell wall. The model is described by a cyclic sequence of translocation steps and proton-binding and -release reactions. Stochastic simulations of the model are carried out in which transitions between the states of the reaction cycle are treated as random events. In this way the rotation frequency and the torque generated by the motor can be predicted as a function of experimental variables such as driving force and viscous load. Furthermore, the effects of microscopic parameters such as the mean jumping frequency of stator elements and the force constant of elastic coupling on the dynamic properties of the motor can be studied.

W-Pos470

THE AMOEBOFLAGELLATE TRANSFORMATION (AFT) IN PHYSARUM POLYCEPHALUM DOES NOT REQUIRE PROTEIN SYNTHESIS. M.R.Adelman, Department of Anatomy, USUHS, Bethesda, MD

The AFT involves striking changes in the cytoskeleton and motility, but SDS-gels show no shifts in concentrations of proteins like actin or tubulin. Cycloheximide (CX, 25 ug/ml) inhibited the incorporation of tritiated amino acids into transforming cells by 80-90% but had no effect on the kinetics of the AFT, even at concentrations in excess of 100 ug/ml. Autoradiography showed all cells were labelled and the distribution of grain densities was approximately gaussian; after inhibition with CX, all cells showed reduced grain densities with no evidence for classes with differential incorporation. Although limited synthesis of minor proteins is not ruled out, these studies strongly argue that massive protein synthesis is not required for the AFT to proceed. The striking changes that occur during the AFT may reflect postranslational modifications of preexisting proteins. USUHS Protocol RO7083.

W-Pos471

ISOFORMS OF MYOSIN I IN DICTYOSTELIUM. T.J. Lynch, H. Brzeska, and E.D. Korn (Intro. by T.I. Bonner) NHLBI, NIH, Bethesda, MD 20892. It has been proposed that myosin I contributes to the extension of pseudopodia and lamellipodia during cell migration and the early events in phagocytosis. These processes should be impaired if the expression or normal function of myosin I were to be disrupted. Recently, Jung and Hammer (see abstract, this meeting) disrupted the gene coding for a myosin I in Dictyostelium, however the resultant myosin I null (MI^-) mutants are capable of chemotaxis and phagocytosis. We have found that the MI^- cells express normal levels of (NH_4^+,EDTA)-ATPase (an activity characteristic of myosin I) and possess a 120-kDa polypeptide that is recognized by an antiserum raised against myosin I from wild-type Dictyostelium. We have partially purified this protein from MI^- cells and have shown that it is an actin-activated Mg^{2+}-ATPase and that this activity is enhanced when the 120-kDa polypeptide is phosphorylated by myosin I heavy chain kinase from Acanthamoeba. This protein is distinguishable from the myosin I isolated from wild-type cells and so appears to be a second isoform of Dictyostelium myosin I. Its presence in MI^- cells may explain the relatively normal motility of these cells.

W-Pos473

A ROLE FOR MYOSIN IN THE REGULATION OF MACROPHAGE (Mϕ) MOTILITY. Allison K. Wilson and Primal de Lanerolle (Intro. by Mrinalini Rao). Dept. of Physiology. Univ. of IL, Chicago, IL 60612.

Myosin has been suggested to be involved in the regulation of mammalian nonmuscle cell motility. Since phosphorylation of the 20 kD light chain of myosin (MLC) by MLC kinase activates Mg^{2+}-ATPase activity and regulates myosin filament formation, we investigated the relationship between MLC phosphorylation (MLC-PO_4) and Mϕ chemotaxis. Inhibition of myosin dephosphorylation or incorporation of a constitutively active form of MLC kinase demonstrate an inverse relationship between MLC-PO_4 and motility. In addition, a greater proportion of the total myosin is associated with the cytoskeleton under conditions of increased MLC-PO_4. Interestingly, incorporation of antibodies to MLC kinase, which are known to inhibit MLC kinase activity, also decrease Mϕ migration. This inhibition of Mϕ migration that is observed under conditions of both increased and decreased MLC-PO_4 suggests that MLC-PO_4 must be regulated within relatively narrow limits to support motility by mammalian cells.

W-Pos472

COMPARATIVE STRUCTURE AND ENERGETICS OF SODIUM AND PROTON DRIVEN BACTERIA FLAGELLAR MOTORS

Jenny Z. Liu, Imran H. Khan, Michaela Dapice & Shahid Khan
Departments of Anatomy & Structural Biology/Physiology & Biophysics. Albert Einstein College of Medicine Bronx, N.Y. 10461

Ongoing studies on sodium driven flagellar motors of *Bacillus* strain YN2000 and *Vibrio alginolyticus* will be presented. SDS-PAGE of isolated hook basal body complexes from YN2000 flagella and the proton driven flagella of *Bacillus subtilis* gives rise, in each case, to three prominent bands. The most intense band for each species represents the hook protein, which bands differently in the two species. The other bands occur at similar positions in the two cases and may represent the proteins of M-S disc complex. The diameter of the M-S disc complex is different between the two *Bacillus* but the polypeptide composition suggests conservation of M-S disc function. At constant membrane potential, *V. alginolyticus* cells are immotile in K^+ and exhibit a 3-fold slower saturation swimming speed in Li^+ compared to Na^+. These data suggest that the dehydrated forms of the ions are transported. Hence, the size of the ion pores coupled to sodium driven motility may not show dramatic difference from proton transporting pathways.

W-Pos474

CREATION OF A DICTYOSTELIUM MYOSIN I MUTANT. G. Jung and J. A. Hammer III, LCB, NHLBI, NIH, Bethesda, MD 20892. We are interested in the possibility that the motile processes retained by Dictyostelium (Dd) myosin II null mutants (chemotaxis, phagocytosis) are supported by nonfilamentous myosin I. We recently cloned a Dd myosin I heavy chain (MIHC) gene and showed that this apparently single-copy gene encodes ~124 kDa HC which is highly similar to the MIHCs of Acanthamoeba (Jung et al., PNAS, 1989). To determine the physiological role of Dd myosin I, we have now disrupted its gene using a gene-replacement vector. By immunoblot analysis, MI null mutants are devoid of MIHC protein. MIHC mRNA is also not detectable. Southern blot analyses indicate that the central ~1/3 of the gene has been replaced by the disruption vector, rendering the gene permanently nonfunctional. These cells grow at a normal rate, are able to undergo chemotactic streaming (although this is delayed), and can complete development, but are impaired in their ability to phagocytose, as accessed by plaque formation on lawns of E. coli and uptake of FITC-labeled E. coli. Therefore, either MI is not essential for chemotaxis and phagocytosis, or Dd contain additional myosin I isoforms. We present new data supporting the latter conclusion.

W-Pos475

EFFECT OF CALYCULIN-A ON 3T3 FIBROBLASTS. L. Chartier, L. Rankin, R. Allen, D.J. Hartshorne, Y. Kato[1], N. Fusetani[1], S. Watabe[1], H. Karaki[2]. Muscle Biol. Grp. Univ. Arizona, Tucson, AZ 85721. [1]Lab. Marine Biochem., Univ. Tokyo, Tokyo 113, Japan[2], Dept. Vet. Pharmacol. Univ. Tokyo, Tokyo 113, Japan.

Calyculin-A (CL-A), an inhibitor of type-1 and 2A phosphatases, was applied to 3T3 fibroblasts. At 0.1 μM CL-A induced a marked increase in protein phosphorylation. An immunoprecipitate (formed with a mAb to gizzard myosin) showed enhanced phosphorylation in vimentin, myosin light chain (20 kD) and a 440-kD component. Neither actin nor tubulin were phosphorylated. CL-A caused marked shape changes in the 3T3 cells. At 0.1 μM CL-A cells rapidly became rounded and detached from the substrate. Stress fibers, prominent in the flattened control cells, were not detected in the rounded cells. By transmission electron microscopy an unusual ball-like structure, 2-3 μm in diameter, was visible in the CL-A-treated cells. Effects of CL-A were reversible. These observation lend support to the idea that cell shape is controlled (in part) by concerted actions of kinases and phosphatases. (Supported by NIH Grants HL-23615 and HL-20984).

W-Pos476

PEPTIDE INHIBITION OF RABBIT PSOAS MUSCLE SKINNED FIBER MECHANICS & MYOFIBRILLAR ATPASE ACTIVITY.

P.B. Chase, J. Bursell and M.J. Kushmerick. Depts of Radiology, Physiology and Biophysics, University of Washington, Seattle, WA 98195

A synthetic peptide matching myosin heavy chain (MHC) around SH_1 (IRICRKG) inhibited force in skinned fibers (1988, JCB **107**:258a) with a K_i similar to that obtained for inhibition of acto-S1 rigor binding (Suzuki et al., 1987, JBC **262**:11410). HPLC purification of this peptide alters the inhibition of fiber mechanics. The apparent K_i of the purified peptide was increased to ≈3 mM), so an unidentified component was responsible for most of the activity described previously. The purified peptide also inhibited myofibrillar ATPase activity and V_{max} with similar K_i's which were greater than that for force inhibition. Force inhibition is diffusion limited, so it was not possible to determine if Ca^{2+} influenced peptide binding (1989, Biophys. J. **55**:406a). Related peptides CNGVLEGIRICRKGFP (the whole conserved region), IRIPRKG, and RICIRGK (scrambled) behaved as IRICRKG. The results with the latter two peptides suggest that the observed inhibition is not a unique property of the native linear sequence of this small region of MHC.

Supported by NIH grants AM36281 and HL31962, and UW MSRTP.

W-Pos477

EFFECTS OF Ca^{2+} ON CROSS-BRIDGE TRANSITIONS MEASURED BY PHOTOGENERATION OF P_i AND ATP.

J.W. Walker and R.L. Moss. Dept of Physiology, University of Wisconsin, Madison, WI 53706

Cross-bridge transitions thought to be associated with the power stroke were measured in skinned single fibers from rabbit psoas muscle. Pulse photolysis of caged P_i to release 0.8 mM P_i decreased active tension in two phases with half-times of 13 ± 3 ms (n=11) and 0.9 ± 0.2 s (n=5) at 15° C, I=0.18 M, SL=2.4 um. Release of 0.9 mM ATP within fibers in rigor increased tension, following a delay, with a half-time of 85 ± 9 ms (n=15). P_i and ATP transients were independent of pCa between 6.4 and 4.5. Following partial removal of troponin complexes then complete removal of troponin C, half-times of P_i and ATP transients at pCa 9, 6.4 and 4.5 were similar to untreated fibers. The results suggest that for cross-bridges that are bound and cycling or are initially in rigor, transitions to the force generating state are not detectably influenced by Ca^{2+}.

W-Pos478

PURIFICATION AND PROPERTIES OF AN APPARENTLY FULL LENGTH NATIVE CARDIAC TITIN.

K.-M. Pan, A. W. Clark, and M. L. Greaser, Dept. of Anatomy and Muscle Biology Lab, University of Wisconsin, Madison, WI 53706

Titin from skeletal muscle normally gives two high molecular weight bands on SDS gels, T1 and T2. The smaller T2 is believed to be a proteolytically derived fragment from T1. Native skeletal titin purified by several other groups is predominantly the degraded T2 form. Methods have been developed in our laboratory to purify native cardiac titin from bovine heart which is predominantly T1. Swollen, washed myofibrils were extracted with 0.15M potassium phosphate, and the protein was purified by hydroxylapatite chromatography. Rotary shadowing of native titin sprayed onto mica revealed structures with diameters of 4-5 nm and lengths ranging from 0.3 to 0.9 microns. Samples prepared using a mica sandwich technique, however, gave structures which were more convoluted and more bead-like. Thus the method of sample preparation appeared to affect the titin morphology.

W-Pos479

TITIN SPACING IN MECHANICALLY PEELED SINGLE FIBERS WITH RESPECT TO FIBER TYPE.

C. E. Kasper and J. R. Townsley. School of Nursing, UCLA, Los Angeles, CA 90024-6918.

Single fibers from soleus and plantaris muscles were dissected in a relaxing solution (pCa 10.0; EGTA 0.05). Fibers were then mechanically peeled (sarcolemma removed), longitudinally split in half, and placed on calf skin coated coverslips. Coverslips were stained with monoclonal anti-Titin 9D10 IgG (M. Greaser, Univ. Wisc.) and incubated with 1:20 diluted FITC conjugated goat anti-mouse IgG. Fibers were washed after each incubation with phosphate buffer pH 7.4. Following incubations fibers were mounted with a DABO/glycerol medium. Stained Titin doublets were measured in addition to sarcomere lengths. A ratio of Titin spacing / sarcomere length revealed that there was a significant difference ($p \leq 0.001$) between slow soleus and fast plantaris muscles. Soleus muscle was 0.380 ± .004 SEM while plantaris ratios were .290 ± .004 SEM. Furthermore, when compared by fiber type, irrespective of muscle of origin, there was a significant difference ($p \leq 0.001$) between fast and slow fibers. Results are consistent with morphometric data from previous ultrastructural studies that have shown that the width of Z bands vary between fiber type with slow (type I) fibers the widest at 1445 Å and fast (type II) fibers narrower at 611-881 Å.

(Supported by NIH:NCNR & NIAMS; NASA)

W-Pos480

VARIATION IN CALCIUM SENSITIVITY OF SKINNED SKELETAL MUSCLE FIBERS AT DIFFERENT SARCOMERE LENGTHS IN SOLUTIONS WITH AND WITHOUT DEXTRAN. B.H.Bressler and L. Morishita, Dept.of Anatomy, Univ. of B.C., Vancouver, B.C.

Rabbit psoas or frog semitendiosus muscle were skinned in a 50% or 25% glycerol solution respectively. Single fiber segments from either muscle were used. Force-pCa curves were obtained at different sarcomere lengths (1.9um, 2.2um, 3.5um) in solutions of varying calcium concentration and 0.2mM,3mM,or 5mM MgATP at pH 7.0. At sarcomere lengths >2.2um the force-pCa curves were shifted to the left. At short sarcomere lengths they either superimposed or were shifted to the right of resting length curve. Concentration of MgATP did not affect this shift. Addition of 5% dextran to the solutions did not result in a shift of the force calcium relation in fibers at 2.2um. The tension length relation at long sarcomere lengths for skinned segments, with or without dextran in the activating solution, was not dissimilar from the intact fiber although the curve was moved to the right. Results indicate that calcium sensitivity and tension of skinned fibers is related to sarcomere length but not necessarily lattice spacing. (Supported by MRC).

W-Pos482

CROSSBRIDGE TURNOVER KINETICS DURING ISOMETRIC AND ISOTONIC STEADY-STATE CONTRACTION. B. Brenner, Universität Ulm, FRG.

We measured force, fiber stiffness, fiber ATPase, and the rate constant of force redevelopment (k_{redev}) both during isometric contraction and during steady-state shortening at different loads. Lowering load at which isotonic shortening takes place, we find an almost linear decrease in fiber stiffness, approaching about 15% of its isometric value at zero load. In contrast, fiber ATPase passes through a maximum of about 160% of the isometric value at relative loads between 25-30%, followed by a decrease to about 140% of the isometric value near zero load. k_{redev} increases almost 10-fold as load approaches zero. Although most quantitative crossbridge models (e.g. A.F. Huxley, Prog. Biophys. 7, 1957; Eisenberg and Hill, Prog. Biophs. Mol. Biol. 33, 1978) can account for the decrease in fiber stiffness, a several fold increase in fiber ATPase is predicted by the assumption that a large increase in g (the rate constant which describes the return to the non-force generating state(s) via ADP-release and rebinding of ATP) is responsible for sufficiently fast detachment at high speeds of shortening. With a two-step attachment process (A. F. Huxley, Proc. Roy. Soc. Lond., B, 183, 1973), the ATPase data can be accounted for but not the stiffness data. We will discuss possible processes other than the large increase in g (e.g. rapid detachment and reattachment to a subsequent site on the actin filament for crossbridges in the force-generating states.) that may provide rapid crossbridge detachment at high-speed shortening. (See also B. Brenner, abstract, this meeting). (Supported by DFG Br 849/1-2,3).

W-Pos481

EVIDENCE FOR REVERSIBLE ACTIN ATTACHMENT OF FORCE-GENERATING CROSSBRIDGES IN Ca^{++}-ACTIVATED SKINNED RABBIT PSOAS FIBERS. B. Brenner, Universität Ulm, FRG. Previously we proposed that in relaxed fibers or in the presence of $MgPP_i$ crossbridges reversibly attach to actin, i.e., they can detach from and reattach to actin rather rapidly compared to active turnover. Whether reversible attachment is a property common to all states has not yet been resolved. In the past, studying the response of force to releases and stretches of different speeds imposed on Ca^{++}-activated fibers was complicated by possible transitions between various attached states (Huxley and Simmons, Nature, 233, 1971). In the present study we succeeded in separating detachment/reattachment reactions from "Huxley-Simmons transitions". Our results imply that force-generating crossbridges can rapidly detach from ($k^- = 50\text{-}1000 s^{-1}$) and even more quickly reattach to actin ($k^+ >> k^-$), and reattachment rapidly leads back to a force generating crossbridge configuration. Note that k^+ and k^- are orders of magnitude faster than the rate constants describing active turnover (f_{app} and g_{app}; Brenner, PNAS, 85, 1988). Thus, both in the weak-and strong-binding states, crossbridges can detach and reattach several times as one crossbridge cycle is completed, i.e. as one molecule of ATP is hydrolysed. Reversible attachment in force-generating states may provide a mechanism for fast crossbridge detachment (with reattachment to a subsequent site in the actin filament) during high speed shortening. This mechanism does not require completion of the ATPase cycle for detachment and could account for a large distance of filament sliding during a single crossbridge cycle.(Supported by DFG,849/1-3)

W-Pos483

EFFECTS OF ISOTONIC SHORTENING ON THE EQUATORIAL X-RAY DIFFRACTION PATTERN OF SKINNED SINGLE RABBIT PSOAS FIBERS. B. Brenner, Y. Maeda[@] and R.M. Simmons[#]. Universität Ulm, FRG; [@]EMBL, FRG; and [#]King's Coll. London UK. We recorded the first two equatorial reflections [1,0] and [1,1] during isometric and isotonic steady-state contraction after modifying the EMBL beamline X-33 at DESY, Hamburg, FRG for small specimen diffraction. During isometric contraction at 5°C and μ = 170mM the average I_{11}/I_{10} ratio was 1.43 compared with 0.73 during relaxation. During isotonic shortening I_{11}/I_{10} decreased almost linearly with load. Near maximum speed of shortening the increase in I_{11}/I_{10} upon activation under isometric conditions was reversed by about 50-55% toward the relaxed value. This is slightly less than observed in an earlier study (Brenner, BJ 41, 1983). Similarly, the decrease in interfilament distance (d_{10}) upon activation was reversed by ≈60% toward the relaxed value when load approaches zero. Control experiments suggest that the observed changes in I_{11}/I_{10} during isotonic shortening are not due to (a) disorder in the filament lattice, (b) misalignment of the filaments during shortening, (c) changes in filament overlap, (d) (passive) sliding of filaments relative to each other, and (e) changes in interfilament distance. Our results suggest that the observed differences in the diffraction patterns between isometric and isotonic conditions reflect changes in the number of attached force-generating crossbridges. The discrepancy between the X-ray results and our stiffness measurements (Brenner, BJ 41 1983; Brenner, abstr., this meeting) will be discussed in view of the effect of Ca^{++} activation on weak-binding crossbridges (See Kraft, Yu & Brenner, abstr., this meeting). (DFG Br849/1-1,2,

W-Pos484

ATTACHMENT OF WEAK-BINDING CROSSBRIDGES CAN ACCOUNT FOR THE VARIOUS TIME COURSES OF MECHANICAL AND STRUCTURAL PARAMETERS OBSERVED DURING THE RISING PHASE OF A TETANUS. B. Brenner, Universität Ulm, FRG. It was previously proposed (Huxley and Kress,JMRCM,6,1985 Ford et al.,J.Physiol.372,1986) that the lead of stiffness or of equatorial X-ray reflections over force, observed during the rising phase of a tetanus, is due to initial crossbridge attachment in a "pre-force generating" state, postulated to be different from the weak-binding crossbridge states first shown in relaxed rabbit psoas fibers at low ionic strength (Brenner et al., PNAS, 79, 1982; Biophys. J. 46, 1984). We now show that not only the various leads and lags between the time courses of mechanical and structural parameters but also the characteristic changes in the rate and amplitude of early tension recovery after quick releases observed during the rising phase of a tetanus can quantitatively be explained by taking into account of the properties of the weak-binding crossbridges found by biochemical, mechanical and structural studies: (a) very fast actin binding kinetics such that equilibrium between attachment and detachment is established instantaneously compared to crossbridge turnover; (b) a small (5 to 10 fold) increase in actin affinity when Ca^{++} is raised; (c) the increase in I_{11} upon attachment is larger than the decrease in I_{10}; (d) only a limited fraction of weakly attached crossbridges is detected even by the fastest stiffness measurements. Our modelling illustrates that all measurements during the rising phase of a tetanus can be accounted for by crossbridges cycling between the weak and strong-binding states and no extra "pre-force generating state" nor cooperative kinetics (Bagni, et al., BJ 53, 1988) needs to be postulated.

W-Pos486

The Rate of ADP Release from Muscle Cross-Bridges. S.K.A. Woodward and M.A. Ferenczi, *National Institute for Medical Research, Mill Hill, London NW7 1AA, U.K.*

We have estimated the rate of ADP release from muscle cross-bridges by investigating the effect of ADP on the time course of stiffness change following the photolytic release of ATP from caged-ATP in single rabbit psoas muscle fibres at 20°C. Stiffness was determined by measuring the tension change following a rapid step increase in length (1%), at various times after a pulse of light which initiated relaxation of an isometric muscle fibre from rigor. Photolysis released 0.7 mM ATP from 2 mM caged-ATP (I=0.2M, pH 7.1, $[Ca^{2+}]<10^{-8}$ M). The time course of stiffness decrease was faster than that of tension. The former could be described by two exponential processes of equal amplitude, with rate constants of 114±23 s^{-1} and 11±3 s^{-1}. When fibres were incubated with a solution containing, in addition, 50 μM ADP or 3'(2')-O-(N-methylanthraniloyl)-ADP, the time course of stiffness change was satisfactorily described by a single exponential process with a rate constant of 12±1s^{-1}. Under these conditions, the majority of active sites contain ADP (the K_d for methylanthraniloyl-ADP measured fluorometrically in fibres was 30 μM). We interpret the rate of 12 s^{-1} for stiffness change as the rate constant for ADP release from the cross-bridge nucleotide binding sites.

W-Pos485

pCA-TENSION CURVES AND KINETICS OF STRETCH ACTIVATION IN SKINNED SINGLE MUSCLE FIBERS FROM DROSOPHILA MELANOGASTER.

M. Yamakawa, J. Molloy, S. Falkenthal*, D. Maughan. Dept. Physiol. & Biophys., Univ. Vermont, Burlington, VT 05405, and *Dept. Mol. Genetics, Ohio State Univ., Columbus, OH 43210.

We report here basic mechanical parameters from skinned indirect flight muscle, a system which is amenable to genetic manipulation (White & Sparrow, Biophys. J. 55:193a, 1989). In wild type, tension and relative stiffness increased sigmoidally between pCa 8 and 4 ($pCa_{1/2}$ at ~6.3), similar to that found in other insect fibrillar flight muscles. A stretch of <1% muscle length was sufficient to produce a substantial delayed tension rise (responsible for powered flight) that was enhanced by >10% following incubation with 1 uM calmodulin and ~10 nM myosin light chain kinase. Mutants are selected on the basis of impaired function; the robust mechanical responses from wild type provide sufficient resolution for structure-function studies. [Supported by NIH R01 DK33833 and GM33270]

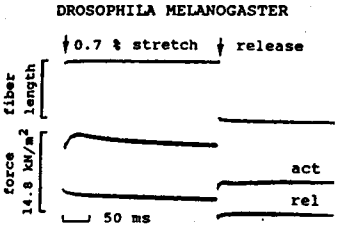

W-Pos487

ELASTIC BEHAVIOR OF TITIN FILAMENTS DURING THICK FILAMENT MOVEMENT IN ACTIVATED SKELETAL MUSCLE Robert Horowits, Koscak Maruyama* and Richard J. Podolsky NIAMS, NIH, Bethesda, MD 20892 and *Chiba University, Chiba, Japan.

We used a monoclonal antibody to study the behavior of titin (also called connectin) in both relaxed and activated skinned rabbit psoas fibers by immunoelectron microscopy. In relaxed fibers, antibody binding is visualized in the I-band as two extra striations per sarcomere arranged symmetrically about the M-line. These striations move away from both the nearest Z-disc and the thick filaments when the sarcomere is stretched, confirming the elastic behavior of titin within the I-band of relaxed sarcomeres as previously observed by several investigators. When the fiber is activated, thick filaments in sarcomeres shorter than 2.8 μm tend to move from the center to the side of the sarcomere. This translocation of thick filaments within the sarcomere is accompanied by movement of the antibody label in the same direction. In that half sarcomere in which the thick filaments move away from the Z-disc, the spacings between the Z-disc and the antibody and between the antibody and the thick filaments both increase. Conversely, on the side of the sarcomere in which the thick filaments move nearer to the Z-line, these spacings decrease. Regardless of whether I-band spacing is varied by stretch of a relaxed sarcomere or by active sliding of thick filaments within a sarcomere of constant length, the spacings between the Z-line and the antibody and between the antibody and the thick filaments increase with I-band length in identical manner. These results indicate that the titin filaments remain bound to the thick filaments in active fibers, and that the elastic properties of titin are unaltered by calcium ions and crossbridge activity.

W-Pos488

RADIAL COMPRESSION OF SKINNED RAT CARDIAC MYOCYTES WITH PVP-40 AND DEXTRAN T-500.

Kenneth P. Roos and Allan J. Brady.
Cardiovascular Research Lab, UCLA School of Medicine, Los Angeles, CA. 90024-1760.

Chemically skinned adult rat cardiac myocytes were bathed in a series of relaxing solutions containing 0-15% concentrations of the long-chain polymers PVP-40 and Dextran T-500. We measured cell width, sarcomere length and striation pattern uniformity from photomicrographs and digital images of single cells. We also measured an index of stiffness at 5 or 70 Hz from cells attached with vacuum suction micropipettes to a perturbator and tension transducer. We found that cell width decreased (down to 70% of control @ 15% concentration) and stiffness modulus increased (by about 10 fold/decade % polymer concentration) with increasing concentrations of either polymer. There were no changes in sarcomere length or in the longitudinal striation pattern uniformity under any condition. As in skeletal muscle, these data are consistent with the view that long chain polymers such as PVP and Dextran are excluded from and therefore compress the myofilament lattice in skinned cardiac cells in accordance with their concentration. Supported by USPHS HL-29671 (KPR) & HL-30828 (AJB).

W-Pos489

FLASH PHOTOLYSIS OF THE CAGED CALCIUM-CHELATOR, DIAZO-2, PRODUCES RAPID RELAXATION OF SINGLE SKELETAL MUSCLE FIBRES.

I.P. Mulligan, S.R. Adams*, R.Y. Tsien*, J.D. Potter+ and C.C. Ashley.
Uni. Lab. of Physiology, Oxford, England, Depts. of Pharm., Uni. of Cal. at San Diego, La Jolla & +Uni. of Miami School of Medicine, Florida.*

Diazo-2 is a calcium-chelator based on BAPTA, whose calcium affinity may be rapidly (2,000 s^{-1}) increased by exposure to near ultraviolet light (K_d changes from 2.2 μM to 0.073 μM), without steric modification of the metal binding site. Photolysis of a 2 mM solution of this compound with a brief flash of light from a frequency-doubled ruby laser (347 nm) caused single skinned muscle fibres from the semitendinosus muscle of the frog *Rana temporaria* to relax with a mean half-time of 60.4 ± 5 ms (range 30-100 ms n=15) at 12 °C [1], which is faster than the relaxation observed in intact muscles (half-time 133 ms at 14 °C) and similar to the rate of the fast phase of tension decay in intact single fibres (20 s^{-1} at 10 °C).

[1]. F.E.B.S. Let., (1989), 255, 196-200.

W-Pos490

RAPID CONTRACTIONS OF SKINNED FIBRE BUNDLES FROM THE SCALLOP STRIATED ADDUCTOR MUSCLE USING LASER-INDUCED PHOTOLYSIS OF NITR-5.

M.J.Fenton, T.J.Lea & C.C.Ashley
University Laboratory of Physiology, Parks Road, Oxford, OX1 3PT, UK

We have used photolysis of nitr-5 for the rapid activation of skinned fibres of a myosin-regulated muscle, the striated adductor of the scallop, **Pecten maximus.** Chemically skinned fibre bundles (diameter 70 - 200 μm) were equilibrated in solutions containing 3 mM nitr-5 (pCa 6.1) and then activated by UV laser pulse (20 ns). Pulses of 60-95 mJ gave contractions of over 90% maximum tension and a mean half-time for tension rise of 43 ms (n = 4) at 12°C; this is similar to the half-time for a tetanus in intact fibre bundles at 12°C. Lower energies gave smaller contractions with longer half-times (260 ms at 12 mJ). A second, slower component of tension development (mean half-time 13.3 s) was often observed. In ATP-free solutions rigor tension developed with a delayed onset. Rapid release of ATP from photolysis of caged ATP (2 mM) at pCa 4.5 then caused a rapid contraction with a mean half-time of 17 ms (n = 4). The fast activation rates are similar to those obtained with skinned fibres of actin-regulated skeletal muscle, although they lacked the slow component.

W-Pos491

DETERMINATION OF RADIAL STIFFNESS OF CROSSBRIDGES IN THE PRESENCE OF VARIOUS ANALOGUES. **S. Xu+, B. Brenner* and L.C.Yu+ +NIH and *Univ. of Ulm, FRG.** **Previously it was determined that crossbridges in rigor and in force generating states of Ca^{++} activated fibers exhibited radial stiffness (Brenner & Yu, BJ, 47, 1985). It was later found that in the radial direction crossbridges behaved as Hookean springs with distinctly different equilibrium positions in those two states. At the equilibrium positions, the radial force is zero. In this study, we measured radial stiffness from fibers in the presence of various nucleotides (MgATPγS, ADP, $MgPP_i$; ±Ca) at two ionic strengths (40 mM and 170 mM) by studying lattice spacings under various concentrations of dextran T_{500}. The results show that the equilibrium positions vary depending on the ligands bound to crossbridges. In addition, when the proportion of rigor and ATPγS crossbridges was varied by titrating [MgATPγS] in Ca^{++}, the radial stiffness changed accordingly, but the equilibrium positions remained the same. The data support the idea that the equilibrium position of the radial elasticity is a unique function of the state of the crossbridges. Implications of variable radial elasticity will be discussed.**

W-Pos492

EFFECT OF ATP ANALOGUE ON EQUATORIAL X-RAY DIFFRACTION PATTERN OF STRIATED RABBIT SKELETAL MUSCLE.

H. Iwamoto and R. J. Podolsky.
Laboratory of Physical Biology, NIAMS, NIH, Bethesda, MD 20892.

Application of ATP analogues (e.g. MgPPi) to rigor muscle fibers of the rabbit accelerates the force decay after stretch while keeping the stiffness constant (Schoenberg & Eisenberg, 1985). To examine whether this effect is accompanied by structural changes in myosin crossbridges, we compared the equatorial reflection intensities of skinned rabbit psoas fibers in the presence of 4mM MgPPi with those of rigor fibers at 5°C. The fibers were alternately stretched and released by 1% fiber length every 4 sec, and X-ray patterns were collected with 2 sec time resolution. During equal numbers of releases and stretches, the average intensity ratio I_{10}/I_{11} in the presence of MgPPi was 36±9% higher than in rigor solution (n=7, mean ± SEM, $P<0.02$). Upon stretch the 1,1 reflection of the MgPPi-treated fibers decreased by 6±3% (n=7, $P<0.05$) while the reflections of the rigor fibers did not show any significant change. These results suggest that MgPPi-bound crossbridges are more compliant than rigor crossbridges.

W-Pos493

EQUILIBRIUM CROSSBRIDGE BEHAVIOR IN THE PRESENCE OF $MgPP_i$. Mark Schoenberg. LPB, NIAMS, NIH. Bethesda, MD 20892

When a step-stretch is applied to a muscle fiber, all the attached crossbridges are strained and a force is generated. That force subsequently decays as the strained crossbridges detach and reattach in positions of lesser strain. For skinned rabbit psoas fibers bathed in a solution containing 3 mM $MgPP_i$ at ionic strength 110 mM, the rate constant of that decay, as estimated from the half-time of the decay, is less than the rate constant with which myosin subfragment-1, under identical conditions, detaches from actin in solution. Anderson and Schoenberg (Biophys. J. 52:1077:1987) postulated that the rate constant for force decay at ionic strength 110 mM was slow because the crossbridge was bound with two heads and only when both heads detached simultaneously could the crossbridge relax a significant fraction of the tension it supported. We have now added this feature to my simple 1985 equilibrium crossbridge model (Biophys. J. 48:467) and calculated the magnitude of the expected reduction in force decay due to binding of the second head. Studying fibers bathed in 3 mM $MgPP_i$, we have obtained strong experimental evidence in support of the model by correctly predicting the ionic strength dependence of the rate constant of force decay. As predicted by the double-headed model, as ionic strength increases from 40 to 200 mM, the rate constant of force decay increases 30-fold to near the subfragment-1 detachment rate constant. Another experimental result successfully predicted by the model is that at high ionic strength, the sigmoidicity in the concentration dependence of the rate constant of force decay greatly decreases.

W-Pos494

THE CALCIUM SENSITIVITY OF WEAKLY-BINDING CROSSBRIDGES PRODUCED BY TREATMENT OF SKINNED MUSCLE FIBERS WITH N-PHENYLMALEIMIDE OR p-PHENYLENE-DIMALEIMIDE. Vincent A. Barnett and Mark Schoenberg. LPB, NIAMS, NIH. Bethesda, MD 20892

It has been previously shown in fibers and in solution that the binding of "strongly-binding" myosin heads is Ca-sensitive. While, in solution, it has been determined that the binding strength of weakly-binding myosin heads (e.g. S1·ATP) is relatively insensitive to Ca^{++}, in fibers, it has been difficult to verify this because Ca^{++} allows crossbridges to cycle into strongly-binding states. We have found that treatment of relaxed skinned muscle fibers with N-phenylmaleimide (NPM) or para-phenylene-dimaleimide (pPDM) produces crossbridges that are locked in a weakly-binding state, with mechanical properties very closely matching those of the weakly-binding rapid-equilibrium M·ATP crossbridge. We have therefore examined the calcium sensitivity of fibers treated with NPM or pPDM under conditions that lock > 95% of the crossbridges in this weakly-binding form. At both physiological (165) and 40 mM ionic strength, calcium (pCa 4.6) induces very little change in either fiber stiffness or crossbridge kinetics. We conclude that, in fibers, as in solution, Ca^{++} has only a small effect on the strength of binding of weakly-binding rapid-equilibrium crossbridges to actin.

W-Pos495

THE USE OF APYRASE IN CAGED-ATP EXPERIMENTS. J.Sleep & K. Burton. MRC Unit of Cell Biophysics, 26-29 Drury Lane, London WC2B 5RL.

In experiments involving activation of rabbit psoas fibres for more than 1 second at 20°C it is essential to use an ATP regenerating system to avoid ATP depletion in the centre of the fibre. This can be a problem in experiments with caged-ATP, which may contain about 5 μM contaminating (ATP + ADP). Since the K_m for ATP is about 15 μM, about 1/4 of the heads are expected to be actively cycling under these conditions. Experimentally, tensions approaching the isometric value (P_o) are generated (half time about 1 min @ 5°C) from an initially low rigor tension (5% P_o). If the fibre is released by 0.5% to reduce the tension to zero, tension recovers somewhat faster. This effect can largely be eliminated by pretreatment of the caged-ATP activating solution with 7 μg/ml apyrase (an ATPase and ADPase) for 1 hour at 20°C which reduces the [ATP] to < 0.05 μM. In this case the steady-state tension is about 15% P_o. Apyrase has also proved useful for simplifying the purification of caged ATP.

W-Pos496

MOVEMENT OF MYOSIN HEADS IN INTACT FROG SARTORIUS MUSCLE UPON ACTIVATION. T. C. Irving, and B. M. Millman. Biophysics Interdept. Group, Dept. of Physics, Univ. of Guelph, Ont. Canada. N1G 2W1. Reflection intensities have been obtained from equatorial X-ray diffraction patterns from relaxed frog sartorius muscles with and without compression of the filament lattice by adjusting the osmolarity of the Ringer's solution (0.06 - 0.4). Phases for the first five orders were established as ++--+ under all conditions. Axially-projected electron density across the A-band filament lattice showed that in relaxed muscle the myosin heads are concentrated in regions between adjacent thick filaments along the 1,0 plane, and that they are pushed against the thick filament backbone as the lattice is compressed. The distribution of myosin heads appears to be more uniform in contracting muscle. In relaxed frog muscle, electrostatic repulsion between the myosin heads and the thin filament prevent interaction but upon activation, this repulsion may be reduced. Thus, activation may involve changes in the disposition of myosin heads that are mainly azimuthal rather than radial contrary to usual assumptions. Supported by the Natural Sciences and Engineering Council of Canada.

W-Pos497

EFFECT OF CONTRACTION AND FATIGUE ON THE FILAMENT LATTICE OF INTACT VERTEBRATE SKELETAL MUSCLE. B.M.Millman, B.Williams, T.Irving & Q.Li. Physics Dept., University of Guelph, Guelph, Ontario, Canada

Small-angle X-ray diffraction has been used to examine the A-band filament lattice of intact frog sartorius muscle during relaxation and active contraction or after fatigue. Lattice spacing was determined from a lattice which was osmotically swollen or shrunken by using Ringer's solution: either diluted, or with added glucose, sucrose or NaCl. As shown previously (Millman et al., 1981, Biophys. J. 33:189), the lattice behaves as if about 70% of its volume is solute-accessible water. During contraction, the lattice showed either an increase or no change in spacing; during fatigue, the lattice swelled. Increases in lattice spacing may involve one or more of: radial movement of thick filament projections, electrostatic forces resulting from a shift of charge positions on the filaments, osmotic swelling from a net influx of ions or sarcomeric shortening.

W-Pos498

EQUATIORIAL XRAY DIFFRACTION STUDIES ON INTACT SINGLE MUSCLE FIBRES OF THE FROG. G. Cecchi*, P.J. Griffiths+, A.M. Bagni*, C.C. Ashley+ & Y. Maeda. DESY Hamburg, FGR. *Dipartmento di Scienze Fisiologiche, Florence, Italy. + University Laboratory of Physiology, Oxford, UK.

Equatorial reflections (1,1 & 1,0) were studied during tetani of single fibres from tibialis anterior of Rana temporaria under sarcomere length-clamped conditions. In the relaxed state, 2,0 and Z line reflections were clearly separated from 1,1. During the rise of tension, integrated equatorial intensities (I1,1, I1,0) and stiffness changes led tension by 19ms (5°C). There was considerable broadening of the 1,1 reflection as well as increase in amplitude. 1,0 decreased principally in amplitude. Length-clamp virtually abolished lattice expansion. In unclamped tetani, lattice spacing (39.43nm at 2.14um) expanded during contraction with a time course similar to that of changes in I1,1 and I1,0. During unclamped relaxation, lattice compression had a time course similar to that of I1,1, I1,0 and stiffness changes (much slower than force). The data show that lattice spacing changes preceed tension development and suggest an increased lattice disorder associated with tension development. Supported by the NIH and EMBO.

W-Pos499

AN EXPLANATION OF THE A-BAND SHORTENING ARTIFACT IN VERTEBRATE STRIATED MUSCLE. Hugh Huxley, Rosenstiel Center, Brandeis Univ., Waltham, MA 02254.

In view of some reports of A-band shortening in vertebrate striated muscle, an e/m study was made of frog muscle contracting below rest length, using conventional fixation methods. As expected, below a sarcomere length of 1.6μ (the length of the A-bands), contraction bands developed at the Z-lines. These represented the crumpled ends of the A-filaments and became more prominent as the sarcomere length decreased. When such over-contracted muscles were re-extended to normal sarcomere lengths and fixed immediately or after a 15 min. interval, the A-filaments were found not be have re-extended. Instead, their end regions had dissolved, often in a regular manner, giving A-bands of much shorter length, down to 1μ or less. If muscles shortened below 1.6μ sarcomere length were left relaxed at that length for 15 min. before fixation, then contraction bands again dissolved, leaving a clearer region around the Z-lines and shortened A-bands in normal-looking sarcomeres. No sign of any of these effects were seen in contraction to sarcomere lengths greater than 1.6μ. These results illustrate the nature of the 'delta state' described by Ramsey and Street in 1940 (J. Cell. Comp. Physiol. 15, 11-34) in muscle fibers allowed to shorten below 2/3 rest length. The compression induced A-filament depolymerization may account for observations of A-band shortening in preparations whose history or loading and stimulus conditions were not appropriately controlled.

W-Pos500

RADIUS OF GYRATION OF MYOSIN S1 WHEN FREE AND WHEN BOUND TO F-ACTIN

R. Mendelson, P. Curmi, D. Schneider, D. Stone, C.V.R.I.* & Biochem./Biophys., U.C., San Francisco, CA and *Brookhaven Nat. Lab., Upton, NY

We have reported (Curmi *et al.*, JMB, *203*, 781, 1988) a search for large-scale changes in myosin S1 structure upon binding to F-actin using neutron scattering with deuterated ("invisible") actin. In order to extend these studies to the longest chords in S1, we have investigated the very low-s portion ($s = 2\sin\theta/\lambda$, 2θ = scat. angle) of the scattering pattern of papain-generated S1 (with LC II) using long wavelength neutrons ($\lambda = 0.64$ nm). When this S1 is dissociated from actin, a bi-phasic Guinier plot is observed with the lowest s-portion yielding a radius of gyration (R_g) of papain-S1 of 4.5 nm. The Rg of free chymotrypsin-generated S1 (without LC II) was 4.0 nm. The free S1 R_g values are in good agreement with recent X-ray studies by Garrigos & Vachette (Biophys. J. *55:* 80a,1989. & personal communication). The difference in R_g of (papain) S1 between when free and when bound to F-actin was 0.03 ±0.18 nm. This lack of observable change upon actin binding supports and extends the conclusions of our previous neutron scattering work. Supported by NIH grant AR 39710.

W-Pos501

TIME-RESOLVED FLUORESCENCE SPECTROSCOPY OF STRIATED MUSCLE FIBRES USING SYNCHROTRON RADIATION.

A. Arner*, R. Rigler** and J. Roslund***. *Dept. Physiology & Biophys, Lund University, **Dept. Medical Biophysics, Karolinska Institute, Stockholm and *** MAX-laboratory, Lund, Sweden.

A beam-line for time-resolved spectroscopy at the MAX-synchrotron (Rigler et al. 1987, Physica Scripta T17, 204) was used to investigate fluorescence and anisotropy in skinned rabbit psoas fibres. Fluorescence from intrinsic tryptophan and a nucleotide analogue, etheno-ADP, were used. Following excitation (300 nm, 50 ps) the intrinsic fluorescence decayed with time-constants in the ns time-range. Anisotropy showed a decay within the first ns followed by a slower decay. These anisotropy changes were slower in rigor compared to the relaxed state. The results show that time-resolved fluorescence and anisotropy in the pico- nanosecond time range can be obtained non-invasively using intrinsic fluorescence. With etheno-ADP, which binds to the nucleotide site on myosin, anisotropy changes similar to those obtained with intrinsic fluorescence in rigor were observed. The data may provide information regarding the link between intramolecular motions and cross-bridge state.

W-Pos502

THE LIFETIME OF VANADATE-TRAPPED NUCLEOTIDE IN INSECT FLIGHT MUSCLE IS VERY LONG.

N. Naber, R. Cooke and C. Lucaveche, M.K. Reedy. Dept. Biochem. & Biophys., UCSF; Dept. of Cell Biology, Duke U., Durham, NC.

A spin-labeled ATP analog (SL-ATP) was trapped with vanadate (Vi) on myosin cross-bridges in insect flight muscle. SL-ADP bound in the absence of Vi showed a well-ordered spectrum. Addition of Vi, calcium and SL-ATP resulted in a spectrum indicative of highly disordered cross-bridges, and characteristic relaxed patterns were seen in both electron microscopy and x-ray diffraction. Competition between SL-ATP and ATP in the presence of Vi showed that the rate of binding of the two nucleotides was similar. In a relaxing solution containing only ATP and phosphate, spin-labeled nucleotides remained trapped by Vi on the myosin head for many hours; upon addition of calcium the rate of release of the nucleotide increased with a half-time of 45 min. After overnight incubation in ATP-Vi, EM's and x-ray diffraction showed stable relaxed patterns up to 1 hr after washing with rigor solution. This shows that the Vi nucleotide state in insect flight muscle is more stable than the corresponding state in fast skeletal muscle where the release of trapped ADP by Ca++ occurs in less than a minute. Supported by USPHS grants AM30868, (RC) and AM 14317 (MKR).

W-Pos503

CONTRACTION OF RABBIT SEMITENDINOSUS FIBERS AS A FUNCTION OF [MgATP].

M. Lin, E. Pate, and R. Cooke, Dept. Biochem. Biophys., UCSF; Dept. Math., Wash. State Univ.

We measured the isometric tension (Po) and maximum contraction velocity (Vmax) of glycerinated rabbit slow fibers (semitendinosus) as a function of [MgATP] over the range 5 μM to 3 mM. The results, when contrasted with similar ones from fast muscle, can test current models of cross-bridge kinetics. We found that Po decreased with increasing [MgATP], while Vmax, determined by extrapolation of Hill fits to the force-velocity data, increased. Vmax exhibited classical, Michaelian, saturation behavior with respect to [MgATP] with half-maximal velocity at 18 μM (=Km) and a value at saturating [MgATP] of 0.6 muscle lengths per sec. These compare with values of 175 μM and 1.6 lengths per sec. in fast (psoas) muscle. Thus compared to psoas, Km decreases by almost a factor of 10 while Vmax decreases by less than a factor of 3. Hence we do not obtain a simple linear scaling of the hyperbolic relationship between Vmax and [MgATP], with the surprising result that at low [MgATP], "fast" fibers actually have a lower shortening velocity than "slow" fibers. Supported by USPHS grants HL32145 (RC) and AR39643 (EP).

W-Pos504

SMALL ANGLE DYNAMIC LIGHT SCATTERING OF LIMULUS THICK MYOFILAMENTS IN SUSPENSION. R. Xu[1], S.F.Fan[2], T.Maeda[1] and B.Chu[1]. [1]Dept. Chem.,[2]Dept. Anat. Sci., HSC, SUNY at Stony Brook, NY 11794.

Dynamic light scattering (DLS) had been used by us to study the crossbridge motions of the isolated Limulus thick myofilaments in suspension at scattering angles (θ)higher than 30° (J. Mol. Biol.,166:329'83; Biophys. J.,47:809'85). In order to estimate the size distribution from pure translational motions we have performed the DLS measurements at θ down to 3° which corresponds to $KL \sim 4.3$ for λ_o = 488 nm with K and L being the magnitude of the scattering vector and the characteristic filament length($\sim$4.8 μm)respectively. We found three unexpected results:(1) The apparent filament length is shorter than 4.8 μm; (2) in the region $4.3 > KL > 2.1$, the Γ/K^2 values were practically constant; and (3) the variance of the linewidth distribution at $KL \sim 4.3$ was very small ($\sim$0.03). Possible factors that can partly explain them include (1) due to crossbridge projecting from the shaft of the filament, the effective viscosity of the solvent is higher than the macroscopic solvent viscosity and/or (2) the apparent mechanical characteristics of the filament along its length is not uniform. (Supported by NSF grant DCB8508897)

W-Pos505

ORIENTATION OF IODOACETAMIDOTETRAMETHYLRHODAMINE (IATMR) PROBES ON MYOSIN LIGHT CHAIN-2 (LC-2) IN RABBIT MUSCLE FIBRES. C. Shrimpton, J. Sleep & M. Irving, Biophysics Dept, King's College London, 26-29 Drury Lane, London WC2B 5RL, England.

Rabbit skeletal LC-2 was labelled with IATMR and exchanged into myosin heads in psoas muscle fibres in EDTA rigor solution. Calcium-activated force was not altered by exchange of ~0.5 LC-2/head. Fluorescence intensity polarisation ratios were fitted using a model with an axially ordered plus an isotropic population of probes (Tregear & Mendelson (1975) Biophys. J. 15,455). In rigor the data suggested ~45% of probes were ordered, with absorption and emission dipoles at ~70° to the fibre axis. When labelled LC-2 was exchanged into isolated Mg-papain heads and these were bound to highly-stretched rigor fibres, the ordered fraction, also at ~70°, was ~65%. This suggests a well-defined relation between dipole and head axes. In relaxed fibres probe orientation was almost isotropic, but in contracting fibres there was a significant ordered fraction. Qualitatively similar results have been obtained by exchanging IATMR-labelled chicken gizzard LC-2 into psoas fibres. (Supported by the Muscular Dystrophy Association.)

W-Pos506

BIREFRINGENCE AND DIFFERENTIAL FIELD RATIO IN RELAXED AND RIGOR FIBERS FROM INSECT FLIGHT MUSCLE R.J. Baskin, S. Shen, and Y. Yeh. Group in Biophysics, Univ. of California, Davis, CA 95616

Relaxed, chemically skinned, single fibers from the dorsal longitudinal muscle of the insect, *Lethocerus colessicus* (full overlap SL = 2.95 μm) show a value of birefringence ($1.76 \pm .08 \times 10^{-3}$) similar to that found in relaxed, chemically skinned frog fibers (full overlap SL 2.30μm) ($1.60 \pm .19 \times 10^{-3}$). The value of the differential field ratio (DFR) defined as $(E_{diff\parallel} - E_{diff\perp})/(E_{diff\parallel} + E_{diff\perp})$ is however quite different, exhibiting a negative value (-0.021 ± .013) in contrast to the normal value found in frog muscle of 0.099 ± .026. When the insect fiber is put into rigor the birefringence shows a small decrease (similar to what is seen in rigor frog muscle) and the value of DFR becomes more negative (-0.062 ± .028). In our theoretical formulation, as applied to insect muscle, we are able to explain these results if we assume the existence in insect muscle of an anisotopic molecular component oriented at right angles to the long axis fiber. There is some evidence that such a component may be present in the Z-membrane (Deatherage, J.F., J. Cell Bio. 108, 1775-1782, 1989). With this assumption our theoretical formulation is able to predict the positive value of birefringence, the negative value of DFR, and the changes in these values that occur when the fiber is placed into rigor. Work is supported by NIH under grant AR 26817.

W-Pos507

ANTI-RIGOR CROSS-BRIDGE ANGLE IN NORMAL SARCOMERES? K. Trombitas and G. H. Pollack, Bioengineering WD-12, University of Washington, Seattle WA 98195

Under rigor conditions, we reported that cross-bridges of insect flight muscle can assume any of three angles: 45° (rigor), 90° (perpendicular), or 135° (anti-rigor), depending on the condition. When rigor develops isometrically, the bridge angle is typically 45°. When rigor develops isotonically, so that the specimen can shorten, many anti-rigor bridges are observed (Trombitas *et al.*, 1986, 1988). Anti-rigor bridge angles were recently confirmed by Reedy *et al.* (1989). In the mutant Drosophila flight muscle that they studied, however, the anti-rigor angles were thought to arise out of actin filaments on either side of the M-line switching places with one another, each becoming "wrongly" polarized. Recent evidence, however, implies that this is not a universal explanation: (1) Reedy's hypothesis predicts chevrons with mirror symmetry on either side of the M-line, but we could often observe the rigor configuration on one side, anti-rigor on the other; and (2) a progressive bridge-angle change could often be observed along thin filaments: e.g., rigor near the Z-line, perpendicular in the mid-region, anti-rigor near the tip. Thus, the anti-rigor angle may be a genuine feature of the rigor state in sarcomeres that are structurally normal.

W-Pos508

DISSOCIATION OF CROSSBRIDGE CYCLING FROM MUSCLE FORCE AT SHORT SARCOMERE LENGTHS IN-VIVO.

A.J.Baker, S.D.Trocha, R.Brandes, M.W.Weiner.
Mag Res Unit. Univ of California, San Francisco.
4150 Clement St CA 94121

The aim of this study was to determine whether the reduced force production of shortened muscles *in vivo* is related to reduced ATP-consuming crossbridge interactions. ^{31}P NMR spectra were continuously acquired (1.4 min averages) at 121 MHz from single frog sartorius muscles stimulated at 0.2Hz. Oxidative ATP production was blocked and ATP utilization inferred from decreases in amplitude of the phosphocreatine (PCr) resonance. Comparisons were made between muscles at optimal length for force production and highly shortened (≈50%) muscles which produced negligible force. The initial time course of PCr decrease was found to be similar at both muscle lengths. With increasing sarcomere lengths above optimal, both force and ATP utilization are known to decrease proportionately. In contrast, the present results show that at reduced sarcomere lengths, muscle force and ATPase are uncorrelated. These results suggest that at short sarcomere lengths, crossbridges continue to cycle but without production of external muscle force. Furthermore, consistent with recent *in-vitro* motility studies (Toyoshima et al;Nature,341,154) the results also raise the possibility that *in-vivo*, myosin ATPase may be activated by interaction with actin filaments having reversed orientation in the double overlap zone.

W-Pos510

DEVELOPMENTAL CHANGES IN CA SENSITIVITY OF SKINNED RABBIT CARDIAC FIBERS.

Ventura-Clapier, R., Hoerter, J. & Murat, I. (introduced by K. Schwartz) U241-INSERM, Université Paris XI, 91405-Orsay, France

Various isoforms of regulatory proteins are expressed during cardiac development. Since the expression of different TnT isoforms affects Ca sensitivity, we measured pCa_{50} during perinatal period. Isometric force-pCa relationship was measured in Triton X-100 skinned bundles from left papillary muscle in foetal (2 days before birth), newborn: 1 ,3 ,8 and 17 days postpartum (dpp) and adult rabbit. Ca sensitivity was high in fetus (pCa_{50}= 5.60±0.01, n=15), decreased abruptly at birth (5.47±0.02, n=20 at 1dpp) and remained low during the first postnatal week (5.46±0.02, n=9 at 3dpp; 5.43±0.02, n=11 at 8dpp) Ca sensitivity reached the adult level (5.54±0.01, n=19) at 17 dpp. The Hill coefficient was similar at all ages. The postnatal increase in Ca sensitivity could be related to change in proportion of the five TnT isoforms found in developing rabbit heart (Anderson et al., Circ. Res.;63:742 1988). The origin of the abrupt decrease in Ca sensitivity at birth remains unknown.

W-Pos509

TRIMETHYLAMINE N-OXIDE (TMAO) PROTECTS SKINNED SKELETAL MUSCLE FIBERS FROM THE DELETERIOUS EFFECTS OF INCREASED IONIC STRENGTH.

R.T.H. Fogaça, M.A. Andrews and R.E. Godt
Dept. Physiol. & Endo., Med. Coll. GA, Augusta GA 30912

The zwitterion TMAO, found in high concentrations in muscle of euryhaline animals, acts to stabilize intracellular enzymes under conditions of increased osmolarity (Yancey et al., *Science 217*:1214-1222, 1982.). Using detergent skinned fibers from rabbit psoas, we tested whether TMAO could reverse the decrease in contractility induced by increased ionic strength (Andrews et al., *Biophys. J. 53*:570a, 1988). Ionic strength was altered over the range 165 to 315 mM by varying the concentration of potassium salt (methanesulfonate, Cl^- or NO_3^-). Optimal concentrations of TMAO (300 mM) significantly increased maximal Ca^{2+}-activated force (19-61%), under all conditions. Other biological zwitterions (sarcosine, glycine and betaine) also increased force but to a lesser extent, while equivalent concentrations of sucrose decreased force. Furthermore, at both high (315 mM) and low (165 mM) ionic strengths, TMAO decreased the tension-cost of isometric contraction (fiber ATPase rate/ force). Our results indicate that the deleterious effects of elevated ionic strength on contraction: 1) are not due solely to ionic screening, which should be unaffected by TMAO, but 2) may involve destabilization of the actomyosin-ATPase, which can be ameliorated by TMAO. (Support: NIH AR31636)

W-Pos511

KINETICS OF A CROSS-BRIDGE STATE TRANSITION IN FIBERS ACTIVATED BY PARTIAL REMOVAL OF TROPONIN.

Joseph M. Metzger and Richard L. Moss.
Department of Physiology, University of Wisconsin, Madison, WI.

The rate constant of tension redevelopment (k_{tr}) has been shown to increase with increases in $[Ca^{2+}]$ and is thought to reflect a transition in the cross-bridge cycle which is rate limiting in terms of formation of the strongly bound, force bearing cross-bridge state (Brenner PNAS 85 3265, 1988; Metzger, Greaser and Moss JGP 93 855, 1989). Rabbit psoas fibers were chemically skinned and activated to contract in the absence of Ca^{2+} by partial removal of troponin (Tn). The remaining Tn units were TnC replete so that maximal activation could be achieved by the addition of Ca^{2+}. As $[Ca^{2+}]$ was varied from pCa 9.0 to 4.5, k_{tr} first decreased before increasing to the maximum value at pCa 4.5 while tension progressively increased throughout the entire pCa range. Thus, in terms of k_{tr}, activation by Tn removal appears to differ from activation by submaximal concentrations of Ca^{2+}.

W-Pos512

ALTERATIONS IN THE KINETICS OF A CALCIUM-SENSITIVE CROSS-BRIDGE STATE TRANSITION IN SKINNED PSOAS SKELETAL MUSCLE FIBERS DUE TO MAGNESIUM.

Joseph M. Metzger and Richard L. Moss. Department of Physiology, University of Wisconsin, Madison, WI.

The rate constant of tension redevelopment (k_{tr}) has been shown to be Ca^{2+} sensitive and is thought to reflect a transition in the cross-bridge cycle that is rate limiting in terms of formation of the strongly bound, force bearing cross-bridge state (Brenner PNAS 85 3265, 1988; Metzger, Greaser and Moss JGP 93 855, 1989). The basis of this Ca^{2+} sensitivity was investigated by examining the k_{tr}-Ca^{2+} relationship with free [Mg^{2+}] set at 1 mM or 10 mM. In maximally Ca^{2+} activated fibers, k_{tr} and tension were unaltered due to changes in free [Mg^{2+}]; however, at submaximal levels of Ca^{2+} activation, k_{tr} and tension were markedly depressed at 10 mM Mg^{2+}. In fibers treated to partially extract myosin LC_2 the effect of Mg^{2+} upon the k_{tr}-pCa relationship was less marked. These results support the hypothesis that LC_2 modulates a Ca^{2+} sensitive cross-bridge state transition in vertebrate skeletal muscle.

W-Pos513

CALCIUM SENSITIVITY OF THIN FILAMENT ACTIVATION IN CARDIAC AND SKELETAL MUSCLE CELLS CHANGES WITH MAXIMUM TENSION.

Nancy K. Sweitzer, Dept. of Physiology, University of Wisconsin, Madison.

We have probed the effects of tension on the level of activation of single cardiac myocytes and psoas muscle fibers. Force was altered by altering temperature (temp) and TnC extraction. Maximum force and the Ca^{2+} sensitivity of force development increased with temp in both muscle types (disparity between published studies will be discussed), having a more pronounced effect in cardiac muscle. TnC extraction from myocytes, by contrast, shifted the midpoint of the tension-pCa curve (pCa_{50}) less than removal of TnC from psoas. In addition, the temp-dependent shift in pCa_{50} was increased by extraction of TnC from psoas muscle. Based on these results, we conclude that pCa_{50} in both cardiac and skeletal muscles varies with maximum tension. Thin filament activation in cardiac muscle is less cooperative than in skeletal muscle, explaining the differential sensitivity of the two systems to the perturbations described here. Reducing thin filament activation in skeletal muscle by TnC extraction results in a temp response similar to that of control cardiac cells.

W-Pos514

CALCIUM BINDING AND CROSS-BRIDGE ATTACHMENT: EFFECTS OF STRETCH INDUCED CROSS-BRIDGE DETACHMENT AND STRAIN

E.B. Ridgway and A.M. Gordon, Depts. of Physiology and Biophysics, Medical College of Virginia, Richmond VA 23298 & Univ. of Washington, Seattle, WA 98195.

Stretch of an active barnacle muscle fiber during the declining phase of the calcium transient (measured with aequorin) causes an increase followed by a transient decrease in free Ca. There is a minimum stretch (>0.2% of muscle length) required to produce the increase. This and other data (Gordon and Ridgway, Biophys.J. 55:276a, 1989) imply that this extra Ca is from activating sites accompanying cross-bridge detachment with stretch. Additional studies show that the amplitude of both the increase and decrease in Ca with stretch are enhanced as the stimulus intensity is increased. If the muscle fiber is allowed to shorten so that force falls to zero, stretches of the fiber at different times during the subsequent redevelopment of force show that both the increase and decrease in Ca with stretch are depressed immediately after the shortening but redevelop toward the control level as force redevelops. This suggests that the transient decrease in Ca with stretch is not just due to an enhanced Ca binding with increased length, but is related to enhanced strain in reattached cross-bridges. Our data support the hypothesis that attached cross-bridges enhance Ca binding to the troponin activating sites and that strained cross-bridges further enhance this binding. (Supported by NIH grants NS08384, AM35597 and the Virginia Heart Association.)

W-Pos515

SARCOMERES SHORTENED BY 1-3% PRODUCE 75% MORE FORCE THAN ISOMETRIC SARCOMERES.

Arie Horowitz and Gerald H. Pollack, Center for Bioengineering WD-12, University of Washington, Seattle WA 98195.

The force-length relation of tetanized, fixed-end fibers is higher than the linear descending limb of sarcomere-length clamped fibers, particularly at long sarcomere lengths. We have found that during tetanus at long lengths, fixed-end fibers contain sarcomere populations that undergo slight shortening. In order to verify if the shortening can account for the elevation of the force-length curve, we imposed small predetermined shortening on tetanized, sarcomere-length clamped fibers, and compared force levels before and after the shortening. Force was substantially higher after the shortening than before it. The increase in force was larger than predicted by the linear descending limb. We examined the dependence of the increase in force on the size, speed and timing of the shortening. Timing (0 to 1.2 sec after stimulus onset) and speed (0.2 to 1.2 μm per sarcomere per sec) had no effect on the amount of force increase. Shortening size (5 to 100 nm per half sarcomere), was the major determinant of the amount of force augmentation. The dependence was not linear: shortening by as little as 20 nm per half sarcomere produced the full force increase, while larger releases had almost no additional effect. This indicates that the augmentation mechanism is of a threshold-dependent nature, triggered by some minimal sarcomere shortening. The average force level after shortening from an initial sarcomere length of 3.2 μm was 75% larger than the force level predicted by the linear descending limb. Thus, the sarcomere-length clamped tetanus may reflect sub-maximal force generation.

W-Pos516

FORCE SUSTAINED BY FAST AND SLOW MUSCLES OF MICE DURING ISOMETRIC, MIOMETRIC AND PLIOMETRIC CONTRACTIONS.
John A. Faulkner and Susan V. Brooks, Bioengineering Prog., Univ. of Michigan, Ann Arbor, MI 49109-0622

We have demonstrated that at optimum velocities of shortening for maximum power and optimum duty cycles for sustained power, fast muscles sustain a greater power (W/kg) than slow muscles (Biophys, J. 51:467a, 1987; 53:570a, 1988). We have now tested the hypotheses that forces (F_m, N/cm^2) sustained by slow muscles are greater than those sustained by fast muscles during repeated isometric contractions, pliometric contractions, and miometric contractions. Velocities of shortening were optimum for development of maximum power by slow muscles. For each of the three protocols, F_m of both fast and slow muscles was measured during contractions at a frequency of stimulation that produced 85% of maximum force (F_o). Isometric contractions were performed after a quick stretch to bring the F_m rapidly to 85% of F_o. Pliometric contractions were initiated after isometric development of 85% of F_o. Isovelocity lengthening was at 0.25 L_f/s through 10% of L_f to prevent contraction-induced injury. Miometric contractions occurred during isovelocity shortening at velocities of 2.0 L_f/s through 10% of L_f. At the optimum duty cycle for sustained F_m, the F_m sustained by slow muscles during isometric (2.5 N/cm^2) was more than two-fold greater than that sustained by fast muscles. In contrast, during pliometric (4.5 N/cm^2) and miometric (0.55 N/cm^2) contractions sustained F_m of fast and slow muscles were not different. NIH AG-06157.

W-Pos517

THE TRANSITION FROM THE ISOMETRIC STATE TO STEADY SHORTENING IN RABBIT SKINNED FIBERS
K. Burton & R.M. Simmons. Department of Biophysics, King's College London, 26-29 Drury Lane, London WC2B 5RL, England.

The timecourse of changes in mechanical properties of a muscle fiber during shortening has been studied using step and ramp length changes to simulate isotonic releases. The shortening was terminated by a test step, here a rapid restretch to the original length (Brenner, B. (1983), Biophys. J. 41:99-102) at different times following the start of the release. The response to the test step was a spike of tension, followed by a minimum level (T_m) and a slow recovery (4-7 s^{-1}, k_r) to the original isometric value. Both T_m and k_r decayed during shortening with a similar time dependence. For tensions of 0-30% P_o during shortening, the time dependence of T_m and k_r was roughly proportional to velocity such that the two quanitities approached completion after shortening of about 4-5.5% (45-60 nm per half sarcomere). The results suggest that the distribution of cross-bridge states takes the equivalent of several (conventional) throws to reach a shortening steady state.

W-Pos518

THE SARCOMERE LENGTH-TENSION RELATION OF SINGLE FROG MUSCLE FIBERS DURING SHORTENING.
DR Claflin, DL Morgan* and FJ Julian, Dept. Anesthesia Research, Brigham & Women's Hospital, Boston, MA 02115; *Monash University, Australia.

A cornerstone of the sliding filament theory for muscle contraction (SFT) is that force (F), measured under length-clamp conditions, linearly decreases with increasing sarcomere length (SL) above plateau values for SL. This shows that F output is determined by the number of cross-bridges attached. It is not possible simply to stretch a fiber to increase the SL, since this produces gross nonuniformity in SL with the ends having a shorter SL than the middle. Stimulation in this case leads to an initial rapid rise of F followed by "creep", a slowly progressive increase in F. Creep is produced by continued shortening of the shorter sarcomeres (S) stretching the longer ones. That is, because of the marked change in slope in the F-speed relationship about the isometric point, the F measured is more nearly equal to the (increasing) isometric capability of the shortening S than the lengthening S. Length-clamping reduces creep by reducing SL nonuniformity. We report here a new technique to significantly reduce the effect of nonuniformities on tension by applying shortening length ramps to remove the complication of lengthening S. Ramps were applied to living single fibers from frogs, both early (500ms) and late (1500ms) in a fixed-length tetanic contraction, at rates of 10, 20, 30 & 50% of unloaded shortening speed. For each speed, F's measured during shortening were a linear function of SL over the range tested (2.3-3.0μm), and were scaled versions of the classic relationship. Furthermore, in contrast to fixed-length contractions, F's measured during ramps were independent of the time the ramp was applied. These results strongly support the SFT and the explanation for creep given above. Support: NIH grants AR07972 (DRC) and HL35032 (FJJ).

W-Pos519

FILAMENT ELASTICITY IN SKINNED SKELETAL MUSCLE FIBERS OF THE FROG.
DWG Jung, T Blangé, BW Treijtel; Physiol. Dept., Univ. of Amsterdam, Netherlands.

The force of isometrically contracting skinned muscle fibers can be varied by alteration of the Ca^{2+} concentration. It appears from model simulations of tension transients of activated fiber segments that the relation of elastic moduli and isometric force is predominantly linear. This is compatible with the idea that the number of cross-bridges increases with increasing isometric force. However, the behaviour of the immediate stiffness suggests that, at least partially, the source of compliance related to this stiffness has to be sought outside the cross-bridge. Furthermore, the elastic impedance of relaxed fibers and low-tension activated fibers increases smoothly with the square root of the frequency. This suggests that in these cases filament elasticity and viscous friction determine the tension response of the sarcomere at fast changes of length. Simulations of the elastic impedance with a model in which filament compliance was incorperated did indeed consistently give better fits in case of relaxed fibers.

W-Pos520

CYTOTOXIC T-CELL & TARGET CELL INTERACTION: ANALYSIS OF MICROMANIPULATION DATA, Aydin Tozeren, K.L.P. Sung & Shu Chien, BMED Program, The Catholic University of America Wash.DC, and the Dept. of AMES, Univ. of California, San Diego.

In our micromanipulation experiments, adhesive energy density between a cytotoxic T-cell (F1, HLA-DR_{W6}) and its target cell (JY:HLA-A2, B7-DRY, W6) increased with the extent of forced disaggregation. In the analysis of this data we have assumed that (1) crossbridges responsible for adhesion attach and detach in a biochemical cycle and (2) are laterally mobile in the plane of the membrane. Adhesive energy density is a measure of the force produced by cross-bridges at the zone of separation. We have solved numerically a set of partial differential equations of parabolic type to determine the density distributions of attached and unattached crossbridges as a function of time and extent of separation. Our numerical experiments show that crossbridge diffusivity and rate of detachment are the two important parameters that effect crossbridge accumulation in the region of conjugation. If crossbridges become immobile when attached, they accumulate at the edge of separation and form a ring as observed in erythrocyte aggregation in the presence of lectins.

W-Pos521

DEVELOPMENTAL TRANSITION IN MYOCARDIAL TROPONIN-T (TnT) ISOFORMS CORRELATES WITH A CHANGE IN CA^{2+}-SENSITIVITY. P.J. Reiser, M. Westfall, R.J. Solaro. Dept. Physiology & Biophysics, Univ. of IL, Chicago, IL 60680.

Recent studies suggest a functional role of TnT in modulating Ca^{2+}-sensitivity of tension production in skeletal muscle. Several reports also show transitions in TnT isoform expression in developing myocardium. The objective of the present study is to ascertain possible changes in the Ca^{2+}-sensitivity of developing mammalian myocardium by comparing tension/pCa relationships in 4 day neonatal and adult rat myocardium at known sarcomere length (1.95-2.05 μm). Tension as a function of $[Ca^{2+}]$ was measured in skinned Purkinje strands and ventricular trabeculae. The neonatal tension/pCa relationship is shifted to higher pCa values by ~0.4 pCa unit at pCa_{50} relative to the adult curve, correlating with a change in TnT from neonatal to adult forms on SDS-PAGE and Western blots using a TnT-specific mAb. Thus, as for skeletal muscle, developmental transitions in TnT isoforms correlate with altered Ca^{2+}-sensitivity of the myocardial tension-generating apparatus. Supported by NIH grants HL-22231 & AR-39652.

W-Pos522

Novel steady-state and pre-steady state kinetics of GTP and ITP hydrolysis by cardiac myosin-S1 and actomyosin-S1. Betty Belknap, Jeanne McDowell, and Howard White, Dept. of Biochemistry, E. Virginia Medical School, Norfolk, Va. 23507.

We have measured the pre-steady-state nucleoside triphosphate hydrolysis of ITP and GTP by bovine cardiac myosin-S1 and acto-myosin- S1. The steady-state hydrolysis of these nucleosides has an unusual dependence upon [actin] that reaches a maximum at relatively low actin concentrations and decreases at higher concentrations of actin The magnitude of the phosphate burst for ITP and GTP are less than 0.1 Pi/myosin-S1. The rate of hydrolysis of GTP and ITP measured in single turnover experiments by bovine cardiac myosin-S1 and acto-myosin- S1, [S1] >> [NTP] are equal to those measured during steady-state hydrolysis. These results indicate that the predominant steady-state intermediate present during the hydrolysis of ITP and GTP are (A)M-(I or G)TP. These results are consistent with the view that a signficant steady-state concentration of AM-NDP-P is required for optimum force development in muscle. This work was supported by grants from NIH, AHA and MDA.

W-Pos523

A Video Cartoon Illustrating the Dynamic Interaction between Actin, Myosin and ATP in Muscle . Howard D. White, Dept. of Biochemistry, Eastern Virginia Medical School, 700 Olney Rd., Norfolk Va 23501.

A computer generated video cartoon will be shown that illustrates the dynamic interaction of actin, myosin, ATP and ADP in a relaxed muscle, isometically contracting muscle, and in muscle contracting at different shortening velocities. The equilibrium constant of the nucleoside triphosphate hydrolysis (A)M-ATP <=> (A)M-ADP-P, the rates of conversion from weakly attached to strongly attached crossbridge states (A)M-ADP-P --> AM-ADP and conversion from strong attached to weakly attached states AM-ADP --> AM --> (A)M-ATP can be varied. Maximum shortening velocity may occur when a sufficiently large number of crossbridges remain tightly bound at the end of the power stroke and produce force opposing the direction of motion. The cartoon illustrates why ADP dissociation from an attached crossbridge rather than the maximum rate of ATP hydrolysis is likely to be the molecular step that limits the maximum shortening velocity. This work was supported by grants from the NIH, AHA and the MDA.

W-Pos524

SHORTENING DEACTIVATES NORMAL BUT NOT HYPERTROPHIED MYOCARDIUM. **B. B. Hamrell, Department of Physiology and Biophysics, College of Medicine, University of Vermont, Burlington, VT 05405.** Short myocardial sarcomere lengths (SL) reduce activation. The slope of a SL-force relationship (SL-P) depends on this inactivation. In contrast, shortening deactivation is characterized by a shift to a new, lower SL-P due to sarcomere shortening (SL-$P_{\delta SL}$). Shortening probably affects thin filament regulatory protein function. If new regulatory protein species appear with pressure overload hypertrophy (POH) effects of shortening may change. I measured SL with laser diffraction[1] (λ = 632.8 nm) of thin rat right ventricular trabeculae at 28°C and 0.2 Hz stimulation. The rats with POH (n = 10) had pulmonary artery constriction for 2 weeks[1]. Resting SL (SL_{rest}) in the normals (n = 8) ranged from 2.13 to 2.53 μm and 2.11 to 2.41 μm in POH. I used a servomotor to produce a shortening ramp followed by a constant shorter muscle length. SL_{rest} was set with a shortening ramp before a twitch. Then peak isometric P and SL were measured to get SL-P. I introduced a shortening ramp during the first 1/3 of contraction and measured redeveloped peak isometric P and SL to get SL-$P_{\delta SL}$. In the normal hearts, SL-$P_{\delta SL}$ was significantly depressed below SL-P such that force decreased by 50± 6% (SEM) at a SL. SL-$P_{\delta SL}$ was not depressed in POH. SL-P and SL-$P_{\delta SL}$ in normal and POH were independent of laser beam location along a muscle and which first order maximum was studied. Therefore, there is shortening deactivation as well as length dependent inactivation in normal cardiac muscle. The absence of shortening deactivation in hypertrophy may be related to variations in thin filament regulatory protein species, which are being characterized.

1. Hamrell/Hultgren, Fed Proc (1986) 45: 2591-2596. Supported in part by HL21182, 31260 and 28001, and the Vermont Affiliate, AHA.

W-Pos525

EFFECTS OF TEMPERATURE ON CA^{2+} AND MG^{2+} DISSOCIATION RATES FROM FROG PARVALBUMIN (PA). T.-t. Hou, J.D. Johnson* and J.A. Rall. Departments of Physiology and Physiological Chemistry*, Ohio State University, Columbus, OH 43210.

Ca^{2+} and Mg^{2+} off rates from PA IV_b were determined from fluorescence stopped flow measurements of the time course of Tb^{3+} binding to Ca-PA or Mg-PA in 20 mM MOPS, 150 mM KCl, 0.07 mM β-ME, pH 7.0 at 20, 10 and 0°C. Rates shown below are based on mono-exponential fits to data. At 20°C time course of Mg^{2+} dissociation was better fit (i.e., 44% less normalized variance) by a sum of two exponentials with about equal amplitudes and with rate constants of 9.4 and 1.8 s^{-1}.

	$k_{off}(Ca)$ s^{-1}	Q_{10}	$k_{off}(Mg)$ s^{-1}	Q_{10}
20°C	1.04		3.40	
		2.3		1.9
10	0.46		1.76	
		2.4		1.9
0	0.19		0.93	

These results are consistent with the suggestion that PA acts as a soluble relaxing factor in frog skeletal muscle. Support by NIH AM20792.

W-Pos526

MECHANISM OF THE LENGTH-DEPENDENCE OF Ca^{2+}-SENSITIVITY IN STRETCHED MUSCLE: IMPLICATIONS FOR STARLING'S LAW OF THE HEART

Jagdish Gulati and Arvind Babu
Albert Einstein Coll Med, Bronx, NY 10461

We have previously shown that the length-dependence of Ca^{2+}-sensitivity of muscle is greater with cardiac TnC than skeletal TnC, directly implicating TnC in the length-transduction mechanism underlying Starling's law of the heart. Effort is now directed to find how TnC senses the sarcomere length change. We test the hypothesis that cross-bridge number modulates the length-dependence of Ca^{2+}-sensitivity. In one study, partially TnC extracted rabbit psoas fibers (to 50% P_o) were used. The length-dependence was found to be unaltered with partial extraction. Secondly, we compared the results between the two TnCs at full and partial filament overlaps in unextracted fibers. The increase in sensitivity for unit length was found to be reduced to 60% at partial overlap compared to that at full overlap. But, the increment with cardiac TnC over skeletal TnC was found to be similar for both overlaps. These results provide further support for the idea that TnC acts as a length sensor and that cardiac TnC is a better sensor than skeletal TnC. The findings also exclude the hypothesis that active cross bridge number is a major mechanism of length transduction in Starling's law. [Supported by NIH]

W-Pos527

DYNAMIC MECHANICAL PROPERTIES OF RELAXED SINGLE CARDIAC FIBERS FROM *CANCER MAGISTER*.

Edgar Meyhofer, Department of Zoology, University of Washington, Seattle, 98195.

Most research on muscle mechanics indicates a very low or negligible viscosity. But recent evidence for rapidly extended fibers suggests that much higher viscosity exists and is required for mechanical stability. Perhaps such high viscosity is not necessary in slowly contracting muscles. To test this hypothesis, I measured the mechanical properties of single cardiac fibers. My model system is large, mechanically dissected single fibers (app. 50 µm diameter, 1000 µm long) from the crab, *Cancer magister*. The elasticity and viscosity were determined from force measurements of relaxed fibers exposed to small (<1.0%) sinusoidal length changes over a wide range of frequencies and sarcomere lengths (0.1-50 hz, 3.6- 6.2 µm). Their total stiffness increases by more than 100-fold in that sarcomere length range, from about 0.01 to 1 MPa, and rises only 3 to 5-fold in that frequency range. The relative energy dissipation (ratio of viscosity to elasticity) decreases monotonically with greater sarcomere lengths and lower frequencies. In the physiological range of frequencies (1-5 hz), strains (0.1 - 0.2) and sarcomere lengths (3.6-4.3 µm) this ratio is about 0.5. I conclude that this viscous component contributes a significant portion of the overall mechanical behavior of cardiac fibers. The values within this physiological range are equivalent to those found for the rapid fiber type. Also, the dissipation is larger at lower frequencies, despite the fact that the total stiffness and viscosity are nearly identical in these cell types. (Supported by the Whitaker Foundation to T. Daniel)

W-Pos528

DEVELOPMENTAL CHANGE IN CONTRACTILE RATE OF CARDIAC MYOFILAMENTS AND EFFECT OF ISOPROTERENOL ON THEIR RATE. T. Shibata, S. Imamura, R. Matsuoka, and A. Takao. Tokyo Women's Medical College, Tokyo, Japan

We studied developmental changes in contraction speed and myosin isozymes of rabbit myocardia and effects of isoproterenol (ISP) on crossbridge kinetics. Ba^{2+}-contracture(24°C) was induced in 4 groups of papillary muscles: (A)0 day-, (B)1 week-, (C) 1 month-, and (D)4 month-old rabbits. Frequency of minimum stiffness (f_{min}), which showed contractile rate of cardiac myofilaments, was determined from dynamic stiffness spectrum (0.05-30 Hz) which was obtained by sinusoidal length perturbations before and after addition of 10μM ISP. The relative amounts of myosin isozymes were analyzed. V1 isozymes of A, B, C, and D were 32±9%, 57±10%, 48±9%, and 22±9%, and f_{min}'s were 1.8±.1 Hz(n=5), 2.2±.1Hz(n=5), 1.9±.2Hz(n=5), and 1.2±.2Hz(n=6), respectively. Linear correlation of Y(Hz)= .02X(%)+.9 (r=0.82) was obtained. ISP increased f_{min}'s of C and D to 108% and 120% of control, respectively, whereas those of A and B were not increased. We concluded that contractile rate significantly varied with development relating to the isozymic pattern of myosin and that the rate was not affected by ISP during newborn period.

W-Pos529

ACCUMULATION OF MITOCHONDRIAL CREATINE KINASE (MiCK) AT PARACRYSTALLINE INCLUSIONS IN MITOCHONDRIA OF ADULT RAT CARDIOMYOCYTES

Riesinger, I., Eppenberger-Eberhardt, M., Schwarb, P., Messerli M., Eppenberger, H.M. and Wallimann, T., Inst. Cell Biol., ETH, CH-8093 Zürich, Switzerland.

Adult rat cardiomyocytes cultured in essentially creatine-free medium for ten days show a varying number of elongated and enlarged mitochondria preferentially arranged in a perinuclear fashion as judged by confocal microscopy (Eppenberger et al., 1989). When exposed to monoclonal anti-MiCK antibody followed by rhodamine-conjugated second antibody, a stronger fluorescence could be observed within these elongated mitochondria as compared to the small round mitochondria also present in the cells. TME of high-pressure frozen and freeze-substituted cardiomyocytes embedded in Epon showed paracrystalline inclusions within the elongated mitochondria, similar to mitochondria of skeletal muscle under ischemia or after feeding animals with the creatine analogue GPA (Hanzlikova & Schiaffino, J. Ultrastruct. Res. 60, 121, 1977; Ohira et al., Jap. J. Physiol. 38, 159, 1988). Postembedding immunogold labelling using polyclonal anti-MiCK antibodies revealed a specific localization of MiCK within the paracrystalline structures suggesting to be one of the major components. These results may point to a compensatory accumulation of MiCK at the mitochondrial inclusions as a consequence of metabolic stress (creatine deficiency).

W-Pos530

NUCLEAR DENSITY IN ISOLATED SINGLE RAT SKELETAL MUSCLE FIBERS WITH RESPECT TO FIBER TYPE. B.S. Tseng, C.E. Kasper and V.R. Edgerton. School of Nursing and Dept. Kinesiology, UCLA, Los Angeles, CA 90024.

Intact skeletal muscle fiber segments from soleus and plantaris muscles of adult female rats were mechanically dissected in a relaxing solution and divided into three pieces for histochemical analysis (S.K. Donaldson, 1984). Two pieces were used for determination of fiber type; either fast or slow as demonstrated by both myosin ATPase @pH 4.4 and 10.4 pre-incubations. The third fiber piece was stained with H & E for determination of the number of nuclei, estimated fiber volume and sarcomere spacing. In order to count only the sub-sarcolemmal nuclei, fiber segments with extraneous fiber debris or disrupted sarcolemma were excluded from this study. Cytoplasmic volume (μm^3) / nucleus differences were found to be significant ($p \leq 0.01$) between the fast and slow fibers (139,116 ± 13,541 SEM vs. 71,843 ± 5776 SEM respectively). Furthermore, significant ($p \leq 0.01$) fiber type differences were found in the number of sarcomere lengths per nucleus (5.98 ± 0.38 SEM in fast versus 3.40 ± 0.21 SEM in slow fibers.) Results of volume / nucleus and sarcomere lengths / nucleus may be interpreted to be theoretical nuclear control domains and are consistent with data from previous biochemical studies that have shown that slow muscles have higher [DNA] than fast. Since lower threshold motor units with slow skeletal muscle fibers are recruited tonically, we interpret our results to reflect a higher protein turnover rate and smaller nuclear control domain necessary for cell maintenance in the slow versus the fast fibers. (supported by NIH:NCNR& NIAMS)

W-Pos531

REDUCTION OF CONTRACTION AND DYNAMIC STIFFNESS OF SINGLE FROG VENTRICULAR HEART CELLS BY HIGH FREQUENCY LENGTH OSCILLATIONS. Leslie Tung and Sanjay Parikh, Department of Biomedical Engineering, The Johns Hopkins University, Baltimore, MD 21205

The dynamic stiffness of muscle is assessed by applying low amplitude length perturbations, which are assumed not to alter the stiffness. Unlike skeletal muscle, the mechanical properties of single cardiac muscle cells have only recently been investigated. In this study, we used a force-fiber technique to apply 100 Hz sinusoidal length oscillations continuously to enzymatically isolated, single frog ventricular heart cells, and to measure the force of contraction and dynamic stiffness of the cell at different resting lengths and stimulus rates. Oscillations were graded in amplitude up to about 2% of the resting cell length, and cells were paced continuously at 0.2-0.8 Hz. Oscillation amplitudes less than 0.2% were sufficient to lower twitch contraction and active stiffness. Higher amplitudes of oscillation decreased force and stiffness monotonically. In contrast, resting force and stiffness were unchanged over the entire range of oscillation amplitudes tested. The simultaneous reductions in twitch force and active stiffness by the high frequency oscillations of cell length are consistent with a reduction in the number of active crossbridges, and the constancy of the resting force and stiffness confirms that these properties arise from structures which are activation independent.

W-Pos532

AFTER-LOADED AND QUICK-RELEASED FORCE-VELOCITY RELATIONSHIPS OF FROG SKELETAL MUSCLES. Brian M. Block, and John A. Faulkner, Dept.of Physiol., University of Michigan, Ann Arbor, MI 48109-0622

For mouse soleus muscles, the stimulation frequency which produces maximum tetanic force (F_0) generates submaximum shortening velocities at any given load, whereas the frequency for maximum rate of force development (dF/dt_0) produces maximum shortening velocities. We hypothesized that the force-velocity relationship of amphibian muscle would be similarly dependent on stimulation frequency. Frogs (*Rana Pipiens*) were anesthetized on ice. Semitendinosus muscles were excised, placed in gassed Ringers solution at 20°C, and tied to the lever arm of a servomotor and a fixed post. Stimulation was through platinum electrodes. The stimulation frequencies of 150Hz and 350Hz, which produced F_0 and dF/dt_0 respectively, were used to generate isotonic shortening contractions to measure velocities at ten loads between 0.025 and 0.50 F_0. Velocities were determined during isotonic after-loaded contractions at 150 Hz and 350 Hz stimulation and by quick releases from 0.90 F_0 to the various loads. Shortening velocity at any load and maximum velocity of unloaded shortening (V_{max}) were not different among protocols (V_{max} = 5.49 ± 0.55). We conclude that unlike mammalian muscles wherein the frequency of stimulation that produces F_0 does not fully activate all cross-bridges until force is almost maximum, amphibian muscles are fully activated by this frequency of stimulation early in the contraction. NIH HL-34164.

W-Pos533

RELENGTHENING FROM RIGOR OBSERVED IN ISOLATED CARDIAC MYOCYTES AFTER PHOTORELEASE OF ATP. E. Niggli and W.J. Lederer, Department of Physiology, University of Maryland, School of Medicine, 660 W. Redwood St., Baltimore MD 21201

Relengthening from rigor contractions of skinned isolated myocytes is slow ($\tau \approx$ several seconds). This has been attributed to delays of solution exchange and diffusion of ATP into the acto-myosin lattice under conditions of ATP consumption (see Nichols C.G., Lederer W.J., Can. J. Physiol. (in press)). We have applied concentration jumps of ATP ($\tau \approx 3$ ms) by photorelease from NPE-caged ATP to observe the passive relengthening properties of intact unloaded myocytes. Rigor contractions were induced by metabolic inhibition in the presence of 10 mM deoxy-glucose and 2 mM NaCN. Individual cells were loaded with 2 mM NPE-caged ATP via giga-seal pipette. Sarcomere-length or cell-length was recorded with a laser-diffraction system or a CCD-video camera and a video dimension analyzer. At cell lengths around 60% of the resting cell length (corresponding to unresolvable sarcomere-lengths of ≈ 1.1 μm) relengthening was found to be as slow as observed after bulk solution changes, despite the rapid concentration change of ATP. However, if ATP was released early during the rigor-contracture (at sarcomere-lengths between 1.8 and 1.6 μm, corresponding to the range prevailing during twitch contractions), passive relengthening was rapid ($\tau \approx 100$ ms) and could be described by a mechanical model incorporating an exponential decay of the rigor force, a compressed elastic element, a viscous damping element and an accelerated mass. We conclude that relengthening of myocytes from severe rigor may be slow due to damage to structural elements inside the cell, whereas relengthening from intermediate sarcomere-lengths is elastic and may provide information about the underlying relengthening forces inside the cell.

W-Pos534

SARCOMERE DYNAMICS IN CAT CARDIAC TRABECULAE; P.P. de Tombe and HEDJ ter Keurs, University of Calgary, CANADA.

The purpose of the present study was to desribe sarcomere dynamics in cat myocardium. Thin trabeculae were dissected from the right ventricle of kittens, mounted in an experimental chamber perfused with a Krebs-Henseleit solution (25C) at varied Ca^{++}. Sarcomere length (SL) was measured by laser diffraction techniques. Slack SL was 1.9 um, passive force (F) increased steeply at SL>2.4 um. Twitch F (F_o)-SL releations were curved concave and convex towards the abcissa at Ca^{++}=6.0 mM and 1.5 mM, respectively. Unloaded velocity of SL shortening (V_o) was constant from 200-300 ms. Both V_o (at 200 ms) and F_o were sigmoidal functions of Ca^{++}; Maximum V_o was 9.8±0.2 um/s. EC_{50} of V_o and F_o was 1.1±0.1 and 1.7±0.5 mM, respectively. F-V relations (Ca^{++}=1.5 mM) were fitted to Hill's hyperbola; Parameter 'a' was 9.7±2.2 %F_o; 'b' was 0.6±0.6 um/s; Vo was 6.5 um/s. V_o was constant at SL>1.9 um and proportional to SL below 1.9 um, at Ca^{++}=6.0 mM. In contrast, V_o was proportional to SL between 1.7 and 2.2 um at Ca^{++}=1.5 mM. These result are comparable to our previous results in rat myocardium, although cat myocardium is less sensitive to Ca^{++}, maximum V_o is 20% lower, and twitch kinetics are 50% slower.

W-Pos535

STIMULATION OF MUSCLE BY HIGH FREQUENCY AND INTENSITY.

Jan P. Koniarek
Columbia Univ., Department of Ophthalmology. 630 W. 168th St., New York, NY 10032, USA.

Stimulating an isometrically held skeletal muscle by a train of high freq. (2000 Hz) and higher than normal intensity pulses or by a long DC pulse elicits a triphasic tension response (arrow) unlike a twitch or a tetanus. An initial rapid rise of tension to about 0.3 P_o is elicited by two or three action potentials. Subsequently steady tension is maintained, but the membrane remains electrically quiescent. After stimulation a final tension increase is generated via anode break excitation.

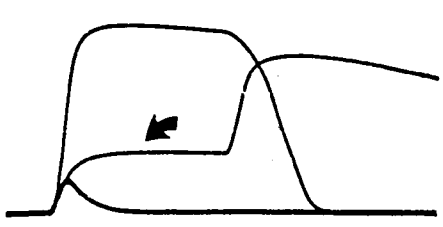

Supported by a Rockefeller Clinical Res. Grant.

W-Pos536

THE ENDOMYSIUM IS A SERIES-ELASTIC ELEMENT IN SKELETAL MUSCLES WITH LONG FASCICLES AND IN ARTERIAL SMOOTH MUSCLE.

J.A. Trotter and L.J. McGuffee, Depts. of Anatomy and Pharmacology, Univ. of New Mexico School of Medicine, Albuquerque, NM 87131.

Skeletal muscles with fascicles longer than a few cm. consist of fibers with tapering intrafascicular endings (Loeb et al. ('87) J.Morph.191:1). Tension is transmitted across the membrane at the tapered ends (Trotter, 1990a, Trans.Orthop.Res.Soc. 36). The absence of myo-myous junctions in these regions and the constant presence of collagenous endomysium indicates that the endomysium transmits tension between muscle fibers. Vascular smooth muscle also consists of tapered muscle cells lacking significant intercellular mechanical junctions and separated by connective tissue (CT). Analysis of these tissues by scanning EM (Ohtani et al., ('88) Arch.Histol.Cytol.51:249) and by transmission EM has shown that the intercellular CT is a continuous network of isotropically arranged collagen fibrils. This fibril arrangement is well suited to elastically transmit shearing loads between contracting muscle cells. [Supported by NIH grants AR39922 (JAT) and HL37015 (LJM)].

W-Pos537

Immunofluorescent Localization of Dystrophin in Smooth Muscle. D. G. Ferguson*, I. E. Gillette*, L. Kao+, J Krstenansky# and Eric Gruenstein+. Physiology and Biophysics*; Molecular Genetics, Biochemistry and Microbiology+, University of Cincinnati; Merrell Dow Research Institute#.

Previous immunofluorescence localization studies from several laboratories suggest that dystrophin is found only in close proximity to the sarcolemma in skeletal muscle. Immunogold EM localization studies have suggested that dystrophin is also associated with the T-system (Watkins et al, Nature 333:863). A polyclonal antibody has been raised against an oligopeptide based on the predicted sequence of dystrophin (Kao et al, PNAS 85: 4491). We have affinity purified this antibody and used it to immunolocalize dystrophin in skeletal and smooth muscle. Our experiments with skeletal muscle tissue confirm that dystrophin is apparently abundant in the subsarcolemmal region. However, a cytoplasmic tubular network was also heavily labeled. Our studies with smooth muscle indicate that dystrophin is very abundant in this tissue. Both gastric and vascular smooth muscle tissues were much more heavily labeled than was identically treated skeletal muscle tissue. In control studies, skeletal and smooth muscle tissues from C57B normal mice were heavily labeled but skeletal and smooth muscle tissues from MDX mice were unlabeled.

W-Pos538

LATERAL STIFFNESS OF SARCOMERE DECREASES GREATLY IN CONTRACTION

Tatsuo Iwazumi, University of Calgary, Calgary, Alberta, Canada T2N 4N1

The myofibrils were obtained from bullfrog atrial cells by mechanical dissection. Their widths were 2-4 μm and their mounted lengths were 10-20 sarcomere long. The lateral stiffness was measured by two 5 μm dia. carbon fibers placed across the diameter of the sarcomere. One carbon fiber was attached to an actuator to apply synthesized white noises and another to a force transducer to detect transmitted vibrations. The white noise was synchronized to a spectrum analyzer allowing a measurement of a complete elastic transfer function covering 5-1000 Hz in just 0.2 s.

The lateral stiffness dramatically diminished when the sarcomeres were activated by calcium (pCa 5.5-6.0) while the stiffness increased when they were exposed to a rigor solution (no ATP with same ionic strength).

The increased lateral stiffness in rigor is readily explained as cross-linking of the thick and thin filament. However, the diminution of the lateral stiffness in contraction cannot be explained by cross-bridge theory. Since the longitudinal stiffness increases in contraction, any theory of contraction must explain the fact that sarcomere stiffness increases in the axial direction while it decreases in the lateral direction at the same time. The only theory that explains this peculiar property of the sarcomere is that of Iwazumi (1970) as one of the intrinsic physical properties of a hexagonal dipole array. Supported by the MRC Canada.

W-Pos539

ANALYSIS OF STOCHASTIC FLUCTUATIONS IN CROSS-BRIDGE SYSTEMS. E. Pate and R. Cooke Depts. Math., WSU & Biochem./Biophys., UCSF

The stochastic nature of the actomyosin interaction should result in force fluctuations. We investigated the tension fluctuations predicted by the Huxley (1957) model. Fractional fluctuations become greater as the number of cross-bridges decreases. Recently, tension measurements have been made on single actin filaments attached to a flexible rod interacting with fewer than 50 cross-bridges. Our analysis shows that in spite of the small number of cross-bridges, the fluctuations in tension are small due to damping within the system. The system is damped because the tension decrease caused by release of one cross-bridge is largely taken up by other cross-bridges that are stretched as the flexible arm relaxes to its new equilibrium position. With only 15 cross-bridges and an arm with a stiffness of 0.6 pN/nm, the expected fluctuation in tension is only 10%. The expected fluctuations of thick filament position within a sarcomere were also analyzed. At full filament overlap, stability remained high with most thick filaments remaining in the center of the sarcomere after 15 seconds. At longer sarcomere lengths stability is only obtained in the presence of a restoring elastic element. Supported by USPHS grants HL32145 (RC) and AR39643 (EP).

W-Pos540

EFFECTS OF HALOTHANE ON MAXIMAL UNLOADED VELOCITY OF SHORTENING (MUVS) AND INTRACELLULAR Ca^{2+} TRANSIENTS IN MAMMALIAN CARDIAC MUSCLE.

E.G. Carton, L.A. Wanek, and P.R. Housmans. Depts. Anesth. and Pharmacol., Mayo Fdn. Rochester, MN 55905.

MUVS and $[Ca^{2+}]_i$ transients detected with aequorin were measured in right ventricular ferret papillary muscle (30°C, 0.25 Hz) with and without halothane(0.5-1.5% v/v). During shortening at zero load there was no difference between the time to peak light and MUVS. Light maintained its peak level for 20-30 ms after MUVS in 4 of 5 muscles. Halothane 1% decreased MUVS from 1.92±0.31 (mean±SD) to 0.99± 0.21 Lmax/s, and decreased peak light to 21.6±11.7% (n=5) of control. The upstroke of the aequorin signal correlates with muscle acceleration at zero load (r^2= 0.89, n=14) with or without halothane, so that the rate of rise of $[Ca^{2+}]_i$ may be an important determinant of MUVS. Support: Mayo Foundation and GM 36365.

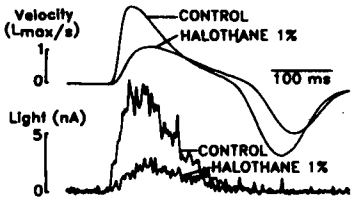

Velocity and aequorin signals of zero-load-clamped twitches.

W-Pos541

HALOTHANE (H), ENFLURANE (E) AND ISOFLURANE (I) DECREASE MYOFIBRILLAR Ca^{2+} RESPONSIVENESS IN INTACT MAMMALIAN VENTRICULAR MUSCLE.

P.R. Housmans, L.A. Wanek and E.G. Carton. Depts. Anesth. and Pharmacol., Mayo Fdn., Rochester, MN 55905.

The negative inotropic effect of H, E and I is mainly due to a reduction of intracellular Ca^{2+} availability. In addition, they may modify Ca^{2+} sensitivity of intact cardiac fibers as was shown in skinned fibers (Murat et al, Anesthesiology 69:892-899, 1988). Ferret right ventricular papillary muscle cells were injected with the Ca^{2+}-regulated photoprotein aequorin. $[Ca^{2+}]_o$ was raised to yield equal developed force in isometric twitches with H, E and I as in control twitches without anesthetic. At equal force, light signals representing $[Ca^{2+}]_i$ were higher in muscles exposed to anesthetic than in control. H, E and I may decrease myofibrillar Ca^{2+} responsiveness by increasing k_{off} of troponin C for Ca^{2+} and/or increasing the cross-bridge cycling rate. Support: Mayo Fdn. and GM 36365.

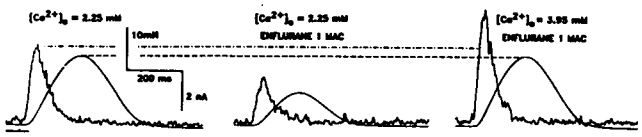

W-Pos542

THE RELATION BETWEEN SARCOMERE LENGTH AND STIFFNESS OF INSECT MUSCLE.

H. Granzier & K. Wang, Chem. Dept., U. of Texas, Austin, Tx., 78712.

To elucidate the mechanical function of elastic cytoskeletal proteins, we investigated the sarcomere length dependence of the steady-state and dynamic stiffness of insect muscle. Glycernated fibers were used, as were skinned fibers dissected from 'fresh' muscle to evaluate the effect of glycernation.

Fibers were dissected from flight and leg muscle of giant waterbug (*Lethocerus griseus)* and honey bee (*Apis mellifera*). Force, fiber length and sarcomere length were measured as described previously (Granzier et al., 1987, J.Muscle Res. Cell Mot., 8, 242). Steady-state force was measured after a ramplike slow stretch and a period of stress-relaxation. Dynamic parameters were measured by stretching the fiber sinusoidally (amplitude: 0.25% of the slack length; frequency range: 0.01-1000 Hz), and recording ensuing changes in force (stiffness) and its phase shift (viscous modulus).

The 'steady-state' stiffness of the dorsal longitudinal muscle of waterbug (PCa 9.5; PMg-ATP 2.3) reached a maximum at about 10% stretch, and remained constant or declined slightly thereafter. Results obtained with fresh and glycernated fibers were similar and confirmed findings by others on glycernated fibers (e.g. White, 1983, J.Physiol., 343, 311).

The dynamic stiffness increased linearly with frequency, with a distinct increase of slope at about 200 Hz. Stiffness increased with length until sarcomeres were about 10% longer than the slack length. The viscous modulus was sarcomere length dependent only at frequencies higher than about 50 Hz. The modulus decreased with prestretch until prestretch reached a value of about 10% of the slack length; the modulus increased thereafter. At all lengths tested, the viscous moduli were smallest at a frequency at about 10 Hz. The modulus approached zero at this frequency, indicating minimal dissipation of strain energy, i.e., fibers behaved purely elastic.

W-Pos543

IMMUNOLOCALIZATION OF NEBULIN IN THE SARCOMERE MATRIX USING MONOCLONAL ANTIBODIES TO FOUR DISTINCT EPITOPES.

Marlena Kruger, John Wright and Kuan Wang. Clayton Foundation Biochemical Institute, Department of Chemistry, The University of Texas at Austin, Austin, Tx. 78712.

Nebulin, a giant myofibrillar protein 600-800 kD that is abundant in a wide range of skeletal muscles, has been proposed to constitute a set of inextensible filaments anchored at the Z line (Wang and Wright, JCB 107, 2199). To evaluate this hypothesis, we have prepared a panel of eighteen monoclonal antibodies that are directed to four distinct epitopes of rabbit nebulin. Due to the weak immunogenicity of nebulin, immunization was done by splenic injection of highly purified, denatured nebulin. The selection of hybridomas to distinct epitopes was enhanced by a double screening with immunoblots of intact and CNBr and NTCB digests of nebulin as well as immunofluorescence of myofibrils.

Epitope localization studies using immunofluorescence and immunoelectron microscopic techniques on both isolated myofibrils and mechanically split muscle fibers indicated that (1) nebulin epitopes maintained a fixed distance to the Z line irrespective of the degree of stretch; (2) each nebulin polypeptide may extend at least 0.85μm from the Z line. Native nebulin is being purified to evaluate this proposal. These results support our earlier polyclonal antibody data and disagree with the claim of elastic stretch of nebulin by Furst et al. (JCB 106, 1563).

W-Pos544

STRUCTURAL MOTIFS OF NEBULIN AS PREDICTED BY PARTIAL SEQUENCES OF HUMAN NEBULIN cDNA. K.Wang, M. Knipfer, A. Osborn, K. Browning, X. Quian* and H. Stedman*, Dept. Chem. Univ. Texas at Austin, TX 78712 and Dept. of Anatomy*, Univ. Pennsylvania Medical School, PA 19104.

Nebulin, a giant myofibrillar protein in most vertebrate skeletal muscles, has been proposed to constitute a set of inextensible longitudinal filaments that are attached to Z lines and are coextensive with actin filaments (Wang & Wright ICB 107, 2199). To complement ultrastructural studies of nebulin, we set out to isolate cDNA clones encoding human nebulin, with the goals of establishing its primary structure and cellular function (Stedman et. al. Genomics 2 1). To date more than 20 kb of the 25 kb nebulin transcript has been cloned by cDNA walking. A total of 10 kb has now been sequenced, giving rise to two long open reading frames. Analysis of the deduced amino acid sequences indicated that (1) both are unusually basic, with pI's around 10; (2) both have a strong propensity for α-helices (~50%), and to lesser extent, for β-sheets (~30%); (3) most prolines are equally-spaced along the sequence with a 32 to 35 residue repeat; (4) the charge and hydrophobic profiles of both fragments exhibit two repeating motifs: a short repeat of 30-37 residues and a long repeat around 220 residues. We speculate that native nebulin is an elongated, highly basic fibrous protein with repeating domains and charge clusters at every ~35 residues along its length. This prediction has significant implications in the putative role of nebulin as a template for the actin filament in the sarcomere.

W-Pos545

THE TROPONIN-ASSOCIATED X-RAY REFLEXIONS FROM STRIATED MUSCLE.
Y.Maéda, D.Popp* and A.Stewart. EMBL at DESY, 2000 Hamburg 52, and *Max Planck Institute for med. Research, Jahnstr.29, 6900 Heidelberg, FRG (sponsored by G.Cecchi).

Striated muscles give rise to a series of reflexions indexed as orders (n) of 770 Å, the even orders being meridional while the odd orders being near-meridional. The reflexions from crustacean muscle have been assigned to extra mass of troponin (Tn) on the actin filaments (Wray et al.1978; Maéda et al.,1979; Maéda,1979,.*Nature* 277:670; Namba et al. 1980). In the present study, (1) the relations of Tn levels between adjacent thin filaments in muscles of different lattice types are elucidated, and (2) biphasic time courses of the intensity changes of these reflexions on activation of frog muscle are interpreted as indicating conformational change of Tn and S1 binding to the thin filaments.

(1) Frog muscle (lattice type 2:1 = thin:thick filament number ratio) gives rise to reflexions n=2,4 and 6 sharply sampled on the meridian, indicating that the levels of Tn are all aligned or staggered by 385 Å. On patterns from lobster fast and insect flight muscle (lattice type 3:1), n=2,4 are missing and n=6 is sampled, indicating the levels are staggered by 770/3 or 770/6 Å between adjacent thin filaments.

(2) Reflexions n=2,4 and 6 from live frog sartorius muscles show a biphasic intensity change during the tension rising phase of tetanic activation. A rapid intensity increase of 10 %, being completed by the time when tension rises to 10 % or less, is followed by a slow intensity decrease down to 50 %, which is associated with the tension rise. In both phases, lateral widths remain unchanged. We interprete the first phase as being caused by conformational change of Tn molecules on the binding of Ca^{2+}, while the second phase being due to direct contribution of the mass of S1 bound to the thin filament. These results indicate that the intensities of the Tn-associated reflexions are a measure of conformation of Tn as well as the binding of S1 to the thin filaments.

W-Pos546

CRYO-ELECTRON MICROSCOPY OF SCALLOP MYOSIN FILAMENTS.
Peter Vibert, Rosenstiel Center, Brandeis University, Waltham, MA 02254.

Native myosin filaments from scallop striated muscle that have been rapidly frozen in relaxing solutions appear to be well preserved in vitreous ice. Electron micrographs of these unfixed, unstained, hydrated filaments were recorded with an electron dose of 10 e/Å^2 on a Philips EM420 using a Gatan cryo-holder at -177°C protected by a Gatan anti-contaminator. A set of images was recorded at 1.5μ defocus, which should emphasize features at about 35 Å resolution. After filament images were straightened by spline-fitting, some transforms showed peaks above background to 24 Å axially and radially, close to the first zero of the contrast transfer function. A preliminary set of layer lines to 27 Å resolution has been collected and corrected for background and for phase and amplitude contrast functions. Helical reconstructions show the myosin heads to be well separated from each other and from the filament backbone. In views perpendicular to the filament axis, individual pear-shaped heads are resolved. The two heads of each molecule appear to be splayed apart axially.

W-Pos547

MYOFIBRIL ASSEMBLY IN DROSOPHILA FLIGHT MUSCLE (IFM): MUTANTS AND DEVELOPMENTAL MODELS. Mary C. Reedy*, Cliff Beall@ and Eric Fyrberg@ *Cell Biol, Duke Univ,Durham,N.C. @Cell Biol, Johns Hopkins, Baltimore, Md.

EM observations of myofibrillar defects associated with mutations of IFM-specific actin or sarcomeric α-actinin genes reveal varying degrees of disruption of sarcomere assembly, especially affecting Z-lines. One site-directed actin mutation, Act88F$^{G6A/T}$, results in multilevel Z-lines, bypassed at the fibril periphery by untethered myofilaments. In the actin mutant Act88F^{I76Val}, peripheries of many Z-lines extend into stress-fiber-like appendages. In several α-actinin mutants, terminal sarcomeres and insertions are preferentially disrupted. Each of these assembly defects fits best with a different contending developmental model: new flight muscle sarcomeres are formed by transverse splitting of existing Z-bands (Auber), myofibrils assemble on stress-fiber templates (Holtzer), or new sarcomeres are added at the ends of the muscle (Goldspink). It is not known whether any of these models describe sarcomere assembly in IFM of Drosophila, since no modern ultra-structural studies of its development in vivo have been reported. We have conducted an EM study of the development of normal Dros. IFM, in order to establish a basis for evaluation of effects of single-site mutations on sarcomere assembly and function.

W-Pos548

THE KINETICS OF O_2 REDUCTION TO WATER BY PURIFIED CYTOCHROME C OXIDASE. B. Reynafarje, The Johns Hopkins Univ. School of Medicine, Baltimore, MD. Current address: NHLBI, NIH, Bethesda, MD 20892

Purified and fully reduced cytochrome c oxidase catalyzes the reduction of O_2 to water in 4 kinetically distinct phases, each of which correlates uniquely with changes in the redox poise of the enzyme. Both, the redox state and the rates of O_2 consumption depend on the concentration of the enzyme and its 3 substrates. Direct kinetic dependence on O_2 concentration is only observed at the beginning of the first phase. Abrupt impairments in the rates of O_2 consumption are associated with back-flow of electrons, net reduction of the oxidase and, depending on conditions, release of bound oxygen. Zero and first order rates of reaction are not strictly observed at any time after the first phase. It is postulated that the respiratory reaction takes place in a cyclic process in which the redox state of the enzyme and the rates of O_2 uptake oscillate with frequencies and amplitudes depending on the conformation of the enzyme and the concentration of protons, electrons and O_2 at its catalytic site.

W-Pos549

MITOCHONDRIAL LIPID PEROXIDATION: ROLE OF NADH AND SUCCINATE DEHYDROGENASES. M. Glinn*, S. Tsang*, L. Ernster# and C. P. Lee*, *Dept. Biochem., Wayne State Univ. Sch. Med., Detroit, MI & #Dept. Biochem., Univ. of Stockholm, Stockholm, Sweden.

In the presence of rotenone and either NADH or NADPH, ADP-Fe^{+3} induced O_2 consumption and malondialdehyde (MDA) formation in beef heart submitochondrial particles. With NADPH the titration curve was hyperbolic (Km = 100 μM); whereas with NADH it was biphasic, descending above 50 μM. Rhein enhanced both O_2 consumption and MDA formation supported by NADH, but not by NADPH. Succinate abolished the NADH/NADPH supported MDA formation. Succinate alone induced oxygen consumption, but not MDA formation. In the presence of TTFA (thenoyltrifluoroacetone), succinate supported MDA formation without the aid of ADP-Fe^{+3}. TTFA mimicked the effects of ADP-Fe^{+3} to a lesser extent in the NADH/NADPH systems. Butylated hydroxytoluene abolished MDA formation in all systems tested. Our data indicate: (A). The flavoproteins and/or non-heme iron sulfur centers of NADH and succinate dehydrogenases participate in the initiation of lipid peroxidation. (B). Initiation of peroxidation by NADPH differs from that by NADH. (C). Ubiquinol may inhibit MDA formation.

W-Pos550

IRON SULFUR CLUSTERS IN THE TWO RELATED FORMS OF the NADH-Q OXIDOREDUCTASE (COMPLEX I) IN NEUROSPORA CRASSA
D.C. Wang, U. Sackman*, H. Weiss*, and T. Ohnishi, Dept. Biochem. & Biophys., Univ. of Penn. Phila. PA 19104, * Dept. of Biochem., Univ. of Düsseldorf, FRG.

Recently Friedrich et al. (1) reported that N. crassa cells grown in the presence of chloramphenicol, a smaller form (13 subunits) of Complex I is synthesized in place of the normal large form (30 subunits). We have resolved EPR spectra of individual clusters by the redox titration and computer simulation. The large form contains four NADH reducible clusters (N-1, N-2, N-3, & N-4). In the chloramphenicol-poised cells, the Complex I content is specifically diminished relative to other respiratory chain iron-sulfur proteins. However, in the isolated small Complex I, clusters N-1, N-3, and N-4 are present, while cluster N-2 is non-detectable. Thermodynamic and EPR properties of these iron-sulfur clusters will be presented (supported by NIH GM30736 and Deutsche Forschungsgemeinshaft).

(1) Friedrich et al. (1989) Eur. J. Biochem. 180, 173.

W-Pos551

CHEMILUMINESCENCE BEHAVIOUR OF WILD AND RESPIRATORY MUTANT STRAINS OF YEAST.
C. KUMAR AND B. CHANCE, DEPT OF BIOCHMISTRY AND BIOPHYSICS, UNIVERSITY OF PENNSYLVANIA, PHILADELPHIA, PA 19104. (Intro by Dr. D. Robertson)

We have studied the chemiluminescence behaviour of wild and mutant strains of yeast in the presence of various respiratory substrates, inhibitors and peroxide. Similar to our earlier studies on rat liver mitochondria (E.Cadenas, A.Boveris and B.Chance, Biochem. J., 186, 659(1980)), wild strains of yeast showed enhanced chemiluminescence on addition of peroxide (Hydrogen Peroxide or Ethyl Hydrogen Peroxide) to micromolar concentrations. Antimycin A incubated yeast showed higher levels of Peroxide induced chemiluminescence. Cyanide incubated yeast showed lower levels of Peroxide induced chemiluminescence. A cytochrome b deficient yeast mutant (W-7, courtesy of P. Brivet-Chevillote) showed high Peroxide induced chemiluminescence even in the absence of Antimycin A. In this case also Cyanide decreased the intensity of peroxide induced chemiluminescence. This may be indicative of a role for Cytochrome Oxidase in Peroxide induced chemiluminescence.

The spontaneous chemiluminescence of the wild type yeast (no Peroxide added) is enhanced several fold in presence of Antimycin A - Menadione. Such enhancement occurred after a pronounced lag phase.

W-Pos552

THE EFFECT OF PRESSURE ON THE MAIN AND PRE-TRANSITIONS IN DMPC, DPPC, DSPC AND DAPC

S. Krishna Prasad*, S. Chandrasekhar*, R. Shashidhar[1,2] and B.P. Gaber[1]
*Raman Res. Institute, Bangalore 560 080, India
[1]Center for Biomolecular Science and Technology, Code 6090, Naval Research Laboratory, Washington D.C 20375-5000
[2]Geo-Centers Inc, 10903, Indian Head Highway, Fort Washington, Maryland 20744

It is known that DMPC, DPPC as well as DSPC, which are successive even members of the same phospholipid series, exhibit both main and pre-transitions at atmospheric pressure (1 bar). The difference between the two transition temperatures decreases with increase of chain length until finally for DAPC, only the main transition is seen at 1 bar. Our pressure studies on these materials have shown that the difference in the values of dT/dP for the main and pre-transition phase boundaries increases with increasing chain length. This effect leads to an interesting novel behavior - the observation of a pressure induced pre-transition in DAPC.

W-Pos553

pH-DEPENDENT EXPRESSION OF TERMINAL OXIDASES IN A FACULTATIVELY ALKALIPHILIC BACILLUS. Robert J. Plass, David B. Hicks, and Terry A. Krulwich, Dept. of Biochemistry, Mount Sinai School of Medicine of CUNY, New York, NY. Bacillus firmus OF4, an obligate aerobe, grows well at both pH 10-11 and at pH 7.5. Reduced vs. oxidized spectra of everted vesicles revealed two striking differences in the terminal oxidase content of log phase, pH 7.5-grown cells vs. pH 10.5-grown cells. First, the cytochrome aa3 content of membranes relative to membrane protein is only half that of membranes of cells grown at pH 10.5, which have about 0.3 nmoles heme a/mg protein. Second, pH 7.5-grown cells express a cytochrome d absent from log phase, 10.5-grown cells. Stationary phase cells at both pH values have cytochrome d. The cytochrome d assignment is based on a reduced vs. oxidized peak at 621 nm and a peak at about 630 nm in the reduced-CO vs. CO difference spectrum. pH shift experiments document the time course of terminal oxidase changes as well as other pH-dependent changes, especially in b- and c-type cytochromes.

W-Pos554

SUBUNIT II SPECIFIC MONOCLONAL ANTIBODIES TO CYTOCHROME OXIDASE: INHIBITORY EFFECTS AND INTERACTION WITH THE CYTOCHROME c BINDING DOMAIN. **Taha, T. and Ferguson-Miller, S.** Biochemistry Dept., Michigan State University, E. Lansing, MI 48824

Subunit II specific monoclonal antibodies are found to completely inhibit the activity of beef heart cytochrome c oxidase. Western blot analysis of tryptic and V8 digests of subunit II reveal that the smallest peptide that retains the ability to bind the antibody is approximately 10 KD with an N-terminal of Val 138, suggesting that the epitope is in the C-terminal region. ETC modification of the oxidase in the presence and absence of antibody or cytochrome c shows that both proteins provide similar protection against labeling of carboxyl residues, indicating significant overlap of the antigenic site and the high affinity cytochrome c binding domain. Kinetic and binding studies will be presented in which ETC and the subunit II-specific antibody are used to assess the role of a second cytochrome c interaction with the oxidase. **Supported by NIH GM26916.**

W-Pos555

CYTOCHROME OXIDASE FROM THERMOPHILIC BACTERIUM PS3 CONTAINS A FOURTH PROTEIN SUBUNIT. Wen-Zai Gai, Shu-Man Sun, Nobuhito Sone* and Samuel H.P. Chan Dept. of Biology, Syracuse University, Syracuse, N.Y.13244 and Dept. of Biochemistry, Jichi Medical School*, Japan.

Cytochrome oxidase from thermophilic bacterium PS3 was originally analysed to contain three protein subunits with molecular weight of 56,000; 38,000 and 22,000. Monoclonal antibodies prepared against subunits II and IV of beef heart cytochrome oxidase were found to cross-react with thermophilic bacterial PS3 oxidase in ELISA assays. The effects of the two antibodies on cytochrome oxidase activity both from beef heart and PS3 are comparable. "Western" blots analyses showed that subunit II antibodies of beef heart recognized subunit II of PS3 and subunit IV antibody likewise recognized a fourth protein subunit on slab gels. This fourth subunit previously thought to be a contaminant or a degradation product has a molecular weight of about 10,500 on SDS gels, and appears to exist in stoichiometric amount with a ratio of 1:1 compared with the three larger subunits. We have extracted this subunit from slab gels and its amino acid composition was determined. We conclude that this fourth protein subunit is a genuine component of the bacterial oxidase. (Supported by a Grant-in-Aid from Amer.Heart Assoc.)

W-Pos556

EVIDENCE FOR A LOW-SPIN CYTOCHROME a_3 TRANSIENT FOLLOWING PHOTODISSOCIATION OF CO-CYTOCHROME OXIDASE. R.B. Dyer[1a], 'O. Einarsdottir[2], J.J. Lopez-Garriga[1b], K.A. Bagley[1b], S.J. Atherton[3], R.A. Goldbeck[2], T.D. Dawes[2], and W.H. Woodruff[1b]. Los Alamos National Laboratory ([1a]CLS-4 and [1b]INC-4), Los Alamos, NM 87545; [2]Department of Chemistry, UCSC, Santa Cruz, CA 95064; and [3]CFKR, University of Texas at Austin, Austin, TX 78712.

Time resolved resonance Raman, kinetics, and photolability suggest that the photodissociation of CO from reduced cytochrome oxidase at room temperature is followed by the formation of a transient, low-spin, non-CO-liganded cytochrome a_3 intermediate which decays with a half life of 1μs. The lifetime of this intermediate is the same as the post-dissociation Cu_B-CO transient as determined by time resolved infrared studies. Its spectral and kinetic characteristics are generally similar to bis(imidizole) ferrous heme a model complexes and proteins. However, we do not observe a typical low spin heme a signal by time resolved magnetic circular dichroism. These observations are significant with regard to the ligand-shuttle function which we have previously proposed, in addition to the established redox role, for Cu_B.

W-Pos557

5-METHYLPHENAZINIUM METHYL SULFATE MEDIATES CYCLIC ELECTRON FLOW AND "UNCOUPLING" IN CHROMAFFIN-VESICLE MEMBRANES. Gordon J. Harnadek and David Njus, Department of Biological Sciences, Wayne State University, Detroit, Michigan 48202.

When 5-methylphenazinium methyl sulfate (also known as phenazine methosulfate or PMS) and ascorbate are added together to a suspension of resealed chromaffin-vesicle membranes, the pH gradient and membrane potential established by the H^+-translocating ATPase are rapidly dissipated. This occurs because the membrane-protein cytochrome b_{561} transfers electrons from external ascorbate to internal PMS, and the reduction of internal PMS eliminates both electron and proton. PMS had been thought to accumulate within the vesicles as a weak base and to recycle via oxidation by intravesicular O_2. The rate at which internal PMSH oxidizes, however, is not fast enough to account for uncoupling. Instead, it appears that reduction of external PMS by ascorbate forms a significant concentration of the neutral free radical. The neutral radical enters the vesicle and protonates once inside. This protonated radical readily accepts an electron from cytochrome b_{561} to form the neutral fully reduced species, which then diffuses out of the vesicle and is oxidized by O_2. The same effect may be observed if NADH is used in place of ascorbate. Since NADH reduces PMS but not cytochrome b_{561}, it appears that PMS species may act as both external donor and internal acceptor for the cytochrome. Supported by NIH Grant GM-33849.

W-Pos558

POTENTIOMETRIC AND SPECTRAL STUDIES WITH THE TWO SUBUNIT CYTOCHROME aa_3 FROM P. DENTRIFICANS. K. Pardhasaradi, R.W. Hendler, and B. Luwdig*, NHLBI, NIH, Bethesda, MD 20892 and *Institut fur Biochemie, Medizinische Universitat zu Lubeck.

We have recently described the complex cooperative redox characteristics of 13 subunit mammalian cytochrome aa_3. A transition at ~200 mV includes two low E_m forms of cyt. a_3 with Soret peaks at 428 and 446 nm. Transitions at ~260 and ~340 mV are due to cooperative interactions between cyt a and a higher E_m form of cyt a_3. In order to see whether the interactive redox behavior depends on the "extra" subunits in the mammalian enzyme we examined the 2-subunit enzyme from P. dentrificans. The latter shows essentially the same 3 transitions as the mammalian enzyme plus an additional one for cytochrome a alone at ~370 mV. The 3 transitions for the bacterial enzyme were at ~215, ~250, and ~305 mV. CO-complexes of the 429 and 446 species of low E_m mammalian a_3 have E_m's of ~225 and ~325 mV, whereas the corresponding complexes from the bacterial enzyme have E_m's of ~270 and ~330 mV. We conclude that the redox characteristics of cyt aa_3 do not depend on interactions involving the "extra" subunits.

W-Pos559

ELECTRON NUCLEAR DOUBLE RESONANCE (ENDOR) OF THE Q_c UBISEMIQUINONE FROM THE MITOCHONDRIAL ELECTRON TRANSPORT CHAIN. John C. Salerno and Marcie Osgood, Dept. of Biology, RPI, Troy, NY 12180, and Yajun Liu, Harold Taylor, and Charles P. Scholes, Dept. of Physics, SUNY Albany, Albany, NY 12222.

ENDOR signals were obtained from protons associated with the bound Q_c ubisemiquinone of the mitochondrial bc_1 complex. We observed strongly coupled protons whose exchangeable nature indicated that they were protons hydrogen bonded to the quinone oxygen(s). Such hydrogen bonds are critical in binding the ubiquinone to the protein, in stabilizing the semiquinone form, and potentially in modulating the thermodynamic properties of bound ubiquinone. Additional proton ENDOR features were assigned to the quinone ring protons and to weakly coupled protons that may be associated with nearby amino acids. (These above assignments were aided by similarity to ENDOR signals from ubisemiquinone in the bacterial photosynthetic reaction center as obtained by Lubitz et al. [1985] BBA 808, 464.) There was also ENDOR evidence from very weakly hyperfine coupled, distant, exchangeable protons that indicated proximity and accessibility of the ubiquinone binding site to the aqueous medium. (This work supported by NIH grants GM-34306 and GM-35103.)

W-Pos560

CATALYSIS AND ELECTRON TRANSFER BY A SOLUBLE TERNARY PROTEIN COMPLEX FROM PARACOCCUS DENITRIFICANS. V. L. Davidson and L. H. Jones, Dept. of Biochemistry, U. of MS Med. Ctr., Jackson, MS 39216.

Three periplasmic redox proteins from P. denitrificans, the quinoprotein methylamine dehydrogenase (MADH), the copper protein amicyanin, and cytochrome c-551i, must form a ternary complex in order to couple methylamine oxidation to cytochrome C-551i reduction. Steady-state kinetic studies yielded Km values of 2.5 uM, 0.22 uM, and 1.3 uM, respectively, for methylamine, amicyanin, and cytochrome c-551i. A kcat/Km of 1100 min^{-1} was measured for the methylamine-dependent reduction of cytochrome c-551i by MADH and amicyanin. In the presence of 0.2 M NaCl, the Km for amicyanin increased 10-fold, with no change in kcat. The kcat/Km for methylamine oxidation by MADH was 3-fold greater when assayed with physiological electron acceptors than when assayed with artificial electron acceptors in the absence of amicyanin. A deuterium kinetic isotope effect was observed with values for methylamine oxidation of ^{D}kcat of 1.5 and ^{D}kcat/Km of 6.7. Supported by NIH grant GM-41574.

W-Pos561

PHOTO-INDUCED ELECTRON EJECTION FROM THE REDUCED COPPER OF PSEUDOMONAS AERUGINOSA AZURIN[1]. Alan F. Corin and Ian R. Gould, Eastman Kodak Company, Research Laboratories, Rochester, NY 14650-2118

Upon reduction from Cu^{+2} to Cu^{+}, the type I blue copper protein from Pseudomonas aeruginosa exhibits enhanced absorption in the UV. Pulsed laser excitation of reduced azurin at 308 nm results in single photon, rapid (<30 ns) oxidation of the copper atom with subsequent formation of the hydrated electron. The quantum yield for this is ca. 0.05. The hydrated electron reacts as expected with scavengers such as nitrous oxide, oxygen, acetone, and nitromethane. In the absence of scavengers, the electron reacts with components of the protein, including the disulfide bond. The latter reaction forms the disulfide radical anion. The overall photophysical event involves a charge-transfer to solvent transition, although the existence of intermediate states cannot be excluded. The existence of each of the photophysical and chemical reactions is inferred from time-resolved transient absorption spectral data.

(1) Corin, A. F. and Gould, I. R. (1989), Photochem. and Photobiol., 50(37), 413-418.

W-Pos562

PHOTOINDUCED ELECTRON TRANSFER IN COMPLEXES BETWEEN RUTHENIUM-CYTOCHROME C AND CYTOCHROME OXIDASE OR PLASTOCYANIN. F. Millett, L.P. Pan, M. Frame, B. Durham, and D. Davis, University of Arkansas, Fayetteville AR 72701

A new technique has been developed to measure intra-complex electron transfer between cytochrome c and its redox partners. Ten different cytochrome c derivatives labeled at single lysine amino groups with ruthenium bis-bypyridine dicarboxybipyridine were prepared as previously described (Pan et al., Biochemistry 27 7180, 1988). Excitation of Ru^{II} with a short light pulse resulted in the formation of the excited state Ru^{II*}, which rapidly transferred an electron to the ferric heme group to form Fe^{II}. Intra-complex electron transfer from the Fe^{II} in cytochrome c to other proteins could then be detected on a microsecond time scale. The derivative modified at lysine 13 at the top of the heme crevice had the fastest electron transfer reaction with plastocyanin, 1900 s^{-1}, while the derivative modified at lysine 27 at the right side of the heme crevice had the slowest, 500 s^{-1}. Molecular modeling studies indicated that the bulky ruthenium group at lysine 13 caused plastocyanin to bind towards the bottom of the heme crevice in a more favorable orientation for rapid electron transfer. The rate for electron transfer between the lysine 13 derivative and cytochrome oxidase was 600 s^{-1}, while the rates for derivatives modified at lysines remote from the heme crevice were much larger. Supported by NIH GM20488

W-Pos563

INTERMEMBRANE IONIC STRENGTH OF INTACT MITOCHONDRIA AS ESTIMATED WITH FLUORESCEIN-BOVINE SERUM ALBUMIN DELIVERED BY PH-FUSION. J.D. Cortese, A.L. Voglino and C.R. Hackenbrock. Dept. of Cell Biology and Anatomy, Univ. of North Carolina at Chapel Hill, Chapel Hill, NC 27599-7090.

The intermembrane ionic strength (IM-IS) of mitochondria can modify electron transport by affecting membrane binding of cyt c. We determined that fluorescein-labelled bovine serum albumin (F-BSA) exhibited a fluorescence change in the presence of monovalent ions with an affinity in the mM-range. Thus, F-BSA can be used as a probe of changes in the IM-IS. We developed a method of controlled pH-fusion to deliver F-BSA to the IM-space without affecting mitochondrial acceptor control. Asolectin liposomes loaded with F-BSA were fused with freshly isolated mitochondria at pH 6.5. The degree of fusion was 37% as monitored by relief of self-quenching of octadecylrhodamine B. With increasing IS, soluble and IM-loaded F-BSA exhibited an increase in fluorescence with similar affinity. This reveals that F-BSA is exposed to the same IS in the IM-space or in solution, and suggests that the IM-IS changes as does the external IS. Supported by NIH.

W-Pos564

DIFFUSION OF MITOCHONDRIAL INNER MEMBRANE REDOX COMPONENTS AND PHOSPHOLIPID IS NOT AFFECTED BY INNER MEMBRANE FOLDING AND MATRIX DENSITY. B. Chazotte and C.R. Hackenbrock, Dept. of Cell Biol. & Anatomy, Univ. of No. Carolina, Chapel Hill, N.C.

We have proposed that diffusion-based collisions of redox components mediate and control mitochondrial electron transport. Recent data reveal that neither the extent of mitochondrial inner membrane folding nor matrix density have a significant effect on the mobility of redox components in mitochondrial electron transport. Data on the diffusion of inner membrane redox components, phospholipid, ubiquinone and Complexes I, III, IV, and V, obtained by submicron beam fluorescence recovery after photobleaching measurements on functionally and structurally intact inner membrane-matrix particles (mitoplasts) revealed essentially the same diffusion coefficients as we reported previously for fused, ultralarge, spherical, matrix-free inner membranes. Theoretical analyses of submicron diffusion measurements and comparisons of diffusion-based collisions to actual electron transport rates confirm diffusion-mediated electron transport at the mitoplast level. Supported by NIH GM28074 and NSF PCM 84-0265 and DMB 88-16611.

W-Pos566

EXOGENOUS UBIQUINONE DEPENDENT UBISEMIQUINONE RADICAL IN SUCCINATE-UBIQUINONE REDUCTASE Chang-An YU, Toshiaki Miki and Linda YU. Dept. of Biochemistry, Oklahoma State University, Stillwater, OK 74078

Two types of ubisemiquinone radicals, one (Q_c) sensitive to antimycin and another (Q_s) sensitive to thenoyltrifloroacetone (TTFA), are involved in succinate-cytochrome *c* reductase (SCR). Q_c is detected in ubiquinol-cytochrome *c* reductase and is bound to a protein of Mr=9.5 kD. The fate of Q_s in succinate-Q reductase (SQR) is less clear. The Q_s radical was only recently detected in reconstituted SQR, but not in isolated SQR (Xu *et al* (1987) BBRC, 144, 315). Fully active, purified SQR contains 5.8 moles flavin and 2.5 moles Q per mole protein but forms very little Q_s-radical without the addition of exogenous Q. The concentration of the Q_s radical increases as the concentration of Q added increases when SQR is dissolved in 50 mM phosphate buffer pH 7.4, containing 10 % glycerol, 2 mM fumarate and 100 mM succinate. The maximal radical concentration is obtained when five moles of Q per mole flavin is used. At 150 K, the radical shows a TTFA sensitive epr signal with g value of 2.005 and a linewidth of 12 Gauss. At pH 7.4 the Em of the two electron step was about 86 mV with E_1=40 mV and E_2=128 mV. In contrast to Q_c, the Q_s radicals do not show power saturation behavior even at 200 mW. (supported in part by grant from NIH GM 30721)

W-Pos565

EPR BEHAVIOR OF BOVINE HEART CYTOCHROME c_1 AND CYTOCHROME c: EFFECT OF HINGE PROTEIN AND A TERNARY c_1-Hp-c COMPLEX FORMATION Chong H. Kim and John C. Salerno, Dept. of Biology, Rensselaer Polytechnic Institute, Troy, NY 12180

Electron Paramagnetic Resonance studies of bovine heart mitochondrial cytochromes c_1 and c, individually and in c_1-Hp-c complex, were conducted to identify changes in the heme site geometry upon formation of a ternary c_1-Hp-c complex with the hinge protin(Hp), a 9.2 kDa subunit of ubiquinol cytochrome c oxidoreductase. EPR spectra of cytochrome c_1 indicated that the g_z value of "two band" c_1 (containing Hp) is slightly higher than that of "one band" c_1 (free of Hp). The "two band" c_1 is also stabilized in a native conformation, whereas "one band" c_1 showed a progressive shift with time to an alternative state, with a cytochrome c like EPR spectrum. Addition of 1% cholate shifted the g_z peak of cytochrome c about 15 gauss to lower field and also produced shoulders corresponding to denatured states. Formation of the ternary complex in 1% cholate shifted the same peak 5-10 gauss to higher field relative to cytochrome c in the absence of the detergent, and more than 20 gauss upfield relative to cytochrome c in cholate (supported by AHA 890662 and NIH GM 34306).

W-Pos567

STRUCTURAL CONSEQUENCES OF NICKEL VERSUS MACROCYCLE REDUCTIONS IN F430 MODELS: EXAFS STUDIES OF A Ni(I) ANION AND Ni(II) π ANION RADICALS. L. Furenlid, M. Renner, C. Chang, M. Smith and J. Fajer. Brookhaven National Laboratory, Upton, NY 11973.

EXAFS results are reported for the Ni(II) complexes of 2,7,12,17-tetrapropylporphycene, anhydromesorhodochlorin XV methyl ester, the corresponding isobacteriochlorin(iBC), and their one-electron reduction products: the Ni(II) π anion radicals of the porphycene and the chlorin, and the Ni(I) iBC anion. The EXAFS data for the parent Ni(II) porphycene and iBC agree within ±0.02 Å with x-ray diffraction results. Reduction to the π anion radicals leaves the nickel environment unperturbed whereas formation of Ni(I) induces distortions in the Ni-N distances of approximately 0.1 Å. Metal, as opposed to macrocycle, reduction thus requires that the macrocycle skeleton be flexible enough to accommodate the Ni(I) ion. This structural requirement may control the sites of reduction in F430, the nickel tetrapyrrole that catalyzes the final steps of CO_2 conversion to methane in methanogenic bacteria, and in Ni porphyrins and hydroporphyrins presently used to model the reactions of F430. (Work supported by the Division of Chemical Sciences, U.S. Dept. of Energy.)

W-Pos568

DEFICIENCY OF CYTOCHROMES IN A PATIENT WITH MITOCHONDRIAL ENCEPHALOMYOPATHY. C. P. Lee*, M. E. Martens*, M. Nigro*, P. L. Peterson*, R. Holmes+, C. H. Chang*, C. Chien*, D. Johns# & O. Hurko#. *Wayne State Univ. Sch. Med., Detroit, MI; +William Beaumont Hospital, Royal Oak, MI; #Johns Hopkins Univ. Sch. Med., Baltimore, MD

A 3-1/2 month old boy presented with respiratory failure, seizures and lactic acidosis. Histochemical and ultrastructural studies suggested disorder of mitochondrial oxidative metabolism. Biochemical studies of mitochondria isolated from a fresh skeletal muscle biopsy revealed that the mitochondria were tightly-coupled and exhibited normal ADP/O ratios with both succinate and NAD-linked substrates. However, the State 3 respiratory rates were severely impaired, ~25% of those seen in controls. The uncoupler and/or Ca^{++}-induced rates were significantly higher. The cyt. contents were exceedingly low, which were 14, 10, 20 and 75% of that of controls for cyts. a, a_3, b and c, respectively. Mitochondrial DNA analyses showed no major DNA deletion and no point mutation associated with Leber's hereditary optic neuropathy. These data indicate that a deficiency of cytochromes and an impaired ATP synthase are associated with this disorder. Supported by NIH (CPL).

W-Pos570

CONTROL OF OXIDATIVE PHOSPHORYLATION IN HEART MITOCHONDRIA OXIDIZING NAD-LINKED SUBSTRATES.

Rafael Moreno-Sánchez and Concepción Bravo (Intro. by A. Peña). Depto. de Bioquímica, Instituto Nacional de Cardiología, México, D.F. 14080 MEXICO.

We determined the flux-control coefficients (C_i) of various steps of oxidative phosphorylation with 5 or 0.5 mM pyruvate and 5 or 230nM Ca^{2+}: in these conditions NAD-dehydrogenase-level control is involved. At low dehydrogenase activity and rates of ATP synthesis (low pyruvate, low Ca^{2+}), control was also exerted by the ATP/ADP carrier (C_i=0.40) and site I of the respiratory chain (C_i=0.28). Activation of dehydrogenases and increase in flux by high pyruvate or high Ca^{2+} brought up an increase in control exerted by the ATP synthase (C_i=0.30-0.50) and the Pi carrier (C_i=0.30). Higher membrane potential values were observed in the presence of high pyruvate or high Ca^{2+} indicating that the limitation of the synthase and Pi carrier is kinetic. Changes in activity of the ATP/ADP carrier and the ATP synthase resulted in a complex variation of the mitochondrial ATP and ADP pools. At physiological values of pyruvate, Ca^{2+}, Pi, Na^+ and pH, oxidative phosphorylation is controlled by the NAD-linked dehydrogenases and the phosphorylating system.

W-Pos569

BRAIN ISCHEMIA, Ca^{++} HOMEOSTASIS AND MITOCHONDRIA INJURY. M. Sciamanna*, J. Zinkel#, A. Fabi* & C. P. Lee*. Departments of *Biochemistry & #Neurosurgery, Wayne State University School of Medicine, Detroit, Michigan.

The 3 vessel occlusion model of Kameyama et al (Stroke, 16: 489, 1985) was adapted with modifications to induce complete reversible rat forebrain ischemia. Mitochondria isolated from ischemic brain (8 - 30 min. ischemia) showed decrease in State 3 respiratory rates and decreased respiratory control indices (RCI). The extent of decrease was proportional to the ischemic time, ~50% decrease in respiratory rates and complete loss of RCI were seen with 20 min. ischemia. Both the respiratory rates and RCI can be restored to control levels upon the addition of EGTA or ruthenium red to the assay mixture. A significant amount of Ca^{++} (~0.6 nmoles/mg protein) was found to be adsorbed to the ischemic (15 min) mitochondria. The decreased respiratory rates and RCI can be restored up to 80% of control levels when the ischemic rats were reperfused in air for 60 min. These data indicate that ischemia disrupted the cellular Ca^{++} homeostasis and resulted excess Ca^{++} adsorption to the mitochondrial membrane.

W-Pos571

^{1}H NMRS OF DEOXYMYOGLOBIN IN HUMAN MUSCLE

E. A. Noyszewski, Z. Wang, K. McCully, and J. S. Leigh, Jr.

Determining the aerobic capacity of skeletal muscle has been controversial, in part because oxygen is difficult to measure in vivo. It has not been established conclusively that O_2 supply to muscle during exercise is adequate to fuel oxidative phosphorylation. We have developed a new technique to obtain information about PO_2 and VO_2 by observing ^{1}H NMRS signals from myoglobin (Mb), the major O_2-binding protein in muscle. The procedure is based on paramagnetic shifts due to interactions between heme group protons and the central iron. When Mb is oxygenated, Fe spin state is S=0 and no interactions occur; Mb proton peaks lie near the water peak and are difficult to observe. However, when deoxygenated, Fe spin state becomes S=2, giving rise to large shifts in the Mb proton peaks (up to 80 ppm) Measurements of changes in these deoxy-Mb signals lead to direct calculations of changes in PO_2 through classical O_2-binding curves for Mb. In addition, by combining this technique with traditional ^{31}P NMRS measurements, we can accurately assess the aerobic capacity of muscle at rest and during exercise.

W-Pos572

CHARACTERIZATION OF THE GENE CODING FOR ATP5 IN YEAST *S. CEREVISIAE*. Misook Uh, Deborah Jones & David M. Mueller. UHS/Chicago Med. School, No. Chgo., IL, USA, 60064. The ATP5 gene codes for subunit 5 of the mitochondrial ATP synthase, is also called the oligomycin sensitive conferring peptide (OSCP). The OSCP links the catalytic sector, the F1, to the membrane sector, the Fo, of the ATP synthase. Here, we report identification and characterization of the ATP5 gene in yeast Saccharomyces cerevisiae. The gene was completely sequenced and its amino acid sequence deduced. The yeast OSCP consists of 212 amino acids with a calculated molecular weight of 23 Kd. The yeast OSCP is 35% identical and 65% homologous with bovine OSCP. The calculated isoelectric point (pI) of yeast OSCP and bovine OSCP was 9.46 and 9.98, respectively, indicating that they are highly basic molecules. The comparison of hydrophobic profile and predicted secondary structure of yeast OSCP and bovine OSCP showed that the overall patterns were similar. Northern blot analysis showed that the message of yeast ATP5 gene was 1.05kb. Gene disruption experiment showed that the OSCP was essential for the function of oxidative phosphorylation. In addition, disruption of the ATP5 gene was occurred at a single chromosomal locus which was proven by Southern blot and tetrad analysis.

W-Pos573

MATRIX FREE Mg^{2+} OF HEART MITOCHONDRIA. D.W.Jung & G.P.Brierley.Dept.Physiological Chem.,Ohio State U., Columbus, Ohio 43210.

The concentration of free Mg^{2+} in the matrix of isolated beef heart mitochondria (BHM) has been monitored using the fluorescent probe furaptra (mag-fura-2). Matrix [Mg^{2+}] averages 0.5-0.6 mM for BHM respiring on succinate or malate+glutamate in a Mg^{2+}-free KCl medium. Addition of P_i (3mM) decreases [Mg^{2+}] by approx 0.2 mM as P_i enters the matrix. Further addition of ADP produces a transient increase in [Mg^{2+}] of approx 0.15 mM lasting until the added ADP is phosphorylated. This effect is oligomycin-sensitive and appears mostly due to the decrease in matrix P_i during oxidative phosphorylation. A second addition of ADP produces a comparable cycle. Uncouplers induce anion efflux and increase matrix [Mg^{2+}] by 0.2-0.3 mM. The presence of 0.5-2 mM external [Mg^{2+}] decreases the P_i-dependent drop in matrix [Mg^{2+}] and results in net Mg uptake. Matrix [Mg^{2+}] decreases with hypotonic swelling and increases with subsequent KCl addition. It is concluded that matrix [Mg^{2+}] changes with ligand availability and may contribute to the regulation of matrix enzymes and membrane transporters.
Supported in part by USPHS grant HL09364.

W-Pos574

MYOGLOBIN MEDIATED OXYGEN UPTAKE IS COUPLED TO MITOCHONDRIAL ATP SYNTHASE. Beatrice A. Wittenberg and Jonathan B. Wittenberg, Department of Physiology and Biophysics. Albert Einstein College of Medicine, Bronx, N.Y. 10461.

Mitochondrial ATP synthesis in the functionally intact isolated cardiac myocyte utilizes dissolved oxygen delivered to cytochrome oxidase and, additively, utilizes oxygen bound to sarcoplasmic myoglobin. This pathway, Myoglobin-Mediated Oxidative Phosphorylation (MMOP), is selectively blocked by carbon monoxide which sequesters myoglobin (Mb) as MbCO without detectable effect on mitochondria (PNAS (1987) 84, 7503-07). Rotenone, which blocks electron flow from mitochondrial NADH to ubiquinone, abolishes MMOP, proving dependence of MMOP on electron flow in the mitochondrial electron transport chain. 4-Bromocrotonic acid, an inhibitor of fatty acid beta-oxidation, also abolishes MMOP. Oligomycin, a specific inhibitor of mitochondrial ATP synthase, abolishes MMOP without importantly diminishing oxygen uptake. This shows that myoglobin-mediated oxygen uptake is tightly coupled to mitochondrial phosphorylation of ADP.
Supported by USPHS grant HL19299.

W-Pos575

AGING EFFECTS ON CO BINDING TO CYTOCHROME OXIDASE. H. James Harmon (Intro. by R.A. Floyd), Oklahoma State Univ., Stillwater, OK 74078

CO recombination to cytochrome oxidase following flash photolysis has been studied in synaptic (S) and non-synaptic (NS) brain mitochondria from 3- and 30-month old rats. Age-dependent differences are observed only in S mitochondria. In NS mitochondria at both ages, CO migration from medium to heme Fe involves two 10.3 kcal/mole barriers separating an inner intermediate region from Fe and the inner region from an outer region. The inner intermediate region can hold one CO; the outer holds two CO. Biphasic Arrhenius plots are observed in 3-month S mitochondria where an inner barrier of approx. 5 kcal/mole and an outer barrier of 10-11 kcal/mole separate regions holding 1 CO. In 30-month S mitochondria, two barriers of 10-11 kcal/mole separate intermediate regions holding 2 CO each.
This research is supported by a grant from the Oklahoma Center for the Advancement of Science and Technology.

W-Pos576

EFFECT OF pH ON CO RECOMBINATION IN CYTOCHROME OXIDASE. BK Stringer and HJ Harmon, Okla. State Univ., Stillwater, OK

Carbon monoxide recombination with cytochrome oxidase in beef heart mitochondria was measured following flash photolysis at low temperatures. At pH 7.4, a monophasic Arrhenius plot is observed in the presence of both 1% and 100% CO with an energy of activation (Ea) of 10.5 kcal/mole. The rate constants with 100% CO are twice those with 1% CO. At pH 5.5 biphasic plots are observed. With 1% CO Ea's of 11.3 and 7.1 kcal/mole are observed below and above 210 K, respectively. In the presence of 100% CO, Ea's of 7.4 and 11.1 kcal/mole are observed below and above 210 K, respectively. The data suggest a model of three intermediate CO holding regions other than the Fe separated by energy barriers. At pH 7.4 all barriers are 10.5 kcal/mole and each region can hold up to 2 CO. At pH 5.5 the barrier between Fe and the innermost region is 7.4 kcal/mole; the other barriers are 11.3 kcal/mole. The innermost and outermost regions can hold 2 CO; the middle region holds only 1 CO.

This research was supported by the Air Force Office of Scientific Research, Air Force Systems Command, USAF, under grant AFOSR 89-0458.

W-Pos577

MUTATIONS IN A RAT LIVER ATP SYNTHASE BETA SUBUNIT PEPTIDE. David N. Garboczi, Philip J. Thomas, and Peter L. Pedersen, Department of Biological Chemistry, The Johns Hopkins School of Medicine, Baltimore, MD.

The ATP synthase beta subunit contains several areas of sequence that are conserved in many nucleotide binding proteins. One of these is a glycine rich region thought to comprise part of the nucleotide binding site. To address the role that this area plays in binding, we generated random amino acid changes within the region and deleted the entire region in a 350 amino acid C-terminal polypeptide of the beta subunit. This wildtype polypeptide has previously been shown to interact with adenine nucleotides (J. Biol. Chem. 263: 15694, 1988). Both the mutant and wildtype proteins were expressed in *E. coli*, purified, and analyzed for their interactions with adenine nucleotides and with fluorescent adenine nucleotide analogs. The results obtained suggest that although the glycine rich region plays a role in the binding of nucleotides by the beta subunit, it may not be absolutely required for such binding. (Supported by NIH grant CA10951 to P.L. Pedersen.)

W-Pos578

MITOCHONDRIAL ATP SYNTHASE: cDNA CLONING, AMINO ACID SEQUENCE, OVEREXPRESSION, AND PROPERTIES OF THE RAT LIVER α-SUBUNIT. James H. Lee, David N. Garboczi, Philip J. Thomas, and Peter L. Pedersen, (Introduced by R.D. Pratt), Department of Biological Chemistry, The Johns Hopkins University School of Medicine, Baltimore, MD

The amino acid sequence of the rat liver mitochondrial ATP synthase α-subunit, predicted from the cDNA sequence, contains the A and B consensus sequences found in many nucleotide binding proteins. A 495 amino acid C-terminal polypeptide fragment of the 510 residue α-subunit, which includes the putative nucleotide binding sequences, has been overexpressed in *E. coli* and purified. This protein, soluble at pH 9.5 or greater, interacts with fluorescent adenine nucleotide derivatives causing a marked fluorescence enhancement. The apparent K_d for the interaction with the nucleotides is in the low micromolar range. Furthermore, the purified α-subunit interacts with millimolar concentrations of Mg^{2+} resulting in precipitation of the protein. The availability of large amounts of pure α-subunit, along with the the ability to change specific residues at will, make this an ideal system for studying nucleotide and metal binding by the α-subunit, proposed to play a role in regulation of the mitochondrial ATP synthase complex. (Supported by NIH Grant CA10951 to P.L. Pedersen)

W-Pos579

PARTIAL AMINO TERMINAL cDNA SEQUENCE OF BOVINE HEART MITOCHONDRIAL COUPLING FACTOR B

Ali Javed, Kathleen Ogata and D. Rao Sanadi, Department of Cell Physiology, Boston Biomedical Research Institute, 20 Staniford Street, Boston, MA 02114.

Bovine heart mitochondrial coupling factor B (F_B) has been shown to be a subunit of the Fo segment of H^+-ATPase (F_o-F_1). F_B is an absolute requirement for ATP-P_i exchange activity in H^+-ATPase and for H^+ conductance in F_o proteoliposomes.

We have previously reported the sequence of 55 amino acids at the NH_2-terminal region of F_B(1). Partial cDNA sequence at the amino terminus of F_B has now been established by amplifying a region utilizing the polymerase chain reaction. Upon subcloning and sequencing it was found that a 96 bp fragment was amplified instead of the expected 165 bp cDNA fragment, possibly due to a stable secondary structure at the mRNA level, and the reverse transcription being non-contiguous because of an mRNA loop, leading to deletion of a segment of cDNA.

1. Huang, Y., Kantham, L. and Sanadi, D.R. (1988) Advances in membrane biochemistry and bioenergetics, (J.J. Diwan et al, editors), Plenum Publishing Corp. pp. 357-362.

W-Pos580

EVIDENCE FOR TWO ENERGETICALLY DISTINCT SPACES WITHIN THE CHLOROPLAST THYLAKOID. R.D. Horner and E.N. Moudrianakis, Biology Dept., The Johns Hopkins Univ., Baltimore, MD 21218.Using chloroplasts in the presence of valinomycin and K^+, amine buffers such as aniline did not delay the initiation of ATP synthesis during illumination (photosynchronous phosphorylation) but did delay the development of the capacity to make ATP after illumination has ceased (postillumination phosphorylation). That these effects were not due to uncouping artifacts was confirmed by making subchloroplast particles, vesicles active in photophosphorylation, in the presence of zwitterionic buffers and observing the same effects on photosynchronous and postillumination phosphorylation. Further study has shown that internal buffers do not affect the rate of decay of the internal potential which drives both forms of photophosphorylation indicating that the two spaces within the chloroplast implied by earlier results are not in a kinetic equilibrium. Rather, experiments which measured the development of photosynchronous and postillumination potentials under increasing illumination have shown that internal buffers result in a constant deficit in photosynchronous phosphorylation potential but a cumulative deficit in postillumination potential. One explanation for these effects is that protons are partitioned between the two energetically distinct spaces.

W-Pos581

DEPENDENCE OF AFFINITY-LABELED AMINO ACID RESIDUES IN F_1-ATPASE ON PROTEIN CONFORMATION. Jui H. Wang, Joe C. Wu, Johnson Lin and Hua Chuan. Bioenergetics Laboratory, Acheson Hall, SUNY, Buffalo, NY 14214.

The hydrolytic site of F_1-ATPase can be labeled with either 3'-O-(5-fluoro-dinitrophenyl)ADP ether (FDNP-ADP) or 3'-O-(5-fluorodinitrophenyl)ATP ether (FDNP-ATP). In both cases each covalent label at the hydrolytic site completely abolishes the ATPase activity of the F_1 molecule. However, FDNP-ADP labels Lys-β162, whereas FDNP-ATP labels Lys-β301. Since both Lys-β162 and Lys-β301 are at the hydrolytic site, we conclude that the different labeling results with these two equally reactive reagents are due to ligand-induced protein conformation change. For labeling with FDNP-ATP, the reaction can be controlled to distinguish two types of Lys-β301 residues. In the absence of Mg^{2+}, two Lys-β"301 residues can be labeled without changing the full ATPase and ITPase activities; but subsequent addition of Mg^{2+} allows the labeling of Lys-β'301 to take place with complete inhibition of ATPase activity. In reconstituted submitochondrial particles, the labeling of either Lys-β'301 or Lys-β"301 inhibits oxidative phosphorylation, but the labeling of Lys-β"301 does not inhibit ATP hydrolysis (USPHS GM 41610).

W-Pos582

MITOCHONDRIAL OLIGOMYCIN SENSITIVITY CONFERRING PROTEIN IS NOT REQUIRED FOR PASSIVE H^+-CONDUCTION THROUGH F_O COMPLEXES.

Saroj Joshi and M.J. Pringle, Intro. by H. Wohlrab, Boston Biomedical Research Institute, Department of Cell Physiology, 20 Staniford Street, Boston, MA 02114

Oligomycin-sensitivity-conferring protein (OSCP) is a water-soluble subunit of bovine heart mitochondrial H^+-ATPase. The requirement of OSCP for passive H^+-conductance through mitochondrial F_O was investigated using F_O proteoliposomes that were deficient in OSCP but not in F_6. The passive proton conductance was measured by time resolved quenching of ACMA (9-amino-6-chloro-2-methoxyacridine) fluorescence following a valinomycin-induced K^+-diffusion potential. The data showed that OSCP-depleted F_O preparations were able to conduct protons and the conductance could be blocked by oligomycin or dicyclohexyl carbodiimide (DCCD). Furthermore, neither the H^+-conductance nor its prevention by the inhibitors were affected by OSCP. The data clearly establish that OSCP is not a necessary component of the F_O H^+-channel nor is its presence required for conductance blockage by oligomycin or DCCD. Supported by NIH grant GM 26420.

W-Pos583

HETEROGENEITY OF THE $P^+Q_B^-$ RECOMBINATION KINETICS IN RCS FROM *RPS. VIRIDIS*

Jiliang Gao, Robert J. Shopes and Colin A. Wraight
University of Illinois, Urbana, IL 61801

In RCs from Rhodopseudomonas viridis, supplemented with ubiquinone as the secondary acceptor (Q_B), the charge recombination of $P^+Q_B^-$ following a short flash was measured at different pH, temperature, viscosity (glycerol concentration) and ionic strength. In general the decay of $P^+Q_B^-$ was not a single exponential but could be well fit by two components. The decay rates of the two components exhibited similar pH dependent behavior: at pH 6.0, the decay rates were $0.85 \pm 0.05\ s^{-1}$ (k_{slow}) and $5.5 \pm 0.5\ s^{-1}$ (k_{fast}), and both increased with increasing pH to maximum values of $3.5 \pm 0.5\ s^{-1}$ and $14 \pm 1\ s^{-1}$ at pH 8.5. Above pH 8.5, the rates of the two components slowed to $2.5 \pm 0.3\ s^{-1}$ and $10 \pm 1\ s^{-1}$ at pH 10.5. From the temperature dependences between 300K and 273K, the apparent activation energies of the two components were the same: 0.53 ± 0.03 eV. The relative amplitudes of the two components were altered by changing pH, viscosity and ionic strength. The amplitude of the fast component increased with increasing pH, from 10% at pH 6.0 to a maximum 45% at pH 8.5, and then decreased to less than 10% at pH 10.5. The relative amplitude of the fast component also increased with high concentrations of glycerol, but decreased with increasing ionic strength.

These results suggest that the heterogeneity of $P^+Q_B^-$ recombination is intrinsic rather than artifactual in nature. Furthermore, the inter-convertibility of the two phases implies the existence of substates within a single population of RCs, rather than permanently distinct populations. A similar heterogeneity was previously described for the $P^+Q_A^-$ recombination reaction in Rps. viridis and it was suggested that to arise, in part, from failure of the $P^+Q_A^-$ state to reach protonation equilibrium prior to the rapid back reaction ($k \sim 1000\ s^{-1}$) [1]. This is very unlikely to be the case here, due to the much longer lifetime of the $P^+Q_B^-$ state, and the present results cast some doubt on the previous description of the $P^+Q_A^-$ kinetics. The possible source of the heterogeneity will be discussed.

[1] Sebban, P. and C.A. Wraight (1989) Biochim. Biophys. Acta 974, 54-65.

Supported by NSF.

W-Pos584

SITE-DIRECTED MUTATIONAL STUDIES ON THE ACCEPTOR QUINONE COMPLEX OF REACTION CENTERS FROM *RB. SPHAEROIDES*

Eiji Takahashi and Colin A. Wraight
Department of Plant Biology and
Department of Physiology and Biophysics
University of Illinois, Urbana, IL 61801

The acceptor quinone complex of reaction centers from *Rb. sphaeroides* is currently under study by means of site-directed mutagenesis of the three protein subunits of the complex--L, M and H. From the x-ray structure, the binding sites for Q_A and Q_B are determined entirely by the M and L subunits, but some cross interactions between the two quinones are implied by their physico-chemical properties. Furthermore, protonation events accompanying the one electron reduction of Q_A and the one and two electron reduction of Q_B strongly implicate the protein, and the existence of proton conduction pathways through the H-subunit to the L and M subunits has been widely considered. The spcific involvement of a buried glutamate residue (Glu^{L212}) in the electron transfer for Q_A^- to Q_B has been supported by site-directed mutation of this residue (1). We will describe further mutagenesis studies on the binding and function of Q_A and Q_B and the associated H^+-ion uptake.

(1) Paddock *et al.*, (1989) Proc. Natl. Acad. Sci. USA. 86, 6602-6606

Supported by NSF, USDA and McKnight Foundation

W-Pos585

CHARACTERIZATION OF M210 (TYR->PHE) MUTANT FROM THE PHOTOSYNTHETIC BACTERIA RB. SPHAEROIDES

Xutong Wang, Peter Gast*, Christine Kirmaier+,
Dewey Holten+ and Colin A. Wraight
Department of Biophysics, *Department of Med. Sciences,
University of Illinois Urbana, IL 61801
+Department of Chemistry, Washington University
St. Louis, MO 63103

The availability of X-ray structure of reaction center from *Rb. sphaeroides* allows the identification of potentially important amino acid in various steps of the electron transfer. M210(Tyr) is in a position relative to the primary donor (P) to be involved in the primary electron transfer to the bacteriopheophytin (I), generating P^+I^- we have altered this residue through site-directed mutagenesis and report here a preliminary characterization of a mutant with phenylalanine at this position, M210YF. The mutant grows well photosynthetically but exhibits some altered properties of isolated RC. The $P^+Q_A^-$ recombination rate($P^+Q_A^- \rightarrow PQ_A$) in the mutant is about 1.5 times ($18\ s^{-1}$) faster than in the wildtype ($11.8\ s^{-1}$) while the forward process of P^+I^- formation is 2 fold slower in the mutant (6 ps) compared to the wildtype (3 ps) The pH dependence of $P^+Q_A^-$ recombination is similar but not identical in mutant and in wildtype RCs; both rates speed up at pH value about 8, but the mutant RCs increase faster. Substitution of native primary ubiquinone (Q) with anthraquinone results in a much faster back reaction due to access of a thermally activated recombination rate of P^+I^-. In the mutant this rate is slower; temperature dependence suggests that it is the primary charge recombination of P^+I^- which is slowed down. EPR of P^+ shows a 10 % increase in the line width of the mutant-- from 9.8 G to 10.9 G, possibly indication of "looser" dimer structure. Also, measuring at 4 K, the polarized triplet state of the mutant has slightly different D and E values, indicating changes in the electronic structure of the special Bchl pair of primary donor.

These results suggest that the polar environment of the dimer is important not only for the forward reaction but also the back reaction of photosynthesis. More dramatic consequences may be expected for non-aromatic substitution at this position, and these studies are underway.

Supported by NSF and USDA

W-Pos586

ELECTRON DONATION TO PHOTOSYSTEM II AT LOW TEMPERATURE.

Michael Atamian and Gerald T. Babcock, Department of Chemistry, Michigan State University, East Lansing, MI 48824.

Low-temperature flash illumination of PSII particles yields an EPR-detectable transient radical species that decays in 4.0 ms. A stable EPR signal at g=2.0026, originally ascribed to a chlorophyll cation, Chl^+, is observed subsequent to the decay of the transient. The linewidths of the static radical are essentially identical in both oxygen-evolving and Tris-washed PSII membranes; spin quantitation indicates one per P_{680}^+. The microwave power saturation profiles of the respective Chl^+ are fully consistent with a radical species that does not experience any appreciable magnetic interactions with either the manganese cluster or the stable tyrosine radical Y_D^+. These properties are to be contrasted to those of the transient. Implications for the identity of the transient and static radicals (P_{680}^+ or Chl^+) will be discussed.

W-Pos587

CHLOROPHYLL DIMERS AND DIAMETER QUANTIZATION IN CYLINDRICAL AGGREGATES OF CHLOROPHYLLS. D.L. Worcester, Biology Division, University of Missouri, Columbia, Mo. 65211. T.J. Michalski, M.K. Bowman and J.J. Katz, Chem. Division, Argonne Nat. Lab, Argonne, Ill. Neutron small angle scattering measurements of several different chlorophylls hydrated in deuterated octane-toluene mixtures show that long, hollow cylinders of aggregated chlorophyll are formed. The cylinder diameters depend on chlorophyll type. Studies of numerous samples show that only certain diameters are formed, which depend on chlorophyll type and are very nearly in the ratio of small integers. This quantization of diameters can be accounted for if water molecules coordinate to magnesium only on one side of the chlorophyll macrocycle in the smallest cylinders, but on either side for larger cylinders giving two types of water coordinated macrocycles which must occur in dimers or higher even numbered aggregates to construct cylinders. The structures are stabilized largely by hydrogen bonding, but also pi orbital interactions. The smallest cylinders are formed by Chlorophyll-a whereas Bacteriochlorophyll-a forms cylinders twice larger in diameter. The additional acetyl group in the latter probably makes two water coordinations possible.

W-Pos589

Q_A AND Q_B SITE CONTROL OF QUINONE ELECTROCHEMISTRY IN THE PHOTOSYNTHETIC REACTION CENTER FROM *RHODOBACTER SPHAEROIDES*. K.M. Giangiacomo, M.R. Gunner and P.L. Dutton, Dept. of Biochemistry & Biophysics, U. of Pennsylvania, Phila., PA. (Intro. by W. D. Bonner)

The E_m values for the quinone/semiquinone (Q/Q^-) couple of a range of tailless quinones in aqueous solution (E_mQ/Q^- (W)) have been compared with E_m values obtained *in situ* for both the Q_A and the Q_B quinone binding sites of the photosynthetic reaction center protein from *Rb. sphaeroides*. Results suggest (see Figure) that the *in situ* E_m values of quinones in the Q_A and Q_B sites exhibit a similar relationship with their aqueous E_m values. The *in situ* E_m values for both the Q_A and the Q_B sites appear relatively insensitive to E_mQ/Q^- (W) values ≥ -150 meV, while for values ≤ -150 meV, the change in the *in situ* E_m values is similar to the change in the aqueous values. We demonstrate that the E_mQ/Q^- (W) has little or no affect on the quinone affinity for the Q_A and Q_B sites. Therefore, applying thermodynamic cycles, our findings suggest that the semiquinone-site binding interaction modulates the *in situ* electrochemistry of the quinone.

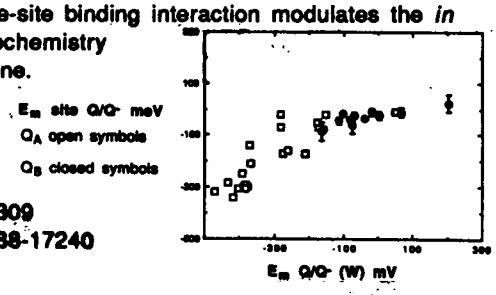

NIH GM 27309
NSF DMB 88-17240

W-Pos588

CHARACTERIZATION OF CYTOCHROME B_{559} AND OF THE PRIMARY ACCEPTOR Q_A OF PHOTOSYSTEM II BY FTIR DIFFERENCE SPECTROSCOPY.

C. Berthomieu[+], E. Nabedryk[+], A. Boussac[+], W. Mäntele[*], J. Breton[+].
[+]Service Biophysique CEN Saclay 91191 Gif/Yvette cedex, France.
[*]Institut für Biophysik, Universität Freiburg, D-7800 Freiburg, FRG.

Illumination at 40K of PS II samples treated with Na-ascorbate induces the simultaneous photooxidation of $Cytb_{559}$ and photoreduction of Q_A. EPR control experiments showed that the $Cytb_{559}^+Q_A^-$ state was formed in 100% of the centers. Light-minus-dark FTIR difference spectra of BBY particles in H_2O and D_2O were recorded under the same experimental conditions. They give informations on the molecular changes associated with the reaction. The feature at 1479 cm^{-1} is assigned to the C=O stretch of the semiquinone anion. The frequency is close to that obtained in bacterial reaction centers, suggesting analogies in the functional group environment. Other features might involve amino acid absorption changes during Q_A reduction (e.g. at 1724/1720 cm^{-1}, 1652 cm^{-1} and 1643 cm^{-1} in the C=O stretching region). Bands at 1660 cm^{-1} and 1624 cm^{-1}, absent in spectra obtained with Tris-treated samples (in which a chorophyll species is photooxidized instead of $Cytb_{559}$) appear specific for $Cytb_{559}$ oxidation. The downshift to 1600 cm^{-1} of the 1624 cm^{-1} band upon deuteration would support the hypothesis of the contribution of the side chain NH group of an amino acid such as the arginine located close to the $Cytb_{559}$ heme.

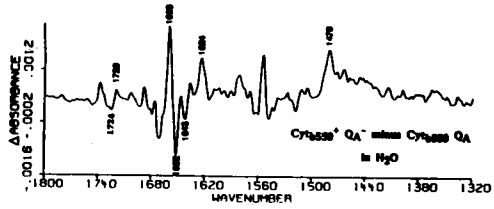

W-Pos590

IDENTIFICATION OF LIGANDS TO MANGANESE AND CALCIUM IN PHOTOSYSTEM II BY SITE-DIRECTED MUTAGENESIS*

R.J. Debus, A.B. Conway, and A.P. Nguyen, Department of Biochemistry, U.C. Riverside, Riverside, CA 92521

The Mn and Ca ions in Photosystem II are believed to be coordinated primarily by carboxyl residues from the lumenally-exposed regions of the D1 and D2 polypeptides. These regions contain 27 carboxyl residues. To rapidly identify those most likely to ligate Mn or Ca, we are constructing a pair of mutations at each. Mutants that grow photosynthetically when Glu is replaced by Asp (or when Asp is replaced by Glu), but not when Glu is replaced by Gln (or when Asp is replaced by Asn) will be characterized in-depth. We are also constructing mutations at lumenally-exposed His and Tyr residues. Mutants are being generated in the unicellular cyanobacterium Synechocystis sp. PCC6803 by a system modified from that previously employed to identify the specific tyrosine residues corresponding to Y_Z and Y_D [1,2].

[1] Debus, R.J., Barry, B.A., Babcock, G.T. & McIntosh, L. (1988) Proc. Natl. Acad. Sci. USA 85, 427-430.
[2] Debus, R.J., Barry, B.A., Sithole, I., Babcock, G.T. & McIntosh, L. (1988) Biochemistry 27, 9071-9074.

*Work supported by the NIH.

W-Pos591

THE STRUCTURE OF THE CAROTENOID IN REACTION CENTERS OF PHOTOSYNTHETIC BACTERIA: A SOLID-STATE MAGIC-ANGLE SAMPLE SPINNING ^{13}C NMR INVESTIGATION OF SPHEROIDENE RECONSTITUTED INTO *Rhodobacter sphaeroides* R-26.

H. de Groot[a], R. Gebhard[a], K. van der Hoef[a], J. Lugtenburg[a], Carol A. Violette[b] and Harry A. Frank[b]. [a]Department of Chemistry, Gorlaeus Laboratories, University of Leiden, 2300 RA Leiden, The Netherlands, and [b]Department of Chemistry, University of Connecticut, Storrs, Connecticut, 06269-3060, USA.

A synthetic scheme for incorporating ^{13}C at specific positions within the carbon chain of the carotenoid, spheroidene, has been developed. Two newly synthesized spheroidene (^{13}C-15', ^{13}C-14') isotopomers have been reconstituted into reaction centers from the carotenoidless mutant *Rb. sphaeroides* R-26. It is known from previous studies (Cogdell, R. J. and Frank, H. A. (1987) Biochim. Biophys. Acta 895, 63-79) that spheroidene reconstituted into reaction centers of *Rb. sphaeroides* R-26 assumes all of the structural and functional characteristics of native spheroidene in *Rb. sphaeroides* wild type strain 2.4.1. Solid-state magic-angle sample spinning (MASS) ^{13}C difference (labelled minus natural abundance) NMR spectra reveal resonances in the 100-150ppm region that are directly attributable to the π-electron conjugated ^{13}C within the labelled spheroidene. The chemical shifts associated with these resonances will be compared with those expected upon isomerization of the carotenoid and used to elucidate the stereochemical structure of the protein-bound spheroidene. This work is supported by grants to H. A. F. from the USDA (88-37130-3938) and NIH (GM-30353).

W-Pos592

EFFECTS OF HYDROSTATIC PRESSURE ON THE FLUORESCENCE PROPERTIES OF CYANOBACTERIA.

Debora Foguel, Jerson L.Silva, Ricardo Chaloub and Gregorio Weber. Dept. Bioq., UFRJ, Brazil and Univ. of Illinois, Urbana IL

At room temperature, the fluorescence of cyanobacteria is due mainly to PSII. PSI fluorescence only appears at temperatures close to 4 Kelvin. Hydrostatic pressure provoked a great increase in the three main emission components (PSII, PSI and APC-PC). At 2.5 kbar, the accessory pigments emission (λ_{max} = 655 nm) increased 11-fold whereas emission of PSII (λ_{max} = 685 nm) only increased 2-fold, suggesting a decrease in the energy transfer from the accessory pigments to clrorophylll a. At one atm, the excited state decay could only be fitted to bimodal distribution of short lifetimes. At 2.5 kbar, the decay was fitted to a single distribution of longer lifetimes confirming the supression of the energy transfer. The emission of PSI also became pronounced at 2.5 kbar (20°C) and the intensity (λ=730 nm) increased many-fold when the temperature was reduced to -5°C.

W-Pos593

CHEMICAL MODIFICATION OF AMINO GROUPS ON PLASTOCYANIN AND THE EFFECT ON ITS INTERACTION WITH CYTOCHROME f.

E. L. Gross and A. Curtiss, Dept. of Biochemistry, The Ohio State University, Columbus, Ohio, 43210

Amino groups on plastocyanin (PC) were modified using 4-chloro-3,5-dinitrobenzoic acid (CDNB). Four singly-modified forms were obtained which were separated and purified using anion exchange FPLC. The modified peptides were identified by amino acid analysis and sequencing after trypsin treatment of the protein. The modifications were located at residues #1, #54, #71 and #77. All modified forms showed stimulation of the reaction with mammalian cytochrome c. However, the forms of PC modified at residues 1, 54 and 77 showed inhibition of cytochrome f (cyt f) oxidation suggesting that they "recognize" the net negative charge on the cyt f molecule. These results taken together with previous studies (Anderson et al. Biochim. Biophys. Acta 894, 386 (1987)) show that both the net charge on the PC molecule and the charge at the binding site for cyt f are important in determining the interactions of the two molecules. Moreover, they suggest that residue #68 as well as #42-45 and #59-61 may be involved in the binding of cyt f.

W-Pos594

MODELING OF THE ELECTROSTATIC POTENTIAL FIELD OF PLASTOCYANIN

Stewart R. Durell*, Jan K. Labanowski+, & Elizabeth L. Gross*; *Biophysics Program, The Ohio State University, 484 W 12th Ave., Columbus, OH 43210, and +The Ohio Supercomputer Center, 1224 Kinnear Rd., Columbus, OH 43212.

It is known that electrostatic interactions affect the rate of reaction of plastocyanin with its reaction partners in the photosynthetic electron transport chain (cytochrome f and photosystem I). The electrostatic potential fields of these proteins influence the rates of association and the locations of the binding domains on the surfaces of the molecules. To better understand these effects we have modeled the electrostatic potential field surrounding plastocyanin with the DelPhi computer program (Honig et al., Proteins 1, 47-59, 1986). The program uses a macroscopic approach which assigns different bulk dielectric constants to the protein and the solvent. Calculations of electrostatic effects on the pKa of nitro-tyrosine 83 and the redox potential of the copper center are used to test the accuracy of the method. The electrostatic potential field of plastocyanin is found to be very heterogeneous, with a region of positive potential over the north pole active site and a region of negative potential over the east face active site. This is why negatively charged reagents associate at the north pole site and positively charged reagents associate at the east face site. The effects of the solvent ionic strength and pH on the calculated potential field is consistent with the experimentally observed effects of these parameters on the rates of reaction of plastocyanin with cytochrome f and photosystem I.

W-Pos595

ULTRAVIOLET CIRCULAR DICHROISM IN THYLAKOID MEMBRANES

J. Kieleczawa, G. Garab[a], J.C. Sutherland and G. Hind.
Biology Department, Brookhaven National Laboratory, Upton, NY 11973.

The ultraviolet CD spectrum of normal barley thylakoids is compared with spectra of membranes defective in Mg ion dependent stacking: (i) a mutant lacking the light-harvesting chlorophyll a/b complex of photosystem II, and (ii) trypsinized thylakoids lacking an amino-terminal, surface-exposed fragment of this same complex. Normal thylakoids undergo membrane stacking in 1 mM Mg ion, whereupon the ellipticity above 205 nm decreases and complex shifts occur below 200 nm. These changes were not seen in mutant or trypsinized membranes. We conclude that an intrinsic change in protein secondary structure occurs when membrane-bound light-harvesting complex interacts with Mg ion, probably including modified ß-sheet and random coil content. (Work supported by U.S. Dept. of Energy).
[a]Biological Research Center, Hungarian Academy of Sciences, Szeged, Hungary.

W-Pos596

EXCITATION TRANSFER IN CHLOROSOMES OF GREEN PHOTOSYNTHETIC BACTERIA

Timothy P. Causgrove, Jian Wang, Daniel C. Brune, and Robert E. Blankenship

Department of Chemistry and Center for the Study of Early Events in Photosynthesis, Arizona State University, Tempe, AZ 85287-1604

Time-resolved fluorescence has been used to measure energy transfer times from BChl *c* (or *d*) to BChl *a* in whole cells and isolated chlorosomes of green photosynthetic bacteria. In the green sulfur bacterium *Chlorobium vibrioforme*, excitations are transferred from BChl *d* to baseplate BChl *a* in 60 ps under anaerobic conditions; in the presence of oxygen, the decay of BChl *d* shortens to 10 ps with an accompanying decrease in transfer efficiency. The effect of oxygen is observed in both chlorosomes and whole cells and can be reversed by the addition of sodium dithionite. In the green filamentous bacterium *Chloroflexus aurantiacus*, excitations originating in BChl *c* are passed to BChl *a* of the baseplate in 15 ps, regardless of the presence of oxygen. In both species, the fluorescence decay at 760 nm is matched by a rise in the BChl *a* emission. Separation of chlorosomes from the photosynthetic membrane results in only a modest increase in BChl *a* fluorescence lifetime, indicating that the isolation procedure induces some type of quenching process not present *in vivo*.

W-Pos597

NMR STUDIES OF THE OXYGEN EVOLVING COMPLEX

T. Bayburt, J.-M. Bovet, and R. R. Sharp, Dept Chem., U. of Michigan, Ann Arbor, MI (Intro. by W. Parkinson)

Redox chemistry of the tetranuclear manganese center that catalyses photosynthetic water oxidation has been studied by flash-induced enhancements in the nmr ^1H solvent T_1 (NMR-PRE). Also, the theory of the nmr-PRE has been developed to describe ions with large zero field splittings (e.g., Mn(III) and Mn(IV)) and used to describe T_1 results for model Mn(III), Mn(IV), and for binuclear Mn(III)/Mn(IV) complexes. The NMR-PRE produced by one and two flashes applied to suspensions of O_2-evolving Photosystem II particles has been measured as a function of temperature (0-31°C) at magnetic field strengths of 0.48 and 1.09 T. These experiments probe magnetic properties of the manganese center in 3 intermediate states of the catalytic cycle (S_0, S_2, and S_3). The nmr-PRE exhibits two well defined temperature regimes. For T<17°C, ^1H relaxation is independent of magnetic field, with temperature dependence characteristic of a chemical exchange-limited process; at T>17°C, R_1's exhibit a mild inverse magnetic field dependence and an extremely rapid inverse temperature dependence, indicative of chemical exchange-mediated relaxation. These data provide an estimate of electron spin relaxation times of manganese. The principal finding is that the ^1H relaxation trap has properties consistent with monomeric Mn(IV) and inconsistent with an exchange-coupled Mn(III)-containing center. On this basis, a two-center monomer-trimer model of the OEC is proposed.

W-Pos598

ELECTRIC FIELD EFFECTS ON P^+Q^- RECOMBINATION KINETICS IN *Rb. SPHAEROIDES* RCs.

S. Franzen & S.G. Boxer, Dept. of Chem., Stanford University, Stanford, CA 94305.

P^+Q^- charge recombination kinetics in *Rb. sphaeroides* RCs have been measured as a function of electric field and temperature for isotropic samples in PVA films. The electron transfer reaction was found to be biphasic at all temperatures. Between 20K and 140K the electric field effect results in an overall slowing of the rate at all fields. Data reduction allows the log(rate) vs. $-\Delta G$ curve to be obtained *experimentally* for both processes (T=80K). The curve can be compared with theory to obtain frequencies ω and coupling constants S for the reaction: ω≈1600 cm^{-1} and ω≈50 cm^{-1} for the faster process; ω≈2500 cm^{-1} and ω≈200 cm^{-1} for the slower process. The overall reorganization energy is about 6400 cm^{-1}. At T>150K the electron transfer rate in the field increases dramatically for some orientations, suggesting a field-assisted activated process. One or both populations of RCs may recombine via the state P^+H^-. Data suggesting the possibility that the state P^+Q^- can be thermally populated in the presence of an electric field is discussed. Comparison of the magnitude of this new effect with known values of ΔG for the reactions is used to estimate the local field correction. Supported by NSF.

W-Pos599

THE NATURE OF THE TRANSIENT ELECTRON SPIN POLARIZED EPR SIGNAL FOUND IN PLANT PHOTOSYSTEM I*

Seth W. Snyder, Richard R. Rustandi and Marion C. Thurnauer, Chemistry Division, Argonne National Laboratory, Argonne, IL and John Biggins, Division of Biology and Medicine, Brown University, Providence, RI

The transient electron spin polarized (esp) epr signal found in plant photosystem I (PSI) is believed to arise from a radical pair consisting of the oxidized primary donor (P_{700}^+) and a reduced quinone-like acceptor.(1) We present evidence that this acceptor is vitamin K_1. Using time-resolved epr techniques we have observed a severe attenuation of transient esp signals when vitamin K_1 was extracted from D144 PSI particles. The signal was restored when vitamin K_1 was reconstituted.(2)

1. M.C. Thurnauer, P. Gast, Photobiochem. Photobiophys. (1985) 9, 29.
2. J. Biggins, P. Mathis, Biochemistry (1988) 27, 1494.

This work was supported by the U.S. Department of Energy, Office of Basic Energy Sciences, Division of Chemical Sciences under contract W-31-109-Eng-38.

W-Pos600

THE PHOTOSYNTHETIC REACTION CENTER COMPLEX FROM *HELIOBACILLUS MOBILIS* ALSO CONTAINS A CORE ANTENNA.

Jeffrey T. Trost, Timothy P. Causgrove, and Robert E. Blankenship

Dept. of Chemistry and Center for the Study of Early Events in Photosynthesis
Arizona State University, Tempe, AZ. 85287-1604, U.S.A.

A photoactive reaction center complex was isolated from *Hb. mobilis*. The complex runs as a single band on SDS-PAGE and shows laser-flash-induced photobleaching with an exponential decay time of 15 ms. RC's and isolated membranes have similar absorption spectra. Difference spectroscopy suggests that there are about 25 BChl *g* per primary donor (P800). Picosecond time-resolved 810 nm fluorescence using 790 nm excitation shows a 23 ps decay accounting for 97% of the amplitude. This suggests that most of the BChl *g* found in the RC act as a core antenna that can efficiently transfer excitations to P800. Emission at 770 nm, with 750 nm excitation, results in a 23 ps decay for 85% of the amplitude. In contrast, membranes excited at 750 nm show only 65% of the 810 nm emission amplitude decaying with a time constant of 24 ps. This suggests that in addition to the core reaction center antenna complex, membranes contain a small amount of peripheral antenna.

W-Pos601

pH DEPENDENCE OF CHARGE RECOMBINATION IN RCs FROM RB. SPHAEROIDES IN WHICH GLU-L212 IS REPLACED WITH ASP*

M.L. Paddock, G. Feher and M.Y. Okamura, UCSD, La Jolla, CA.

Glu-L212 near the Q_B binding site on the L subunit of the reaction center (RC) from *Rhodobacter (Rb.) sphaeroides* was replaced with Asp. Cytochrome photooxidation turnover rate and electrochromic shift measurements at 760nm after a three-electron reduction of the quinones (forming $Q_A^-Q_B^{2-}$) indicate a rapid two-proton transfer to Q_B^{2-} (τ < 10 ms at pH7.5). This is in contrast to the slow (τ ~ 170ms) uptake of the second proton observed in mutant RCs where Glu-L212 is replaced by the non-acidic Gln residue (see preceeding abstract) and supports the proposal that Glu-L212 acts as a proton donor to Q_B^- in native RCs (1). The charge recombination rate ($D^+Q_B^- \rightarrow DQ_B$) is fast for both the ED212L (Glu-L212 → Asp) mutant and native RCs at pH above 11 (see k_{BD} in Figure). As the pH is lowered, k_{BD} decreases. In native RCs the decrease from above pH 11 to ~ 9.5 is assigned to protonation of Glu-L212 (1) and from pH ~ 6 to ~ 4 to another nearby residue(s) (e.g. Asp-L213). In the ED212L mutant the decrease occurs from pH ~ 6 to below pH 4 and is ascribed to a combined effect of Asp-L212 and other nearby residue(s). The surprisingly large difference between the pK_a values of Glu-L212 and Asp-L212 is at present not understood.

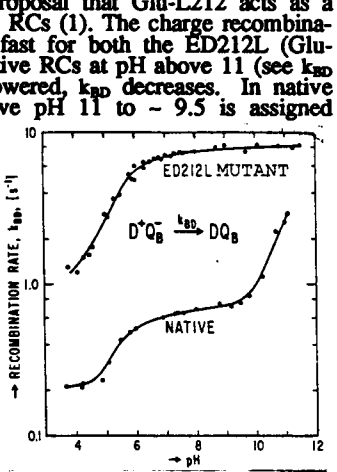

Figure. The pH dependence of k_{BD} for the ED212L (Glu-L212 → Asp) mutant and the native RCs.

(1) M.L. Paddock, S.H. Rongey, G. Feher, and M.Y. Okamura (1989), *Proc. Natl. Acad. Sci. USA* 86, 6602-6606.
*Supported by NSF, NIH and UC Biotechnology Program.

W-Pos602

X-RAY DIFFRACTION STUDIES OF CYTOCHROME C AND PHOTOSYNTHETIC REACTION CENTER MONOLAYERS BOUND TO LB FILMS AND SELF-ASSEMBLED MONOLAYERS.

J.M. Pachence, S. Amador, J. McCauley, A. Smith, J.K. Blasie, Chemistry Department, University of Pennsylvania, Philadelphia, PA 19104.

We have employed nonresonance x-ray diffraction to determine the location of a monolayer of cytochrome *c* either electrostatically or covalently bound to the surface of various Langmuir-Blodgett(LB) lipid films. The location of the heme-Fe atoms within the electron density profile of the cytochrome *c*/LB lipid film was indicated to $\pm 3\mathring{A}$ accuracy using resonance x-ray diffraction. Optical linear dichroism was used to further determine the orientation of the cytochrome *c* heme group relative to the plane of the surface. Monolayers of cytochrome *c* and cytochrome *c*/photosynthetic reaction center complexes have also been bound covalently to self-assembled monolayers of trichlorosilylundecyl thiol attached to synthetic inorganic multilayer substrates. X-ray diffraction techniques using monolayers of these protein complexes have enabled the direct determination of their profile structures at ~ 8 $\mathring{A}$ resolution.

W-Pos603

LIGHT AND DARK STEADY STATES OF CYTOCHROME b-559 IN D1D2 REACTION CENTRES: MODULATION BY DBMIB. **P.Nicholls,K.Barabas & J.Barber** Dept.Biol.Sci., Brock Univ., St.Catharines Ont., Canada; Inst.Biophys., Hung. Acad. Sci., Szeged, Hungary; Dept. of Pure & App. Biol., Imperial College, London, England. Cytochrome b-559 in pea D1D2 (PSII) complexes is reduced in the light by donors like $MnCl_2$ if decylPQ is present. It is reduced in the dark by ascorbate. The redox levels in light or dark indicate a single species in a steady state from reductant to O_2. Dibromomethylisopropyl quinone (DBMIB) decreases the photo reduction level by increasing the O_2-dependent reoxidation; it also increases the rate of dark reduction by ascorbate. Titration of both effects involves [DBMIB] at or below the level of [cyt. b-559] suggesting a very tight DBMIB binding site. A second Q binding site can be occupied either by decylPQ or by a second DBMIB molecule. At high DBMIB concentrations b-559 is photo reducible in absence of either $MnCl_2$ or decylPQ. A model that accounts for the observations involves a dimeric structure for the complex and close relationships between b-559 and two Q-binding sites. Supported by NSERC (Canada) grants to PN and AFRC (UK) grants to JB.

W-Pos604

INTERSPECIES RECONSTITUTION OF THE PHOTOSYSTEM I COMPLEX FROM THE P700 AND F_X-CONTAINING REACTION CENTER CORE PROTEIN AND THE F_A/F_B POLYPEPTIDE

Tetemke Mehari & John H. Golbeck (Intr. by: A.D. Pickar) Portland State University.

The interspecies reconstituted PSI complexes show a slightly different EPR signal for the F_A/F_B Fe-S cluster from that of the controls. A reconstituted PSI complex from the Synechococcos sp. PCC 6301 core protein and spinach psaC protein produces an identical EPR spectrum for the F_A/F_B Fe-S cluster to that obtained from the spinach psaC protein associated with a spinach PSI core. However, PSI complexes reconstituted from the same species show identical EPR signals as that of the controls. This study suggests that the EPR spectral differences seen among various species is inherent to the psaC gene product but not to the specific interactions between this protein and the core.

W-Pos605

P-BAND (15 GHZ) EPR OF THE S_2-STATE SIGNALS OF THE O_2-EVOLVING COMPLEX Alice Haddy, William R. Dunham, and Richard H. Sands, Biophysics Research Div., Univ. of Michigan, Ann Arbor, Michigan 48109

P-band (15 GHz) frequency EPR has been applied to the two S_2-state signals of the O_2-evolving complex. Earlier difficulties interpreting these signals at X-band (9 GHz) has indicated the need for extending the range of study to include both higher and lower (S-band) frequencies.

The P-band "multiline" signal, which arises from a Mn multimer, appears much as its X-band counterpart with 17-20 main lines about g=2.0. However while the wings of the X- and P-band signals are quite similar, the central regions show many differences in peak splittings. The P-band signal at g=4 appears to have a g-value anisotropy (or splitting) of about 0.2 g-value and is broader than the simple X-band signal. Possible sources of this are discussed.

W-Pos606

A MUTATION, (M)L214H, CATALYZES THE INCORPORATION OF BCHL INTO THE BPh_L SITE OF THE R. SPHAEROIDES RC.

C. Schenck[1], D. Gaul[1], C. Kirmaier[2] & D. Holten[2], [1]Dept. Biochem., Colorado S.U., F.C., CO 80523 & [2]Dept. Chem., Washington U., S.L., MO 63130

The RC is an oligomeric integral membrane protein that catalyzes the light-induced electron transfer reactions of photosynthesis. The RC contains 4 BChls whose Mg^{++} atoms are axially coordinated by 4 evolutionarily conserved histidines. Other tetrapyrroles are present in the protein as 2 BPhs with no coordinating protein ligands and no metals. BPh_L functions as an electron transfer intermediate, being reduced in 3 ps.

We have modified the protein primary structure in the vicinity of BPh_L; a Leu side chain at position 214 of the M subunit ((M)L214) has been replaced by His, a potential ligand to MgBChl. The mutant strain grows photoheterotrophically. The RC electronic spectrum is consistent with the replacement of BPh_L by BChl. Metals analysis shows that the mutant contains 4.6+0.4 Mg/RC, whereas the wild-type RC contains 3.9+0.4 Mg/RC. Fs and ps absorption spectroscopy show no evidence for appearance of bands associated with the transient reduction of BPh_L in the mutant. We observe a new intermediate that forms in 3ps and decays in 300ps and shows novel features near 780nm. We conclude that the RC is in some sense an autocatalytic protein that participates in its own assembly. Support by NSF & NIH.

W-Pos607

SPECTROSCOPIC AND ELECTROCHEMICAL RESOLUTION OF THE HIGH POTENTIAL HEMES IN THE REACTION CENTER OF *CHROMATIUM VINOSUM* USING ORIENTED LANGMUIR-BLODGETT FILMS. G. Alegria and P.L. Dutton. Dept. of Biochemistry & Biophysics, U. of Pennsylvania, Phila., PA.

Subchromatophore particles (Thornber's fraction A) containing the RC-cyt c complex of *C. vinosum* were used to fabricate Langmuir-Blodgett (LB) films. LB films deposited on quartz slides were analyzed using standard and linearly polarized spectroscopy in combination with redox potentiometry. The following results were obtained: i) The particles in the LB films show uniaxial orientation. ii) Redox titrations of the photo-oxidation of the high potential hemes reveal two distinct redox centers with E_{m8} values of 372 and 211 mV. iii) The resolved components exhibit different absorption spectra in the γ-band with maxima at 423 and 421 nm respectively. iv) Dichroic ratios at the maxima (0.7 and 0.55 respectively) indicate different orientations of the heme planes relative to the slide plane. The structural implications and relationship with the analogous *Rps. viridis* RC-cyt c complex will be discussed. Supported by PHS grant GM41048.

W-Pos608

BOTH CARBONYL GROUPS ARE NECESSARY FOR STRONG INTERACTION OF THE SEMIQUINONE AT THE Q_A SITE OF PHOTOSYNTHETIC REACTION CENTER PROTEIN. K. Warncke and P.L. Dutton, Dept. of Biochem. and Biophys., Univ. of Pennsylvania, Phila., PA 19104. (Introduced by J.H. Parkes)

The *in situ* midpoint potentials (E_m) for the non-quinonoid compounds 2,4,7-trinitrofluorenone (TNF, -380 mV) and 10-thionyl anthrone (TA, -57 mV) at the Q_A site of reaction center protein (RC) from *Rhodobacter sphaeroides* R26 have been determined from the observed temperature-dependence of charge recombination between $[BChl]_2{+}A^-$ and $[BChl]_2A$ states through the thermal intermediate state, "X" (Woodbury *et al.*, (1986) *BBA 851*, 6-22). The *in situ* E_m values are shifted +42 (TA) and -295 mV (TNF) from values determined in dimethylformamide solution, compared to the characteristic large positive shifts seen with quinones (e.g., anthraquinone (AQ), +379 mV). These results show that: (1) the Q_A site is capable of dramatic destabilization, as well as strong stabilization, of redox couples relative to the aprotic solution environment, and (2) both carbonyl functions are required for the large positive E_m shifts experienced by quinone couples bound at the Q_A site. Thus, although only one carbonyl group contributes to the interaction of the oxidized quinone with the Q_A site (Warncke and Dutton, in press), both carbonyl groups are essential for strong semiquinone interaction. Supported by NSF grant DMB 88-17240.

W-Pos609

RED PEAK OF CHLOROPHYLL a IN SOLUTION FILM AND CRYSTALLINE STATES: ABSORBANCY AND MOLECULAR DENSITY. Germille Colmano Dept. Biomedical Sciences, VA-MD Region. Coll. Vet. Med., VPI & SU, Blacksburg, VA 24060. A model, combining the absorption spectra of chlorophyll a in solution, film, and crystalline states with the molecular orientation of these states, was constructed and coupled with quantum chemistry techniques. It is shown, that the knowledge of the physical parameters of chlorophyll a in different spatial orientation may explain the correlation of peak position of the red absorption for molecules in solution, film, and crystalline states, with the intermolecular distance, which is inversely proportional to the molecular radius.

W-Pos610

How *Does* Manganese Oxidize Water for Photosynthetic O_2 Production?

G. C. Dismukes[1], J. E. Sheats[2], P. Mathur[1], R. Czernuszewicz[1]; [1]Princeton University, Dept. of Chemistry, Princeton, NJ and [2]Rider College, Lawrenceville, NJ.

The molecular mechanism of photosynthetic water oxidation has been investigated with synthetic dimanganese complexes which mimic three reactions: 1) reversible water binding, 2) successive oxidations at a fixed potential < 1.0V, and 3) catalase activity. Water exchanges with the bridging (μ) oxo ligand in 1, $LMn^{III}O(RCO_2)_2Mn^{III}L$. $1e^-$ oxidation $1 \rightarrow 1^+$ initiates the binding of a second water molecule forming the di-μ-oxo species 2, $LMn^{III}O_2(RCO_2)Mn^{IV}L$. The $1e^-$ oxidations $1 \rightarrow 1^+ \rightarrow 1^{2+}$ occur at 0.9 and 1.5V, while $2 \rightarrow 2^+$ is lowered to 0.9 V. Added H_2O_2 disproportionates at the WOC catalytically cycling between the S_0 and S_2 states. Dimanganese(II) complexes which mimic this reaction do so by a two-step mechanism: $2e^-$ oxidation by insertion of μ-oxo, followed by reduction $H_2O_2 + Mn^{III}OMn^{III} \rightarrow O_2 + H_2O$ (Mathur et al (1987) JACS 109, 5227). Conclusion: The activated form of water leading to photosynthetic O_2 production is μ–oxo. Support: NIH GM39932.

W-Pos611

A Calcium-Specific Site Influences the Structure and Activity of the Manganese Cluster Responsible for Photosynthetic Water Oxidation.

J. Tso, M. Sivaraja, M. Baumgarten, J. Philo and C. Dismukes. Intro. by E. Braswell. Dept. of Chemistry, Princeton University, N. J. 08544.

Depletion of Ca from PSII membranes of spinach by a low pH treatment results in the modification of the manganoenzyme responsible for the photooxidation of water to O_2 (Sivaraja et al, 1989, Biochemistry). Ca depletion in the dark results in a modified S_1' which can be photo-oxidized above 250K to form an altered S_2' state which exhibits a modified multiline EPR signal. The modified S_1' and S_2' states are more stable as seen by the higher temperature required for S_1'-> S_2' and the longer life time of the S_2' . Ca reconstitution results in the reduction of the oxidized tyrosine residue $^{161}Y_D^+$. Photo-oxidation of the S_2' state above 250K leads to formation of a new EPR signal at g = 2.004 and symmetric linewidth of 163+3G. Stepwise turnover of the Ca-depleted samples at 273K using laser flashes indicate that this new signal can formally be attributed to an S_5 or S_4 state. This state is photoaccumulated and decays to the S_2' state. The signal could arise from an aminoacid in magnetic contact with the Mn cluster or from the Mn cluster itself, consistent with the temperature dependence and large linewidth. This signal is also observed in fluoride treated PSII membranes. Calcium depletion results in loss of the large first flash magnetic susceptibility signal seen untreated samples.

W-Pos613

^{13}C MAS-NMR STUDY OF THE TYROSINE PROTONATION STATES IN RHODOBACTER SPHAEROIDES R26

H. de Groot[1], J. Raap[1], C. Winkel[1], A. Hoff[2] and J. Lugtenburg[1]
[1]Gorlaeus, and [2]Huygens Labs., Leiden, The Netherlands.

The first Magic-Angle-Spinning NMR results with atomic resolution on R26 photosynthetic reaction centers are presented. The spectral data indicate that all 28 tyrosines in R26 are protonated. A synthetic medium was developed to prepare [4'-^{13}C] tyrosine R26. The incorporation was measured with mass spectrometry and is better than 75%. A ~25mg sample was obtained and studied with ^{13}C CP/MAS NMR. Only one broad [4'-^{13}C] tyr resonance is observed, centered around 156 ppm. Surprisingly, the resonance exhibits fine structure, and may be deconvoluted into five well-defined MAS patterns with slightly different (< 4ppm) isotropic shifts and different intensities. Two low-intensity signals appear upfield from the bulk, and are probably due to an individual tyrosine each.

W-Pos612

ROLE OF SOLVATION IN QUINONE FUNCTION

J. M. KESKE, J. M. BRUCE, AND P. L. DUTTON, Dept. of Biochemistry and Biophysics, Univ. of Pennsylvania, Philadelphia, PA. 19104

The quinone binding sites of photosynthetic bacterial reaction centers demonstrate the potential to create an environment capable of manipulating the functional properties of bound ubiquinone. A constituent of this manipulation resides in the binding sites' differential "solvation" of the quinones oxidized and reduced forms. In order to understand the basis of the solvation process, we have utilized partition coefficients of a variety of solutes related to ubiquinone, obtained between water and alkanes, alkanols, and chloroform. This multiple solvent approach has allowed the resolution of hydrophobicity, dipolar forces, and hydrogen bonding contributions to the solvation of quinones and related molecules. Correlations of oxygen lone pair basicity with its aqueous solvation (Keske et al.; this meeting) permits estimates of hydrogen bond strength changes on quinone reduction. pK shifts observed for the quinone (carbonyl), its conjugate semiquinone (phenolate) and hydroquinone anions suggest large increases in the energy of aqueous solvation upon quinone reduction. For example, reduction of quinone (pK ~ -4) to semiquinone (pK~6) anion will be accompanied by an estimated -4 to -6 Kcal increase in aqueous hydrogen bond strength.

Supported by PHS GM 27309 and NSF DMB 88 77240.

W-Pos614

STRUCTURAL, FUNCTIONAL AND EVOLUTIONARY ASPECTS OF BAND-3 PROTEIN.

D.L. Mullan and H. Mizukami. Division of Regulatory Biology and Biophysics, Department of Biological Sciences, Wayne State University, Detroit, Michigan 48202

Band-3 protein is a permease which catalyzes a one-for-one anion exchange. Like many transport proteins, it consists of a catalytic domain comprised of multiple sets of membrane spanning regions and a cytoplasmic domain with the amino and carboxyl tails in the cytosol. We have compared human and mouse erythroid and non-erythroid band-3 to other membrane proteins that are generally similar in structure and function, but have dissimilar specific functions. Analyses of base and amino acid sequence, secondary structure predictions, matrix homology, and intron-exon compostion suggest that certain peptide domains may share a common evolutionary ancestry with band 3.

W-Pos615

SMOOTHING AND GRAPHICAL ANALYSIS OF SEDIMENTATION VELOCITY DISTRIBUTION FUNCTIONS.

Hayes, D.B. & Laue, T.M. Dept. of Biochem., U. New Hampshire, Durham, NH 03824.

Methods for minimizing the effects of diffusion on sedimentation velocity distribution functions are limited fundamentally when boundaries are not well resolved. In these cases, simple graphical presentation of the empirical distribution function is preferred. Both integral, $G(s^*)$, and differential, $g(s^*)$, apparent sedimentation coefficient distribution functions are useful, but, as expected, the derivative needed for $g(s^*)$ is sensitive to noise. Smoothing using sliding polynomials distorts the data and is insensitive to the regional complexity of the curve. A graphically-interfaced, parametric spline smoothing and fitting package for sedimentation data has been developed using the FITPACK subroutines. The advantages of this are: 1) smoother data result with less distortion than is found with polynomial procedures, 2) the experimenter can place additional knots in the fit at regions of particular interest, 3) faster and more accurate interpolation result, 4) large data sets are reduced considerably without loss of significant information and 5) derivatives are smoother than methods relying solely on local data. Supported by NSF BBS-8615815.

Th-AM-Sym I-1

STRUCTURE, ASSEMBLY AND INTERACTIONS OF THE NUCLEAR LAMINA (NL) AND THE NUCLEAR PORE COMPLEX (NPC) STUDIED BY HIGH-RESOLUTION ELECTRON MICROSCOPY (EM)

U. Aebi, Biocenter, University of Basel, Switzerland

We have developed specimen preparation methods to visualize the NL, an intermediate filament (IF)-like protein meshwork lining the nucleoplasmic surface of the inner nuclear membrane, *in situ*. Using highly purified nuclear lamins, we have investigated the structure, assembly, and dynamics of this new class of IF *in vitro* by high-resolution EM and analytical ultra-centrifugation. The NPC is an elaborate membrane-bound organelle interposed between the inner and outer nuclear membrane, which serves as a gateway through the nuclear envelope (NE) for a variety of nuclear and cytoplasmic substances. Using isolated nuclear envelopes from *Xenopus laevis* oocytes and other sources, we have explored differential extraction procedures (i.e. by varying pH, ionic strength, multivalent cations, and detergents) combined with variations in specimen preparation to visualize by conventional EM (CTEM) and scanning transmission EM (STEM) intact NPCs and distinct NPC components, including cytoplasmic and nucleoplasmic "rings", "spoke" and "plug-spoke" complexes, and plugs. Reproducible structural features to a resolution of better than 10 nm have been gathered from intact NPC and NPC components after correlation averaging of negatively stained and unstained single particle images. A correlation between structure and mass distribution of the intact NPC and of the distinct NPC components has been determined by quantitative STEM. Acordingly, the intact NPC has a mass of 124 MDa, the cytoplasmic ring of 32 MDa, the nucleoplasmic ring of 21 MDa, the spoke complex of 52 MDa, the plug-spoke complex of 66 MDa, and the central plug of 13 MDa.

Th-AM-Sym I-2

SYNTHESIS AND TRANSPORT OF A SPECIFIC PREMESSENGER RNP PARTICLE STUDIED BY ELECTRON MICROSCOPE TOMOGRAPHY.

H. Mehlin, A. Lonnroth, U. Skoglund, and B. Daneholt. Department of Molecular Genetics, Medical Nobel Institute, Karolinska Institutet, Box 60400, S-10401 Stockholm, Sweden.

Balbiani ring genes in the dipteran *Chironomus tentans* are selectively expressed in the larval salivary glands and encode large-sized secretory proteins. These 37 kb long genes can be studied in situ, and the synthesis and transport of the transcription product visualized in the electron microscope. In our studies, a new ultrastructural method, electron microscope tomography, has been applied permitting 3-D analysis of the transcription on a molecular level. It has been shown that the Balbiani ring premessenger RNP particle attains a specific, toroid-like shape, that the particle is formed in a well-defined two-step process and that the particle translocates through the nuclear pore in an ordered fashion with the 5' end of the transcript in the lead.

Th-AM-Sym I-3

ANALYSIS OF NUCLEAR PROTEIN IMPORT AND A PUTATIVE TRANSPORT RECEPTOR, Stephen Adam and Larry Gerace, Dept. of Molecular Biology, Scripps Research Institute, La Jolla, CA 92037

Import of most proteins into the nucleus is thought to occur by mediated transport across the nuclear pore complex, and is directed by short amino acid stretches within nuclear proteins called nuclear location sequences. We have performed binding and crosslinking studies with synthetic peptides to analyze cellular proteins that interact with the nuclear location sequence of the SV40 T antigen (Nature 337:276-279). This work identified one major polypeptide that binds this sequence with the specificity and high affinity expected for a transport receptor. We recently isolated this protein from nuclear envelopes, and are using antibodies to the protein to analyze its functions in a cell-free nuclear protein import system that we recently devised. This system involves digitonin-permeabilized cultured mammalian cells, whose nuclei (which are functionally intact) strongly accumulate fluorescently-labelled proteins containing nuclear location sequences from the surrounding medium when the permeabilized cells are incubated at 33°C in the presence of ATP and cytosol.

Th-AM-Sym-I-4

CYTOSOLIC FACTORS REQUIRED FOR NUCLEAR TRANSPORT IN VITRO. D.D. Newmeyer, K.S. Lundberg, and D.J. Forbes, La Jolla Cancer Research Foundation and Dept. Biology, U.C. San Diego.

To help understand the mechanisms of protein transport into the cell nucleus, we developed an *in vitro* system that displays authentic signal-mediated nuclear import. Rat liver nuclei are placed in a mixture of cytosol and membrane vesicles from *Xenopus* eggs; the transport of TRITC-labeled proteins is assayed by fluorescence microscopy. Transport *in vitro* is temperature- and ATP-dependent, requires a functional nuclear location signal in the transported protein, and is mediated by the nuclear pores. The process involves at least two steps: 1) ATP-independent nuclear pore binding and 2) ATP-dependent pore translocation. The transport inhibitor, wheat germ agglutinin, blocks only the translocation step, suggesting that pore glycoproteins are involved in translocation. We have identified an NEM-sensitive cytosolic factor, NIF-1, required for the pore-binding step. A second cytosolic factor, NIF-2, acts synergistically with NIF-1 in promoting nuclear protein import.

Th-AM-Sym I-5

APPLICATION OF PHOTOBLEACHING TECHNIQUES AND CONFOCAL LASER SCANNING MICROSCOPY TO NUCLEAR CYTOPLASMIC EXCHANGE

R. Peters, Max-Planck-Institut f. Biophysik D-6000 Frankfurt 71, Fed. Rep. of Germany

Fluorescence photobleaching techniques have been widely used to study the lateral mobility of macromolecules in membranes and inside cells. We employ the method also to analyse transport through membranes and will present a new approach to the measurement of fluorescent tracer flux through single transmembrane pores. Nuclear cytoplasmic exchange was studied by combining photobleaching with confocal laser scanning microscopy (CLSM). Hybrid proteins consisting of short segments of the Simian virus 40 T-antigen and the almost complete β--galactosidase were expressed in E. coli, labeled fluorescently and injected into the cytoplasm of cultured cells. Photobleaching and CLSM studies confirmed that the karyophilic signal of the T-antigen (residues 128-132) is necessary and sufficient for nuclear transport. However, transport kinetics strongly depended on sequences flanking the karyophilic signal. Since nuclear transport was only promoted by those sequences containing phosphorylation sites it appears possible that posttranslational modification plays a decissive regulatory role in nuclear transport.

Th-AM-Sym II-1

THE STRUCTURE AND DYNAMICS OF THE Ca^{2+}-ATPase OF SARCOPLASMIC RETICULUM (SR). Anthony N. Martonosi, Dept. Biochem. Mol. Biol., SUNY HSC, Syracuse, NY 13210.

The ATP-dependent Ca^{2+} transport in SR involves transitions between several structural states of the Ca^{2+}-ATPase, that occur without major changes in the secondary structure. The rates of these transitions are modulated by the lipid environment and by interactions between ATPase molecules. Although the Ca^{2+}-ATPase restricts the rotational mobility of a population of lipids, there is no evidence for specific interaction of Ca^{2+}-ATPase with phospholipids. Fluorescence polarization and energy transfer (FET), using site specific fluorescent indicators and monoclonal antibodies, combined with information from two-dimensional Ca^{2+}-ATPase crystals yields a refined structural model of the enzyme, in which the location of the various functional sites are tentatively identified. Analysis of the temperature dependence of FET between fluorophores attached to different regions of the Ca^{2+}-ATPase indicate the existence of "rigid" and "flexible" regions within the molecule characterized by different degrees of thermally-induced structural fluctuations. (Supported by NIH, NSF and MDA).

Th-AM-Sym II-2

RANDOM COLLISION ELECTRON TRANSPORT IN THE MITOCHONDRIAL INNER MEMBRANE. Charles R. Hackenbrock, Department of Cell Biology and Anatomy, School of Medicine, University of North Carolina at Chapel Hill, Chapel Hill, N.C.

Studies from this laboratory indicate that the redox components of the mitochondrial inner membrane are independent diffusants having collision frequencies sufficient to influence the overall kinetic process of electron transport. Experimental changes in membrane protein density, temperature and solvent viscosity affect the electron transport rates and diffusion coefficients of all redox partners directly, as would be predicted in diffusion-based, bimolecular electron transfer reactions. The efficiency of cytochrome c in transporting electrons from and to its membrane-bound protein redox partners is maximal at physiological ionic strength where its diffusion is maximal and in three dimensions, and where its concentration at the membrane surface, its affinity for the membrane surface and its occupancy time on the membrane surface are lowest. Supported by NIH, NSF.

Th-AM-Sym II-3

ROTATIONAL DYNAMICS & REDISTRIBUTION OF CELL SURFACE COMPONENTS IN $Fc_\varepsilon RI$-MEDIATED EXOCYTOSIS. *Thomas M. Jovin*[1], *Enrique Ortega*[2], *& Israel Pecht*.[2]. [1]Dept. of Molecular Biology, Max Planck Institute for Biophys. Chem., Göttingen, F.R.G. [2]Dept. of Chem. Immunology, The Weizmann Institute of Science, Rehovot, Israel.

The allergic response is triggered by the aggregation of receptors ($Fc_\varepsilon RI$) on the surfaces of mast cells, either via IgE molecules tethered to the $Fc_\varepsilon RI$ or via receptor-specific mAbs. Recently, another cell surface antigen (G63) has been identified; cross-linkingwith mAbs leads to *inhibition* of $Fc_\varepsilon RI$-mediated exocytosis. There are $3\text{-}6\cdot10^5$ $Fc_\varepsilon RI$ but only $2\cdot10^4$ G63 Ag molecules per rat mucosal mast cell (RBL-2H3 line).

We have studied the surface dynamics of the $Fc_\varepsilon RI$ and G63 Ag by determinations of rotational diffusion using time-resolved phosphorescence anisotropy of erythrosin conjugated to three $Fc_\varepsilon RI$-specific mAbs (intact and FaB fragments), anti-DNP monoclonal IgE, and mAb G63 (Fab fragment). The results indicate that (1) IgE and the $Fc_\varepsilon RI$-specific Abs bind in a non-random orientation to the cell membrane and their motions reflect the flexibility of the respective $Fc_\varepsilon RI$ segments for which they are specific. (2) The differences in rotational flexibility may be correlated with the relative effectiveness of the three $Fc_\varepsilon RI$-specific mAbs in triggering exocytosis. (3) Cross-linking of $Fc_\varepsilon RI$ leads to rotational immobilization of the G63 Ag, suggesting that the latter is induced to redistribute and interact directly with the $Fc_\varepsilon RI$. These findings provide physical evidence for a role of the G63 Ag in secretion.

Th-AM-Sym II-4

PLASMA MEMBRANE DOMAINS AND MEMBRANE ORGANIZATION Michael Edidin, The Johns Hopkins University, Baltimore,MD 21218

Plasma membranes of many types of cells are organized into membrane domains, specialised in composition and function. We have used the method of fluorescence photobleaching and recovery, FPR to investigate micrometer-sized domains. FPR recovery curves contain information about the fraction of the fluorescent probe that is immobile on the time-scale (minutes) of an FPR measurement. This fraction is not expected to depend upon the size of the spot bleached. However, we find that in three different types of cells the immobile fractions of several different probes are a function of spot size, with the smallest immobile fractions observed for the smallest spots. This is not seen for one probe, NBD-PC in liposomes, or for another lipid probe, diI, in cells. It appears to reflect the organization of the plasma membrane into domains, several micrometers in diameter. Results on inositol-lipid linked proteins strongly suggest that the domains are organized by an underlying cytoskeleton.

Th-AM-Sym II-5

Translational diffusional dynamics and fluid phase connectivity in two-component phosphatidylcholine bilayers. Winchil L. C. Vaz, Max-Planck-Institut für biophys. Chemie, D-3400 Göttingen, F.R.G.

Fluorescence recovery after photobleaching (FRAP) was used to study the translational diffusion of a fluorescent lipid probe, NBD-PE, in bilayers formed from binary phosphatidylcholine mixtures. The probe is soluble in fluid phase but not in the gel phase bilayers. Isomorphous, monotectic, peritectic and eutectic mixtures were studied. The FRAP results give information regarding the "fluidity" and the "connectivity" of the fluid domains in the systems when fluid and gel phase domains co-exist in the same bilayer. The connectivity of the fluid phase lies in some cases close to the fluidus, in some cases close to the mid-points of the tie-lines in the two-phase region and in some cases close to the solidus. The first case above suggests some domain structures in which a small fraction of gel phase ($\leq$ 20%) in a largely fluid bilayer may subdivide the membrane in non-connected fluid domains. This sort of domain structure may control important diffusion-controlled reactions in the plane of a membrane.